HIGHWAY RESEARCH RECORD

Number 190

Behavior: Piles, Stabilized Soils, and Remolded Clays, and CBR Sampling

6 Reports

Subject Area

61 Exploration-Classification (Soils)
62 Foundations (Soils)
63 Mechanics (Earth Mass)

HIGHWAY RESEARCH BOARD

DIVISION OF ENGINEERING NATIONAL RESEARCH COUNCIL
NATIONAL ACADEMY OF SCIENCES—NATIONAL ACADEMY OF ENGINEERING

Washington, D.C., 1967 Publication 1521

Price: $2.80

Available from

Highway Research Board
National Academy of Sciences
2101 Constitution Avenue
Washington, D.C. 20418

Department of Soils, Geology and Foundations

Eldon J. Yoder, Chairman
Joint Highway Research Project
Purdue University, Lafayette, Indiana

Chester McDowell, Vice Chairman
Materials and Tests Soils Engineer
Texas Highway Department, Austin

HIGHWAY RESEARCH BOARD STAFF

J. W. Guinnee, Engineer of Soils, Geology and Foundations

DIVISION B

H. Bolton Seed, Chairman
Department of Civil Engineering
University of California, Berkeley

COMMITTEE ON STRENGTH AND DEFORMATION CHARACTERISTICS OF PAVEMENT SECTIONS
(As of December 31, 1966)

Carl L. Monismith, Chairman
University of California, Berkeley

Bonner S. Coffman, Department of Civil Engineering, Ohio State University, Columbus
B. E. Colley, Manager, Paving Development Section, Portland Cement Association, Skokie, Illinois
F. N. Finn, Chief Engineer, Materials Research & Development, Woodward-Clyde-Sherard & Associates, Oakland, California
Raymond A. Forsyth, Senior Materials and Research Engineer, Materials and Research Department, California Division of Highways, Sacramento
William S. Housel, University of Michigan, Ann Arbor
W. Ronald Hudson, Research Engineer and Assistant Professor of Civil Engineering, Department of Civil Engineering, The University of Texas, Austin
R. L. Kondner, Department of Civil Engineering, University of Maryland, College Park
H. G. Larew, Department of Civil Engineering, University of Virginia, Charlottesville
T. F. McMahon, U. S. Bureau of Public Roads, Washington, D.C.
Bryan P. Shields, Research Council of Alberta, University of Alberta, Edmonton, Alberta, Canada
James F. Shook, The Asphalt Institute, College Park, Maryland
Eugene L. Skok, Jr., Department of Civil Engineering, University of Minnesota, Minneapolis
J. E. Stephens, Professor of Civil Engineering, University of Connecticut, Storrs
Aleksandar S. Vesic, Professor of Civil Engineering, Duke University, Durham, North Carolina

COMMITTEE ON MECHANICS OF EARTH MASSES AND LAYERED SYSTEMS

(As of December 31, 1966)

Robert L. Schiffman, Chairman
University of Illinois at Chicago Circle
Department of Materials Engineering
Chicago, Illinois

Richard G. Ahlvin, Chief, Flexible Pavement Branch, U. S. Army Waterways Experiment Station, Vicksburg, Mississippi

William Baron, Assistant Professor of Civil Engineering, Purdue University, Lafayette, Indiana

Donald M. Burmister, Professor Emeritus of Civil Engineering, Columbia University, New York, N. Y.

J. C. Christian, Assistant Professor of Civil Engineering, Massachusetts Institute of Technology, Cambridge

Lawrence A. DuBose, Testing Service Corporation, Wheaton, Illinois

Jacob Feld, Consulting Engineer, New York, N. Y.

A. A. Fungaroli, Associate Professor of Civil Engineering, Department of Civil Engineering, Drexel Institute of Technology, Philadelphia, Pennsylvania

Delon Hampton, Research Engineer, Soil Mechanics Section, IIT Research Institute, Chicago, Illinois

Milton E. Harr, Professor of Soil Mechanics, School of Civil Engineering, Purdue University, Lafayette, Indiana

R. L. Kondner, Department of Civil Engineering, University of Maryland, College Park

Charles C. Ladd, Associate Professor of Civil Engineering, Massachusetts Institute of Technology, Cambridge

Ulrich Luscher, Assistant Professor of Civil Engineering, Department of Civil Engineering, Massachusetts Institute of Technology, Cambridge

T. F. McMahon, U. S. Bureau of Public Roads, Washington, D. C.

Robert L. McNeill, Chief Engineer, Woodward-Clyde-Sherard & Associates, Oakland, California

Z. C. Moh, SEATO Graduate School of Engineering, Sanamma Road, Bangkok, Thailand

K. Nair, Materials Research and Development, Inc., Oakland, California

A. M. Richardson, Associate Professor of Civil Engineering, Department of Civil Engineering, University of Pittsburgh, Pittsburgh, Pennsylvania

F. E. Richart, Jr., Chairman, Department of Civil Engineering, University of Michigan, Ann Arbor

Bruce B. Schimming, Assistant Professor of Civil Engineering, Department of Civil Engineering, Notre Dame University, Notre Dame, Indiana

Werner E. Schmid, Department of Civil Engineering, Princeton University, Princeton, N. J.

F. H. Scrivner, Research Engineer, Texas Transportation Institute, Texas A and M University, College Station

Eugene L. Skok, Jr., Department of Civil Engineering, University of Minnesota, Minneapolis

Aleksandar S. Vesic, Professor of Civil Engineering, Duke University, Durham, North Carolina

H. E. Wahls, Associate Professor of Civil Engineering, Department of Civil Engineering, North Carolina State University, Raleigh

William G. Weber, Jr., Senior Materials and Research Engineer, California Division of Highways, Sacramento

Russell A. Westmann, Dept. of Engineering, University of California, Los Angeles

DIVISION C

O. L. Lund, Chairman
Assistant Engineer of Materials and Tests
Nebraska Department of Roads, Lincoln

L. F. Erickson, Vice Chairman
Materials and Research Engineer
Idaho Department of Highways, Boise

COMMITTEE ON EXPLORATION AND CLASSIFICATION OF EARTH MATERIALS
(As of December 31, 1966)

Preston C. Smith, Chairman
Principal Research Engineer (Soils), Materials Division
U. S. Bureau of Public Roads
Washington, D.C.

Frederick M. Boyce, Jr., Soils Engineer, Maine State Highway Commission, Bangor
Robert C. Deen, Assistant Director of Research, Kentucky Department of Highways, Lexington
William P. Hofmann, Director, Bureau of Soil Mechanics, New York State Department of Public Works, Albany
James H. McLerran, Assistant Division Chief, Photographic Interpretation Research Division, U. S. Army Cold Regions Research & Engineering Laboratory, Hanover, New Hampshire
Olin W. Mintzer, Department of Civil Engineering, The Ohio State University, Columbus
R. Woodward Moore, Highway Research Engineer, Materials Division, U. S. Bureau of Public Roads, Washington, D. C.
L. T. Norling, Senior Soil Cement Engineer, Paving Bureau, Portland Cement Association, Chicago, Illinois
Arnold C. Orvedal, Chief, World Soil Geography Unit, Soil Survey, Soil Conservation Service, Hyattsville, Maryland
R. L. Schuster, Civil Engineering Department, University of Colorado, Boulder
D. O. Tueller, Senior Highway Engineer, Materials and Research Department, California Division of Highways, Sacramento
Walter H. Zimpfer, Civil Engineering Department, University of Florida, Gainesville

COMMITTEE ON SOIL AND ROCK PROPERTIES
(As of December 31, 1966)

G. A. Leonards, Chairman
Head, School of Civil Engineering, Purdue University
Lafayette, Indiana

George B. Clark, Director of Research Center, School of Mines and Metallurgy, Rolla, Missouri
Robert W. Cunny, Chief, Soil Dynamics Branch, U. S. Army Engineer Waterways Experiment Station, Vicksburg, Mississippi
Robert C. Deen, Assistant Director of Research, Kentucky Department of Highways, Lexington
Victor Dolmage, Consulting Geologist, Vancouver, B.C., Canada
Wilbur I. Duvall, Supervisory Physicist, Applied Physics Laboratory, U. S. Bureau of Mines, Denver, Colorado
Austin H. Emery, Assistant District Engineer, New York State Department of Public Works, Watertown

Charles L. Emery, Head, Department of Mining Engineering, University of British Columbia, Vancouver, Canada

John A. Focht, Jr., McClelland Engineers, Inc., Houston, Texas

Emmericus C. W. A. Geuze, Professor of Soil Mechanics and Foundation Engineering, Chairman, Civil Engineering Department, Rensselaer Polytechnic Institute, Troy, N. Y.

Bernard B. Gordon, Staff Soils Engineer, California Department of Water Resources, Sacramento

James P. Gould, Associate, Mueser, Rutledge, Wentworth, Johnston, New York, N.Y.

Ernest Jonas, Head, Soils and Foundations Department, Tippetts, Abbett, McCarthy, Stratton, New York, N.Y.

Robert L. Kondner, Department of Civil Engineering, University of Maryland, College Park

Charles C. Ladd, Department of Civil Engineering, Massachusetts Institute of Technology, Cambridge

T. F. McMahon, U. S. Bureau of Public Roads, Washington, D. C.

Victor Milligan, Associate, H. Q. Golder and Associates, Ltd., Toronto, Ontario, Canada

Roy E. Olson, Department of Civil Engineering, University of Illinois, Urbana

Shailer S. Philbrick, Ithaca, N. Y.

Ronald F. Scott, Division of Engineering and Applied Science, California Institute of Technology, Pasadena

T. H. Wu, Ohio State University, Columbus

Foreword

The six papers in this RECORD are of special interest to those concerned with the strength of soils and the deflections of pavements. Included are reports on strength of soils related to subgrade support, foundation soil, pile performance, and a method for obtaining undisturbed soil samples.

Stephenson, Karrh, and Koplon put forth a method for estimating CBR by grain size distribution and soil binder analysis. It is suggested that this method may be useful in comparing soil strength data from many different sources.

Khera and Krizek present the results of a study to determine the effect of a consolidation stress path and the principal consolidation stress ratio on the strength response of a homogeneous clay remolded to possess a given primary inherent anisotropy.

Seed, Mitry, Monismith, and Chan make a significant contribution in defining the factors which influence resilient deformation of pavements. Repeated-load triaxial-compression tests indicated a unique relationship between the modulus of resilient deformation and confining pressure, indicating that the modulus can vary considerably over the range in stresses usually encountered in pavements. Repeated-load plate tests indicated that the modulus of resilient deformation increased with confining pressure and the thickness of the base. It would appear that results of repeated load tests on paving materials can be used within the framework of available theory to predict transient pavement deflections.

Schimming and Garvey present an example of the Monte Carlo simulation technique in the prediction of design variables, such as mean length, for friction piles driven into a two-layer soil deposit overlying rock. As pointed out in this example, the use of the technique should benefit the designer in arriving at his decision whether or not to consider pile foundations.

Harris and Laguros explore the use of equivalent beam approximations in the analysis of stabilized soil layers on elastic foundations to determine stresses and deflections in these layers. This provides a means of determining how much strength the stabilized layer should have to meet the design conditions.

Uppal, Singh and Bahadur present a method for obtaining an undisturbed soil sample when making CBR determinations on natural ground and under a more controlled laboratory environment. This should be beneficial in providing a closer correlation between laboratory and field results.

Contents

Compacted Soil Strength Estimated From Grain Size Distribution and Soil Binder Analysis

HENSON K. STEPHENSON, JOHN B. KARRH, and NORMAN A. KOPLON
Respectively, Professor of Civil Engineering, Research Associate and Research Assistant, University of Alabama

This paper presents a mathematical approach to the problem of estimating the strength of a compacted soil from a routine laboratory report on its grain size distribution and soil binder analysis. A means for estimating CBR for a soil obtained by the Alabama 2000-psi compaction method is also presented. This approach is suggested as providing the means for crossing state lines with soil strength data so that soil strength data measured in terms of other parameters for any given state might be converted into comparable data for any other state or agency.

•THIS PAPER is concerned with the development of a method for estimating strength characteristics of a compacted soil from a routine laboratory report on its grain size distribution and soil binder fraction analysis, without actually having to conduct strength characteristics tests in the laboratory. Also, a means for estimating the CBR for such a compacted soil obtained by the 2000-psi static-compaction method presently used in Alabama is presented. The 2000-psi static-compaction method is substantially the same as that originally presented in the late 1920's by O. J. Porter of the California Division of Highways. For design purposes, the Alabama Highway Department uses the lesser of the two CBR values reported for 0.1- and 0.2-in. penetrations. There is strong evidence that this same method also should apply to soil strengths measured by other procedures and parameters.

On a logical basis, the more coarse-grain material contained in a soil the higher the CBR and, conversely, the more fine-grain material the lower the CBR. Also, the plastic properties of a soil should have some influence on CBR. Research on properties of the binder fraction of soils at the University of Alabama indicates that the Atterberg limits of a particular soil are related to the percent clay in the binder fraction. It is recognized that the type of clay included in the binder fraction should have some bearing on compacted soil strength. However, the nature of Alabama soils in general, as well as those included in this study, are such that kaolinite is the predominant clay mineral. Illite and montmorillonite clays are rarely if ever encountered. For all practical purposes, the clays used as a basis for this study were assumed to be of the same type. The influence of the plastic properties of a soil, therefore, probably is some function of the percent clay, plastic limit and liquid limit. If it is assumed that each of these effects may be approximated by a parabolic curve, the resulting mathematical model could be written as follows:

$$\Phi(\text{CBR}) = a + bX_1 + cX_1^2 + dX_2 + eX_2^2 + fX_3 + gX_3^2 \qquad (1)$$

Paper sponsored by Committee on Exploration and Classification of Earth Materials and presented at the 46th Annual Meeting.

where

$\Phi(CBR)$ = some function of CBR,
a, b, c, d, e, f and g = multiple-regression analysis constants,
X_1 = some function of grain size distribution,
X_2 = some function of percent clay, and
X_3 = some function of the Atterberg limits.

The characteristic effect of grain size distribution on the value of CBR is illustrated by the gradation curves shown in Figure 1. The grain size data for each curve were taken from routine reports of the Alabama Highway Department soils laboratory. Examination of the 6 curves in Figure 1 will show that CBR is an inverse function of the area under a given curve. That is, the CBR values tend to decrease as the area under the curves increases.

Numerous multiple-regression analyses were made to determine the function $\Phi(CBR)$ that would correlate best with selected forms of the variables X_1, X_2 and X_3 (Eq. 1). The data used as a basis for these multiple-regression analyses were obtained from some 350 soil laboratory reports of the Alabama Highway Department in which the CBR values ranged from very low to very high. Of all the multiple-regression analyses investigated, the one that resulted in the highest correlation coefficient was the one in which the function $\Phi(CBR)$ and the variables X_1, X_2, and X_3 in Eq. 1 were defined as follows:

$\Phi(CBR)$ = log CBR (common logarithm)

X_1 = %4 + %10 + %40 + %60 + %200
(% of total sample passing each sieve size as indicated)

X_2 = %clay
(% of No. 10 fraction as determined by elutriation test)

X_3 = (plastic limit)/(liquid limit - 15) = PL/(LL-15)

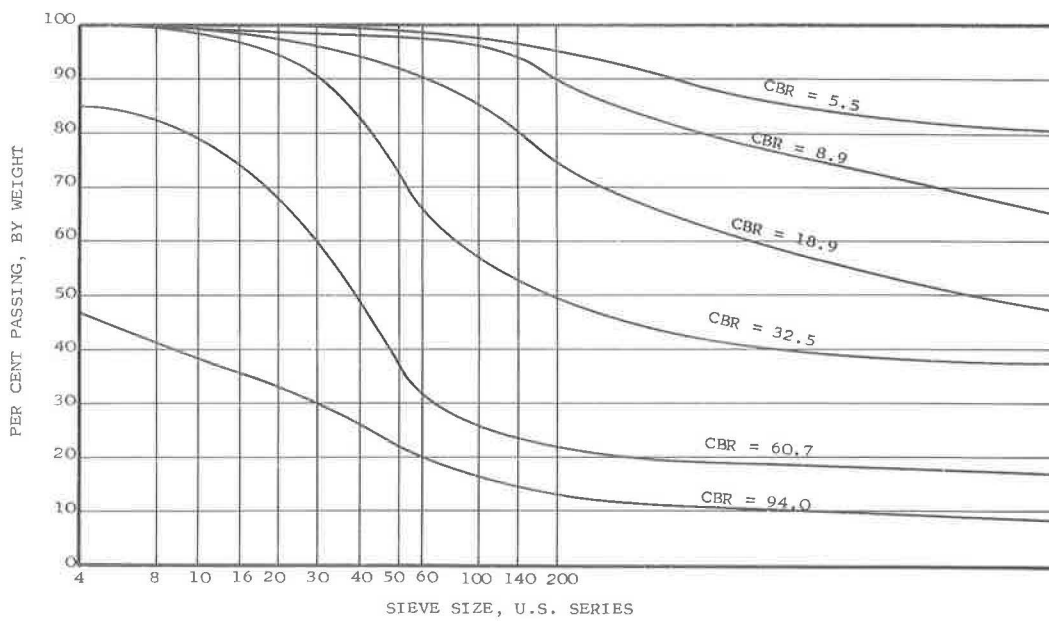

Figure 1. Typical grain size distribution curves.

together with the following multiple-regression constants:

a = 2.446826
b = -0.003272
c = 0.000001
d = -0.007582
e = 0.000003
f = -0.000184
g = 0.000000—negligible

which resulted in the following equation:

$$\log CBR = 2.446826 - 0.003272X_1 + 0.000001X_1^2 - 0.007582X_2 + 0.000003X_2^2 - 0.000184X_3 \quad (2)$$

This multiple-regression equation resulted in a correlation coefficient, R = 0.878112 with R^2 = 0.7711, which means that Eq. 2 explains 77.11 percent of the variation in log CBR.

Only a casual review of Eq. 2 is required to see that the terms involving X_1^2 and X_2^2 have very little effect on the value of log CBR. Similarly, the term involving X_3 has but little effect on the value of log CBR. By eliminating these relatively unimportant terms, it was decided that reasonably accurate values of CBR could be obtained from a simpler mathematical model such as:

$$\log CBR = a + bX_1 + cX_2 \quad (3)$$

where

X_1 = %4 + %10 + %40 + %60 + %200
(% of total sample passing each sieve size as indicated), and
X_2 = %clay
(% of No. 10 fraction as determined by elutriation test)

Based on the mathematical model in Eq. 3, a multiple-regression analysis was run using data from the same 350 soil laboratory reports employed in the multiple-regression analysis that resulted in Eq. 2. The constants resulting from this analysis were as follows:

a = 2.334984
b = -0.002425
c = -0.006920

which when substituted in Eq. 3 gives the following equation:

$$\log CBR = 2.334984 - 0.002425X_1 - 0.006920X_2 \quad (4)$$

The multiple-regression analysis that resulted in Eq. 4 had a correlation coefficient, R = 0.8774 with R^2 = 0.770, which means that Eq. 4 explains 77.0 percent of the variation in log CBR. By comparing this with the 77.11 percent of the variation in log CBR explained by Eq. 2, it will be seen that reasonably accurate CBR values should result from using Eq. 4. This is further evidenced in that the standard error of estimate of log CBR is 0.224 or standard error of estimate of CBR is 1.67. The principal advantage of using Eq. 4 is its simplicity, since all three of the terms can be shown graphically on one page, whereas Eq. 2 would require many pages. A graphical representation of Eq. 4 is given in Figure 2.

In Figure 2, the variable X_1 is shown on the horizontal scale; it is equal to the sum of the percentages of the entire sample passing the No. 4, 10, 40, 60 and 200 sieves. The variable X_2 = %clay (the percent of the fraction passing the No. 10 sieve, as determined by the elutriation test) is shown on the vertical scale. The use of Figure 2 may be illustrated by referring to the typical soils laboratory report shown in Figure 3.

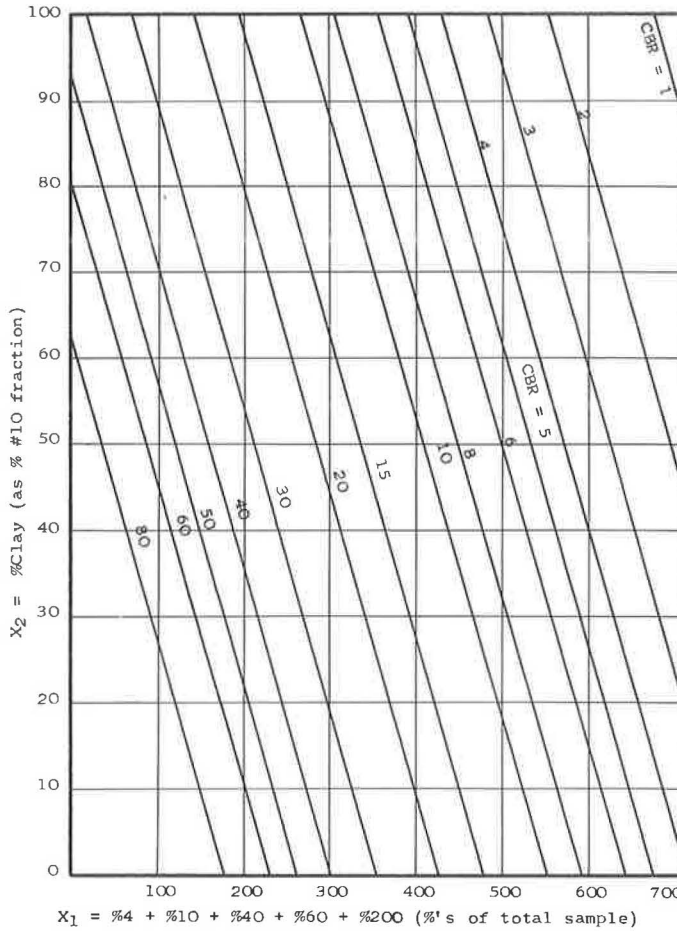

Figure 2. Chart for estimating CBR based on 2000-psi method used by Alabama Highway Department.

From the mechanical analysis, it will be found that $X_1 = 100 + 100 + 100(98 + 96 + 88.1)/100 = 482.1$ and the %clay, $X_2 = 70.4$. For these values of X_1 and X_2, Figure 2 indicates an estimated value of CBR = 4.9, which compares favorably with the design CBR = 5.1 at 0.2-in. penetration as determined by the Alabama Highway Department soils laboratory (Fig. 3).

The question now arises as to how well the observed CBR values agree with the calculated values obtained by use of Eq. 4. Figure 4 shows this relationship. Although this curve gives calculated values of CBR in the higher ranges which are on the conservative side, note that for values of CBR = 60 or less the calculated and observed agree quite well.

The observed CBR values, indicated by the dots in Figure 4, show considerable scatter about the regression curve. This, however, is to be expected since, in addition to grain size, soils in nature have other highly variable characteristics, such as grain angularity and surface roughness, which have a marked influence on soil strength. Research indicates that for sand-size soil grains, the effect of grain shape and roughness on the CBR is quite small compared to that of the coarser soil grains. Furthermore, it is well known that even small variations in compactive effort and molding moisture content will also have a marked influence on soil strength as indicated by the CBR.

STATE OF ALABAMA
HIGHWAY DEPARTMENT
MONTGOMERY

Form CBR-1

INFORMATION TO ACCOMPANY SAMPLE FOR TESTING — LAB NO. 414

Project F-352(13) Division 7 County Montgomery — Date 11-22-63

Materials Sub-Subgrade Marks — Density 116.9 Lbs. Cu. Ft.

Producer Left. R. W. — Optinium Moist 12.5 %

Source Sta. 837+00 — Run By: Athey

Quantity Represented — Compressed at 2000 PSI

Remarks: BPR Check CBR

Sampled By: Tatom & B. Wilkes Date 11-7-63

Submitted By: Kilpatrick Address

Title S. A. Cut

BEARING VALUES

UNSOAKED					SOAKED				
Penetration Inch	Total Load Pounds	Pounds Per Sq. Inch	Standard	% Standard	Penetration Inch	Total Load Pounds	Pounds Per Sq. Inch	Standard	% Standard
0.1			1000		0.1	180	60	1000	6.0
0.2			1500		0.2	230	77	1500	5.1
0.3			1900		0.3	260	87	1900	4.6
0.4			2300		0.4	260	87	2300	3.8
0.5			2600		0.5	280	93	2600	3.6

SWELL DATA

Height in Mold		Inches	
Initial Reading		.100	
Reading After 1 Day		.	
Reading After 2 Days		.	
Reading After 3 Days		.	
Reading After 4 Days		.564	
Total Swell .464	Inches	9.28	%

Moisture-Top 1 Inch	33.7	%
Moisture Bottom 1 Inch	19.0	%
Moisture Average	26.4	%

ANALYSIS

Passing ¾ Screen	100.0	%
Passing # 4 Screen	1000	%
Passing # 10 Screen	100.0	%
Material Passing 10 M Sieve		
Clay	70.4	%
Silt	17.7	%
Total Sand	11.9	%
Pass 40 M	98.0	%
Pass 60 M	96.0	%
Pass 200 M	88.1	%
Field Moisture	37.1	%
Liquid Limit	56.9	%
Plastic Limit	23.0	%
Plasticity Index	33.9	%
Shrinkage Limit	18.9	%
Volume Change	31.9	%
Lineal Shrinkage	8.82	%
Shrinkage Ratio	1.75	%
	A-7	
	A-7-6(19)	

REMARKS: 10# Surcharge Used
Design CBR - 5.1
Std. P. D.
Max. Density - 99.6
Optimum Moisture - 21.6

Testing Engineer

Figure 3. Typical soils laboratory report.

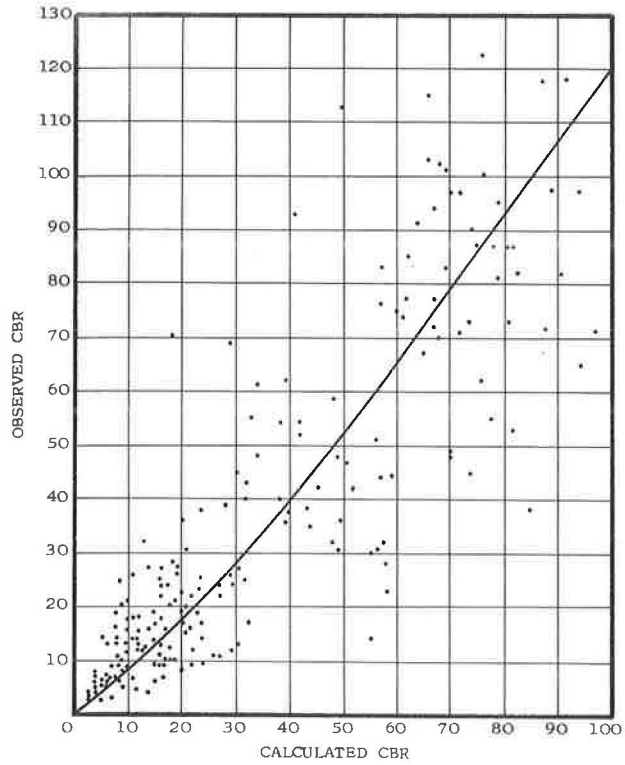

Figure 4. Regression curve showing relationship between observed and calculated CBR.

Experience has shown that replicate CBR tests, based on the 2000-psi static-compaction method, made under carefully controlled conditions have resulted in an average coefficient of variation of about 16 percent. This observation is illustrated by the data in Table 1 which resulted from a series of carefully controlled replicate CBR tests on twelve different materials, accounting for a total of 56 CBR tests. The soils for these tests were selected so that the CBR values would range from very low to very high. In the right hand column of Table 1, notice that the coefficient of variation ranged from a low of 7.1 percent to a high of 31.3 percent, with an average of 16.0 percent, which indicates a rather high degree of variability.

TABLE 1

RESULTS OF A REPLICATE CBR TESTING PROGRAM

Material	Number of Sample	Range of CBR Values	Average CBR	Standard Deviation	Coefficient of Variation (%)
1	5	4.67 to 8.00	6.44	1.29	20.0
2	4	1.20 to 2.00	1.63	0.26	15.9
3	7	4.16 to 5.00	4.66	0.40	8.6
4	5	46.60 to 70.00	57.82	8.50	14.7
5	5	72.80 to 112.00	93.14	12.73	13.7
6	5	50.00 to 100.00	70.00	17.89	25.6
7	5	79.33 to 183.33	115.20	36.05	31.3
8	4	66.50 to 80.00	74.45	5.29	7.1
9	4	80.90 to 107.90	87.70	11.64	13.3
10	4	62.50 to 90.00	77.50	9.85	12.7
11	4	81.00 to 102.50	87.50	8.72	10.0
12	4	72.50 to 113.50	93.63	16.68	17.8

NOTE: Average coefficient of variation = 16.0 percent.

It will be recalled that, on a statistical basis, Eq. 4 explained about 77 percent of the variation in log CBR. By comparing this with the difficulty of obtaining a reliable CBR value from a single test, it would seem that a CBR value obtained on a statistical basis, such as that resulting from Eq. 4 and shown in Figure 2, should provide a reasonably satisfactory estimate for a given soil under ordinary circumstances.

CONCLUSION

If the strength of a soil can be estimated satisfactorily from its physical characteristics by an approach similar to that suggested, it should provide a means for crossing state lines with soil-strength data. In other words, if this approach should prove to be feasible, soil-strength data from any given state or agency could be readily converted into comparable data from any other state or agency. Although this paper only illustrates a method for estimating the CBR resulting from the Alabama 2000-psi compaction method, it is believed that some function of grain size distribution, percent clay, and Atterberg limits could provide the means for estimating the CBR for any one of the many variant static and dynamic compaction methods now in use. Furthermore, such an approach might possibly be used for estimating soil strength obtained from the triaxial, stabilometer, or other test forms.

Strength Behavior of an Anisotropically Consolidated Remolded Clay

RAJ P. KHERA, Newark College of Engineering, New Jersey, and
RAYMOND J. KRIZEK, Northwestern University

If a soil specimen is consolidated under any conditions other than those to which it has been previously subjected, its structure will be altered and a change in its strength characteristics will result. This investigation is concerned with the effect of the secondary inherent strength anisotropy caused by variation of the consolidation stress path and the principal consolidation stress ratio on the strength response of a homogeneous clay remolded to possess a given primary inherent anisotropy.

The following conclusions are drawn. Strength characteristics are influenced by the initial soil structure before anisotropic consolidation, or primary inherent strength anisotropy, as well as the structural rearrangement of particles due to anisotropic consolidation, or secondary inherent strength anisotropy. The stress path followed to obtain a given principal consolidation stress ratio influences the soil response. Pore-pressure values during a strength test decrease with increasing values of the principal consolidation stress ratio. With one exception, the respective failure strains for both the maximum $(\sigma_1' - \sigma_3')$ and the maximum σ_1'/σ_3' failure criteria were approximately equal. Water content for a given octahedral normal consolidation stress decreases with increasing values of the principal consolidation stress difference.

•IN nature, most soils are anisotropic due to the mode of deposition or as a result of subsequent changes caused by various stresses acting on them. Also, compacted embankments may exhibit marked anisotropic behavioral characteristics. Safety factors calculated in the design of earth slopes and determination of bearing capacity values are influenced by strength anisotropy. Therefore, a further understanding of the behavior of anisotropic soils is required.

Whatever the initial structure, such as flocculated or dispersed, of a sedimented clay deposit, subsequent one-dimensional consolidation causes a preferred arrangement of flat or elongated particles with their long axes perpendicular to the direction of the principal consolidation stress. The resulting anisotropy may be termed primary inherent strength anisotropy. When a so-called undisturbed specimen of such soil is tested by means of a standard consolidated, undrained triaxial testing procedure, it is subjected to a laboratory consolidation stress which is generally different from that in the field; most often this is a hydrostatic consolidation stress. In recent work, this consolidation has been accomplished under a principal stress difference.

If this latter consolidation procedure is performed under any conditions other than those which existed in the field or in one-dimensional consolidation, the soil structure will be altered, and this will, in turn, affect its stress-strain and strength responses; such anisotropy may be called secondary inherent strength anisotropy. In addition, the

Paper sponsored by Committee on Soil and Rock Properties and presented at the 46th Annual Meeting.

application of a shear stress during the strength test will cause additional anisotropy, which may be referred to as induced strength anisotropy.

The purpose of this study is to contribute to current knowledge regarding the effect of secondary inherent anisotropy on strength response of cohesive soils. The experimental program is designed to investigate the effect of consolidation stress path and principal consolidation stress ratio on the strength characteristics of a homogeneous clay remolded to possess a given primary inherent anisotropy.

SOIL TESTED

The soil used in this study was primarily an illite clay known by the trade name Grundite. It was mined in the Goose Lake area of Grundy County, Illinois, and marketed by the Illinois Clay Products Company. The clay was upper Pennsylvania in age and was somewhat weathered and desiccated due to erosion of the overlying sediments. Grim and Bradley (1) have discussed its origin and properties, and other engineering characteristics are given in Table 1.

SAMPLE PREPARATION

The test specimens were prepared from a dry, powdered form by mixing with a predetermined amount of distilled, de-aired water to yield a final water content of approximately 42 percent. The additional water was added in small amounts and mixed by hand to obtain a fairly homogeneous moisture distribution. The clay-water mixture was then passed through a "Vac-Aire" sample extruder similar to that used by Schmertmann and Osterberg (2) and described in detail by Matlock, Fenske and Dawson (3).

The soil was passed through the extruder three times and in this process the moisture content decreased about one percent. During the last extrusion, as the clay passed through the 3.56 cm diameter die, specimens about 10 cm long were cut with a wire saw. These were immediately covered with several coats of a flexible wax composed of a mixture of half paraffin and half petrolatum and were stored in a humid room until they were ready to be tested. From their study on Grundite, Perloff and Osterberg (4) found no evidence of thixotropic hardening during a 6-week storage period, and their finding was verified in this experimental program.

Although the extruded samples are homogeneous in moisture content, the screw action of the auger causes the clay platelets to become oriented in a definite pattern. Because the molding moisture content is high, the shear stresses acting tangentially on the soil mass as it travels through the extruder cause the clay particles to align themselves parallel to the axis of the sample. Therefore, a structure similar to that of a dispersed soil is developed, except that the clay platelets are aligned vertically in a direction parallel to the axis of the specimen instead of horizontally or perpendicular to the direction of the specimen axis, as would normally be the case for a tube sample or a compacted sample molded wet of optimum. Also, the soil structure exhibits a radial symmetry about the central axis of the specimen; this is evidenced by spiral crack patterns observed upon desiccation. Since these extruded specimens have a preferred particle orientation parallel to the specimen axis, there is a similarity between such test specimens and those trimmed from a conventional dispersed soil mass in such a manner that particles are aligned parallel to the central axis of the specimen.

TABLE 1

SOIL PROPERTIES

Liquid Limit (%)	Plastic Limit (%)	Plasticity Index (%)	Specific Gravity	Particles Less Than 2μ (%)
54.5	26.0	28.5	2.74	85

SCOPE OF TEST PROGRAM

Two series of tests on extruded specimens, designated as the S and M series, were conducted in this experimental program. The letters refer to the strain rates at which the strength tests were performed. In the S (slow) series, a constant deformation rate of 1 centimeter per 372 min was used. The principal consolidation stress ratios for an octahedral normal consolidation stress of 1.00 kg/cm^2 were 1.00, 1.25, 1.50, 1.75 and 2.00, whereas they were 1.00 and 2.00 for an octahedral normal stress of 2.00 kg/cm^2. For the M (medium) series, the deformation rate was 1 centimeter per 37.2 min, and an octahedral normal stress of 1.00 kg/cm^2 with principal consolidation stress ratios of 1.00, 1.50, and 2.00 was used. In all of the cases mentioned, the octahedral normal consolidation stress was applied in increments while maintaining the principal stress ratio constant. In addition, for principal consolidation stress ratios of 1.25, 1.50, and 1.75 at an octahedral normal stress of 1.00 kg/cm^2, specimens in the M series were first consolidated isotropically and then subjected to additional axial load to obtain the specified principal consolidation stress ratios.

For convenience, the tests are described by a legend consisting of a letter designating the series, as described previously, both preceded and followed by a number. The number preceding the letter indicates the ratio of principal consolidation stresses (1 corresponds to 1.00; 2 to 1.25; 3 to 1.50, etc.). The number following the letter designates the value of the octahedral normal consolidation stress (1 corresponds to 1.00 kg/cm^2 and 2 corresponds to 2.00 kg/cm^2).

EXPERIMENTAL PROCEDURE

When ready to be tested, the wax-covered samples were taken from the humid room and immersed in lukewarm water for about 2 min; after the wax covering became soft and pliable, it was easily removed. Then, the specimen was placed in a cradle and its ends were trimmed with a thin wire saw. Immediately after this operation, the test specimen and its ends were weighed separately. The water content of the ends was computed subsequently to provide a check on the initial water content of the specimen. Initial data on test specimen dimensions, weights and water contents, together with variations, are given in Table 2.

To eliminate the possibility of entrapping air during the process of mounting the specimen, the bottom of the triaxial cell was immersed in distilled de-aired water. The test specimen was placed on the stainless steel base which had been lubricated with a thin layer of silicone grease and covered with a circular piece of latex rubber membrane. A filter paper drain was wrapped around the specimen and covered the radial drainage holes in the bottom plate. The specimen was then covered with a latex membrane. Approximately 20 sec were required for this underwater mounting procedure.

The entire assembly was subsequently removed from the water, and the membrane surface was dried and coated with Dow-Corning 200 silicone fluid. A second membrane was then placed around the first, and the top and bottom of both membranes were sealed to the cap and pedestal, respectively, by silicone grease and three rubber O-rings on each end. The drainage line at the bottom of the specimen was connected to a precision-bore glass tubing calibrated in centimeters.

The triaxial chamber was filled with distilled de-aired water, and chamber pressure was applied by placing weights on a precalibrated constant pressure cell. A constant

TABLE 2

INITIAL DATA FOR TEST SPECIMENS

Height (cm)	Diameter (cm)	Weight (gm)	Water Content (%)	Void Radio
8.01 ± .01	3.56	144.4 ± .1	41.7 ± .3	1.152 ± 0.008

back pressure of 2.0 kg/cm^2 was applied by compressed air to ensure complete saturation during consolidation.

Isotropic consolidation was achieved either by applying the total load in one increment and permitting consolidation for 24 hours (usually the complete volume change took place in the first 12 hours) or by applying the load in increments of 0.25 kg/cm^2. Depending on the value of the final consolidation stress, the latter procedure took from 4 to 7 days for consolidation.

Anisotropic consolidation was also accomplished by two different techniques. In the first method, radial stresses and axial stresses were applied simultaneously in octahedral normal stress increments of 0.25 kg/cm^2 while maintaining constant the principal consolidation stress ratio; complete consolidation was permitted before adding the next increment. The time required for completion of primary consolidation was about 6 hours, but load increments were applied only every 12 hours. Following application of the final load increment, the specimen was allowed to consolidate for 24 hours before being tested. The second technique consisted of consolidating the specimens first under a single increment of isotropic chamber pressure and then increasing the axial load in a single increment to achieve the desired ratio of principal consolidation stresses. Two days were required to complete consolidation.

On completion of consolidation, the lever system used for anisotropic consolidation was clamped in position, and the load hanger was removed; the triaxial specimen with the load hanger was then placed in a loading press. The valve between the pore pressure gage and the specimen was opened, and the one between the specimen and the pipette was closed. A constant rate of deformation was then applied to the specimen; axial deformation was measured with a dial gage, and a steel proving ring provided load measurements. Pore pressures were measured with a Bourdon gage connected to the null gage. Radial deflections were measured by micrometers mounted in the wall of the pressure chamber. These measurements provided an excellent check on volume changes and a comparison of axial and radial strains during consolidation. A more detailed description of this technique, together with a study of end platens, is given by Khera and Krizek (5).

EXPERIMENTAL RESULTS AND INTERPRETATION

Data associated with the anisotropic consolidation phase of the experimental program are given in Table 3. Tables 4 and 5 contain data and calculated parameters associated with two different failure criteria.

TABLE 3

EXPERIMENTAL DATA ON CONSOLIDATION RESPONSE

Sample Number	Water Content		Void Ratio		Dimension Changes		Consolidation Stresses	
	Initial	Final	Initial	Final	Height (cm)	Diameter (cm)	σ'_{1c}	σ'_{3c}
1-S-1	42.30	38.10	1.155	1.039	-0.139	-0.069	1.00	1.00
2-S-1	42.14	37.24	1.156	1.022	-0.235	-0.061	1.14	0.92
3-S-1	42.17	36.61	1.155	1.003	-0.350	-0.045	1.29	0.86
4-S-1	42.08	37.63	1.152	1.030	-0.416	-0.019	1.39	0.79
5-S-1	41.52	36.84	1.147	1.018	-0.642	-0.003	1.48	0.74
1-S-2	41.79	34.12	1.149	0.939	-0.290	-0.116	2.00	2.00
5-S-2	42.10	32.43	1.151	0.886	-1.020	+0.008	2.99	1.50
1-M-1	42.03	37.86	1.153	1.039	-0.143	-0.064	1.00	1.00
2-M-1a	41.93	37.06	1.152	1.018	-0.270	-0.056	1.15	0.92
3-M-1	42.08	37.29	1.154	1.022	-0.330	-0.043	1.29	0.86
3-M-1a	42.13	38.26	1.157	1.051	-0.378	-0.018	1.28	0.86
4-M-1a	41.96	37.00	1.152	1.016	-0.447	-0.014	1.40	0.80
5-M-1	41.98	36.69	1.150	0.978	-0.630	-0.003	1.51	0.75

TABLE 4

EXPERIMENTAL DATA FOR $[\sigma_1' - \sigma_3']_{max}$ FAILURE CRITERION

Sample Number	Failure Strain	$\frac{\sigma_1' - \sigma_3'}{2}$ (kg/cm²)	$\frac{\sigma_1' - \sigma_3'}{2\sigma_{1c}'}$	$\frac{\sigma_{1c}'}{\sigma_{3c}'}$	u (kg/cm²)	A
1-S-1	0.080	0.326	0.323	1.010	0.500	0.770
2-S-1	0.085	0.404	0.354	1.240	0.415	0.705
3-S-1	0.090	0.422	0.329	1.498	0.345	0.825
4-S-1	0.100	0.450	0.327	1.753	0.280	0.906
5-S-1	0.055	0.490	0.330	2.001	0.145	0.620
1-S-2	0.125	0.723	0.361	1.000	1.010	0.700
5-S-2	0.035	0.872	0.292	1.990	0.190	0.740
1-M-1	0.095	0.398	0.398	1.000	0.340	0.427
2-M-1a	0.105	0.433	0.378	1.246	0.320	0.495
3-M-1	0.090	0.460	0.339	1.497	0.220	0.445
3-M-1a	0.080	0.440	0.345	1.492	0.225	0.551
4-M-1a	0.080	0.485	0.347	1.749	0.145	0.386
5-M-1	0.050	0.527	0.351	2.007	0.030	0.100

The relation between the principal consolidation stress ratio $\sigma_{1c}'/\sigma_{3c}'$ (σ_{1c}' and σ_{3c}' are the major and minor principal consolidation stresses) and the water content w is shown in Figure 1. In the direction of increasing values of $\sigma_{1c}'/\sigma_{3c}'$ for an octahedral normal stress of 1.00 kg/cm², the data for both series indicate a decreasing trend in water content with increasing values of $\sigma_{1c}'/\sigma_{3c}'$. A similar trend is observed for the limited data with an octahedral normal consolidation stress of 2.00 kg/cm². These results indicate that water content is not a function of octahedral normal stress alone, but is also dependent on the ratio of principal consolidation stresses. This behavior is contrary to that reported by Whitman, Ladd and da Cruz (6) and Henkel and Sowa (7) who found water content to be only a function of average consolidation stress. Because volume decreases during shear for normally consolidated clays (8), such behavior should be expected when consolidation is accomplished under a principal stress difference.

Data for the radial and axial deformations during consolidation are given in Table 3 and plotted in Figure 2. Specimens with the subscript a were first consolidated under hydrostatic stress followed by application of axial load in a single increment to obtain the desired value of $\sigma_{1c}'/\sigma_{3c}'$. Figure 2 shows that such specimens exhibit a smaller

TABLE 5

EXPERIMENTAL DATA FOR $[\sigma_1'/\sigma_3']_{max}$ FAILURE CRITERION

Sample Number	Failure Strain	$\frac{\sigma_1' - \sigma_3'}{2}$ (kg/cm²)	$\frac{\sigma_1' - \sigma_3'}{2\sigma_{1c}'}$	$\frac{\sigma_{1c}'}{\sigma_{3c}'}$	u (kg/cm²)	A
1-S-1	0.080	0.326	0.323	1.010	0.500	0.770
2-S-1	0.085	0.404	0.354	1.240	0.415	0.705
3-S-1	0.108	0.420	0.328	1.498	0.350	0.416
4-S-1	0.100	0.450	0.327	1.753	0.280	0.906
5-S-1	0.060	0.488	0.329	2.001	0.153	0.660
1-S-2	0.125	0.723	0.361	1.000	1.010	0.700
5-S-2	0.065	0.857	0.287	1.990	0.265	1.160
1-M-1	0.095	0.398	0.398	1.000	0.340	0.427
2-M-1a	0.110	0.434	0.338	1.246	0.325	0.372
3-M-1	0.090	0.460	0.359	1.497	0.220	0.445
3-M-1a	0.107	0.434	0.338	1.492	0.280	0.323
4-M-1a	0.100	0.482	0.345	1.749	0.160	0.166
5-M-1	0.050	0.527	0.351	2.007	0.030	0.100

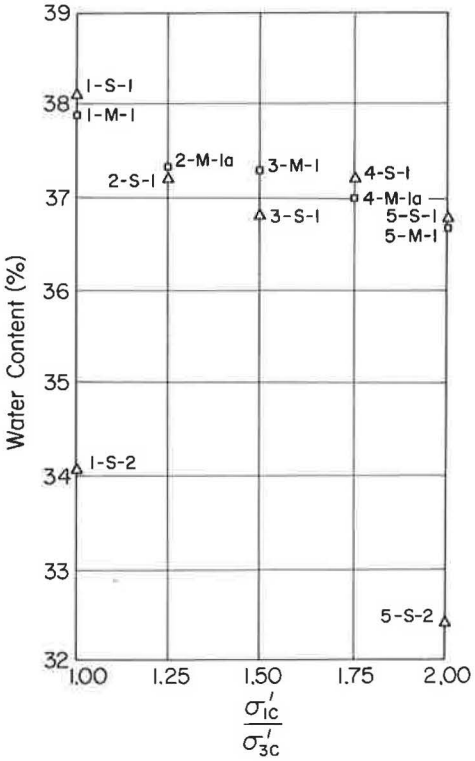

Figure 1. Water content vs principal consolidation stress ratio.

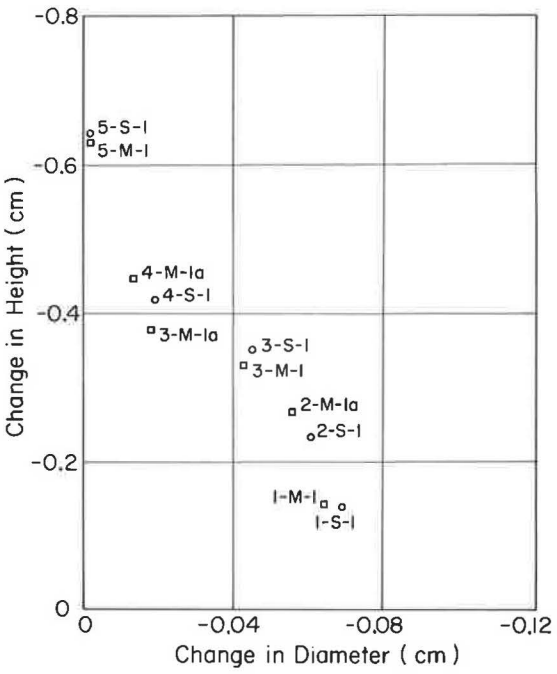

Figure 2. Change in height vs change in diameter.

decrease in diameter at the end of consolidation (both isotropic and anisotropic) than specimens where axial and lateral consolidating loads were applied simultaneously in small increments; the reverse is true for height measurements. After isotropic consolidation, the application of a principal stress difference in a single increment caused high pore pressures to develop. Thus, the effective stresses in the specimen were reduced considerably, and its shear resistance decreased. This resulted in a greater axial deformation and a lesser decrease in diameter, as can be seen in Figure 2 by comparing the response of specimens 4-M-1a and 4-S-1, specimens 3-M-1a, 3-S-1 and 3-M-1, and specimens 2-M-1a and 2-S-1.

Pore-pressure values (Figs. 3 and 4) decrease as $\sigma_{1c}'/\sigma_{3c}'$ values increase. The largest pore pressures are observed in isotropically consolidated specimens, whereas the smallest values are associated with a principal consolidation stress ratio of 2.00 (the largest value used in this investigation). Also, the values of pore pressure developed in the S series are higher than those in the M series for corresponding values of consolidation stresses. Because the strain rate for the M series was ten times greater than that for the S series, the time for the development of pore pressure was not adequate in the former case.

Note that the pore-pressure curve for test 3-M-1a lies above that for test 3-M-1, although the final values of consolidation stresses were the same for both specimens. However, specimen 3-M-1a was first consolidated under isotropic conditions and then axial load was applied to achieve the desired degree of consolidating stress anisotropy, whereas specimen 3-M-1 was consolidated under small load increments while maintaining a constant value of $\sigma_{1c}'/\sigma_{3c}'$ for each increment. In the case of test 3-M-1a, the specimen probably acquired a structure similar to that for the isotropic case, and this structure could not be altered significantly by the subsequent application of an axial consolidation stress. Due to the incremental load procedure employed on specimen 3-M-1, the soil structure probably changed to a greater degree. The higher pore-

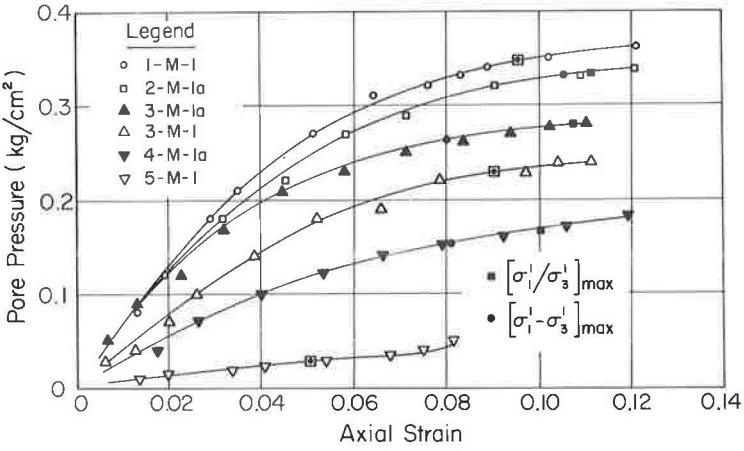

Figure 3. M series: Pore pressure vs axial strain.

pressure values developed in specimen 3-M-1a indicate that it had a particle orientation somewhere between that of specimens 3-M-1 and 1-M-1. Therefore, in studying the effects of anisotropic consolidation, it is important that the consolidation stress be applied in small increments while maintaining $\sigma_{1c}'/\sigma_{3c}'$ constant for each load addition. For example, Lowe and Karafiath (9) presented test results from specimens consolidated isotropically followed by the application of axial-load increments to obtain the desired consolidation stress anisotropy. The work reported herein indicates that a different response would probably have been observed if their specimens were consolidated in increments while keeping the principal stress ratio constant.

For tests on specimens consolidated under zero lateral strain, Simons (10) observed that the failure strain associated with the maximum σ_1'/σ_3' failure criterion was many times greater than that for the maximum $(\sigma_1' - \sigma_3')$ failure criterion; such strains in the former case ranged from 5.4 to 8.4 percent, whereas for the latter case they ranged from 0.4 to 0.9 percent. In this experimental test program, specimens 5-S-1, 5-S-2, and 5-M-1 may be approximately categorized as consolidated under zero lateral strain, since diameter changes were very small (-0.003 to +0.008 cm), as can be seen in Table 3. However, the behavior noted here was different than that reported by

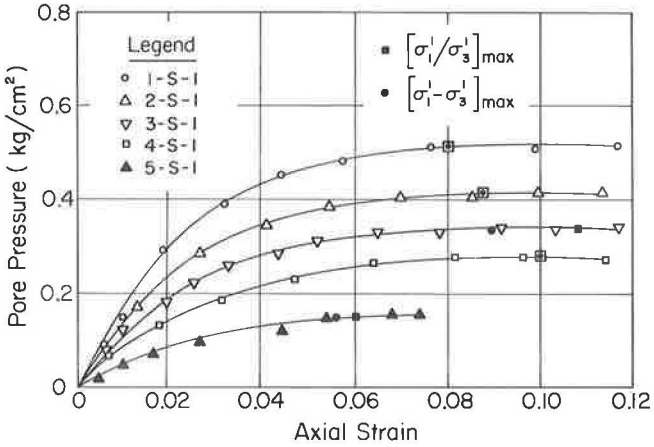

Figure 4. S series: Pore pressure vs axial strain.

Simons (10). For specimen 5-S-1, which is associated with an octahedral consolidation stress of 1.0 kg/cm^2 and a principal consolidation stress ratio of 2.00, the failure strains associated with the maximum ($\sigma_1' - \sigma_3'$) and the maximum σ_1'/σ_3' failure criteria are 5.5 and 6.0 percent, respectively, whereas for specimen 5-S-2 at an octahedral consolidation stress of 2.0 kg/cm^2 and a principal consolidation stress ratio of 2.00, the failure strain for the maximum σ_1'/σ_3' failure criterion is only about twice that for the maximum ($\sigma_1' - \sigma_3'$) failure criterion, or 6.5 vs 3.5 percent, respectively. In addition to the stated variation in magnitude between the failure strain relationship for different failure criteria, this work indicates that the octahedral consolidation stress influences not only the value of failure strain, but also the relationship between the respective failure strains using different failure criteria.

Comparison of specimens 5-S-1 and 5-M-1 indicates that the faster deformation rate tends to lower the failure strain slightly (about 0.5 to 1.0 percent) from that associated with the slower deformation rate; however, failure strains for both failure criteria are essentially equal, and this strain-rate variation is quite small. The observed strain-rate variations are too limited and too small to justify any statement.

The test data of Simons (10) and Ladd (11) indicate that pore pressures continue to increase after maximum ($\sigma_1' - \sigma_3'$) has occurred, but such was not the case in this study, except for specimen 5-S-2. However, even though pore pressures did increase in specimen 5-S-2, the magnitude of the increase was less than previously observed. Because consolidation stress history is known to affect pore-pressure response, triaxial consolidation tests were conducted to determine the preconsolidation stress of these specimens. This stress was found to be 0.6 kg/cm^2, and all specimens were consolidated to a stress greater than 0.6 kg/cm^2 to ensure normal consolidation. For example, the minimum value for any of the principal consolidation stresses was 0.74 kg/cm^2.

The curves in Figures 5 and 6 show the experimental stress-strain data for specimens consolidated under an octahedral stress of 1.0 kg/cm^2. Stress-strain curves obtained by Simons (10) and Ladd (11) for K_0 and isotropic consolidation are shown in Figure 7. For the K_0 consolidated specimens, there is not much similarity between

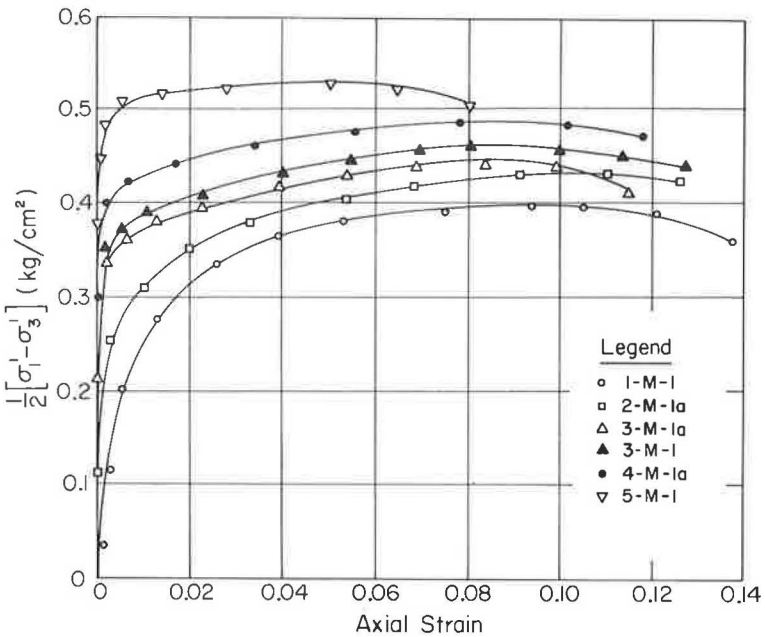

Figure 5. M series: Shear stress vs axial strain.

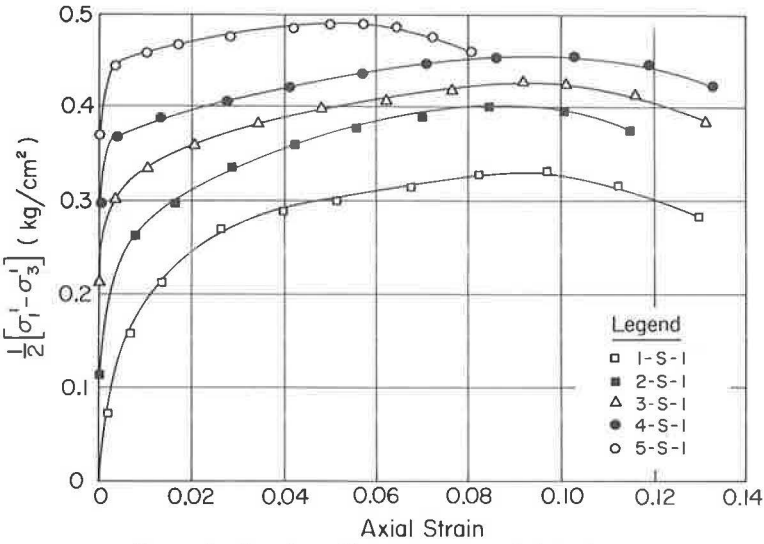

Figure 6. S series: Shear stress vs axial strain.

the stress-strain curves shown in Figure 7 and those obtained in this investigation and shown in Figures 5 and 6. Since their investigations were conducted on either undisturbed specimens, which were consolidated in nature under a principal stress difference, or remolded specimens, which were consolidated one-dimensionally, the clay particles probably had a preferred orientation perpendicular to the direction of the consolidation stress. Therefore, before commencement of anisotropic consolidation, the arrangement of clay platelets for the specimens in their studies was probably significantly different from that in this study. Hence, for these respective studies, the difference in the stress-strain behavior due to anisotropic consolidation possibly may be explained on the basis of this difference in initial particle arrangement. In each case, a rearrangement of the clay particles takes place as a result of applying the principal consolidation stress difference. Thus, the strength response is a function of both the

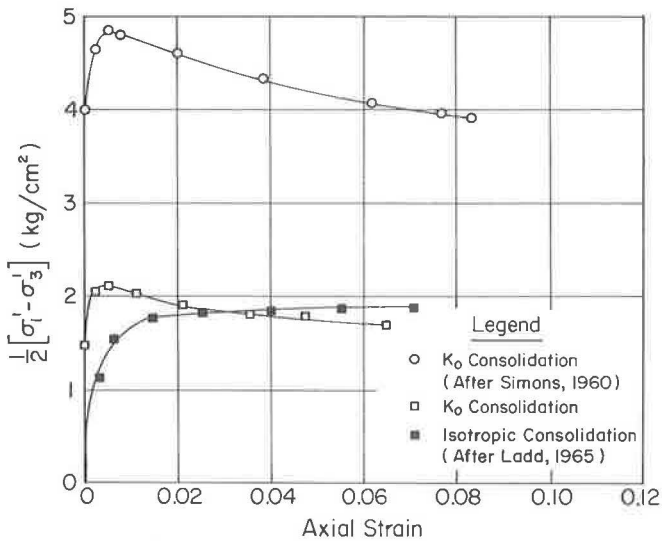

Figure 7. Shear stress vs axial strain: comparison values.

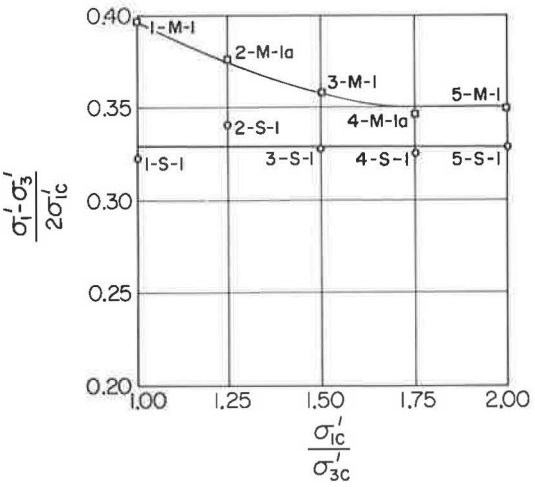

Figure 8. Strength parameter vs principal consolidation stress ratio.

initial soil structure before anisotropic consolidation, or primary inherent strength anisotropy, and the rearrangement in structure due to anisotropic consolidation, or secondary inherent strength anisotropy. An additional induced strength anisotropy occurs when the specimen is subjected to a strength test, such as the constant rate, undrained triaxial test used in this program.

Values of $(\sigma_1' - \sigma_3')/2\sigma_{1c}'$ are shown in Figure 8 for various values of $\sigma_{1c}'/\sigma_{3c}'$. It can be seen that $(\sigma_1' - \sigma_3')/2\sigma_{1c}'$ remains constant for the complete range of $\sigma_{1c}'/\sigma_{3c}'$ values in the S series, whereas for the M series it decreases with increasing values of $\sigma_{1c}'/\sigma_{3c}'$. Ladd (11) found a slight decrease in the values of $(\sigma_1' - \sigma_3')/2\sigma_{1c}'$ for the case of K_o consolidation, but made no study of rate effects. In the present study, it is seen that $(\sigma_1' - \sigma_3')/2\sigma_{1c}'$ is also affected by the strain rate during shear.

CONCLUSIONS

1. Water content for a given octahedral normal consolidation stress decreases with increasing values of the principal consolidation stress difference.
2. Pore-pressure values during a strength test decrease with increasing values of the principal consolidation stress ratio.
3. The stress path followed to obtain a given principal consolidation stress ratio influences the soil response.
4. With one exception, the respective failure strains for both the maximum $(\sigma_1' - \sigma_3')$ and the maximum σ_1'/σ_3' failure criteria were approximately equal.
5. Strength characteristics are influenced by the initial soil structure before anisotropic consolidation, or primary inherent strength anisotropy, as well as the structural rearrangement of particles due to anisotropic consolidation, or secondary inherent strength anisotropy.

REFERENCES

1. Grim, R. E., and Bradley, R. F. A Unique Clay from the Goose Lake, Illinois, Area. Jour. Amer. Ceramic Soc., Vol. 22, No. 5, pp. 157-164, May 1939.
2. Schmertmann, J. H., and Osterberg, J. O. An Experimental Study of the Development of Cohesion and Friction with Axial Strain in Saturated Cohesive Soil. Proc. of the Res. Conf. on Shear Strength of Cohesive Soils, ASCE, Colorado, pp. 643-694, 1960.
3. Matlock, H., Jr., Fenske, C. W., and Dawson, R. F. De-aired Extruded Soil Specimens for Research and for Evaluation of Test Procedures. ASTM Bull. 177, pp. 51-55, 1951.
4. Perloff, W. H., Jr., and Osterberg, J. O. Effect of Stress History on Strength of Cohesive Soils. Highway Research Record 48, pp. 49-71, 1964.
5. Khera, R. P., and Krizek, R. J. Measurement and Control of Radial Deformation in the Triaxial Test. Tech. Rept., Northwestern Univ., 1966.
6. Whitman, R. V., Ladd, C. C., and da Cruz, P. Discussion. Proc. of the Res. Conf. on Shear Strength of Cohesive Soils, ASCE, Colorado, pp. 1049-1056, 1960.
7. Henkel, D. J., and Sowa, V. A. The Influence of Stress Paths in Undrained Triaxial Tests on Clay. ASTM Spec. Tech. Publ. No. 361, pp. 280-291, 1963.

8. Casagrande, A., and Albert, S. G. Research on the Shear Resistance of Soils. Rept., MIT, Cambridge, 1932.
9. Lowe, J., III, and Karafiath, L. Effect of Anisotropic Consolidation on the Undrained Shear Strength of Compacted Clays. Proc. of the Res. Conf. on Shear Strength of Cohesive Soils, ASCE, Colorado, pp. 837-858, 1960.
10. Simons, N. E. The Effect of Overconsolidation on the Shear Strength Characteristics of an Undisturbed Oslo Clay. Proc. of the Res. Conf. on Shear Strength of Cohesive Soils, ASCE, Colorado, pp. 747-764, 1960.
11. Ladd, C. C. Stress-Strain Behavior of Anisotropically Consolidated Clays During Undrained Shear. Proc. Sixth Internat. Conf. on Soil Mech. and Found. Eng., Montreal, Canada, Vol. 1, pp. 282-286, 1965.

Factors Influencing the Resilient Deformations of Untreated Aggregate Base in Two-Layer Pavements Subjected to Repeated Loading

H. B. SEED, F. G. MITRY, C. L. MONISMITH, and C. K. CHAN
Respectively, Professor of Civil Engineering; Formerly Graduate Research Assistant; Professor of Civil Engineering; and Associate Research Engineer, Institute of Transportation and Traffic Engineering, University of California, Berkeley

•IN RECENT years, a large body of knowledge has developed relating the cracking of asphalt-concrete pavements to the transient deflections of the pavements measured under specific axle loads (1, 2). Cracking of this type has been attributed to fatigue failures of the asphalt-concrete surfacing (1, 3) resulting from repeated stresses or strains induced by traffic loads over a period of time. Although it is recognized that the induced stresses and strains in the asphalt surfacing are associated with the curvature of the deflected pavement surface, it is to be expected that they will increase in a general way with the magnitude of pavement deflections. Thus, prediction of deflections from representative tests on paving materials in advance of construction would be a valuable first step in solving the problem of preventing load-associated pavement cracking. Recently, the California Division of Highways instituted such a procedure on a trial basis for special conditions (4).

From available data, it would appear that fatigue distress results from instantaneous and recoverable deflections in the pavement components and is not necessarily associated with any plastic or permanent deformations. Thus, it might be reasonably concluded that the deflections which produce this form of distress could be calculated, at least approximately, from an appropriate elastic theory for layered systems.

To use such a theory, however, requires appropriate values for the material properties of the paving materials (e.g., elastic modulus and Poisson's ratio). Although Poisson's ratio for most paving materials appears to lie in a comparatively narrow range (0.3 to 0.5) for the conditions of stress encountered in the pavement, the same cannot be said of the elastic moduli, or more appropriately the deformation moduli, of the constituents of the pavement. This would appear to be particularly true for untreated-aggregate-base materials.

At the 1962 International Conference on the Structural Design of Asphalt Pavements it was noted (5):

> On the basis of the results reported at this Conference there would seem to be a great need for increased emphasis on the study of base-course materials. The base-course characteristics may play a large part in determining both transient pavement deflections and curvature, yet apart from the new device, the resiliometer, there are no laboratory testing techniques available to evaluate base-course characteristics in this regard. The large scatter of values for base-course moduli reported by different authors is somewhat disturbing and the development of new procedures for evaluating the transient deformation characteristics of base-course materials, together with a systematic study of different materials and conditions, would be highly desirable.

Paper sponsored by Committee on Strength and Deformation Characteristics of Pavement Sections and presented at the 46th Annual Meeting.

In recent years, a number of laboratory test procedures have been developed and used to measure the behavior of pavement materials under conditions of load similar to those created by moving traffic. These methods include repeated-load triaxial-compression tests for fine-grained soils and various dynamic tests to measure the stiffness of asphalt concrete. It appears that developments in this area are sufficiently advanced so that the repeated-load triaxial-compression test can be applied to study the behavior of aggregate bases. When used in conjunction with similar tests on subgrade soils and some form of stiffness measurement of asphalt concrete, it is possible that the results can be used to develop, within the framework of suitable theory, a measure of the response of the pavement to moving traffic.

Thus, the objectives of this research are to study and evaluate those characteristics of untreated base-course aggregates which determine the deflections of asphalt-concrete pavements under moving wheel loads, and from these evaluations to predict the transient deflections of prototype pavements for various load conditions.

Data are presented showing the results of laboratory repeated-load triaxial-compression tests on a variety of granular materials including a well-graded gravel, a uniform sand and disturbed, recompacted samples of untreated-base and subbase materials from in-service pavements. In addition, the deflections observed in repeated-load plate tests on prototype pavements, consisting of two-layer systems of the untreated gravel and a compressible, fine-grained subgrade, are presented together with the results of analytical procedures for predicting the deflections from the results of laboratory tests.

Even though it is recognized that conventional asphalt-type pavements consist of at least three layers, it would appear that definitive information on the role of the untreated aggregate in the pavement system can best be studied in as simple a structure as possible (in this instance, two layers) where the results will not be complicated by the presence of overlying layers.

The ultimate objective of such research is to provide an additional method of design to the paving engineer so that he can attempt to minimize, for the design life of the structure, the form of distress resulting from fatigue failure of the asphalt surfacing. Hopefully, the studies on granular base reported here will add to the knowledge required for the development of such a design procedure.

BACKGROUND

To provide a basis for the data, a brief summary of the existing information on laboratory-determined resilience characteristics of untreated aggregates in repeated-load triaxial-compression tests is included. In addition, a brief summary of a more detailed review (6) of the results of plate-load tests and their interpretation within the framework of elastic theory is also presented. The deformations under consideration are elastic in the sense that they are recoverable; however, they are not necessarily proportional to stress or instantaneous. Thus, in keeping with the terminology introduced by Hveem (1), recoverable deformations will be referred to as resilient deformations and the corresponding moduli as resilient moduli.

Repeated-Load Triaxial-Compression Tests on Granular Materials

Whereas repeated-load triaxial-compression tests have been performed on cohesive soils for over a decade, it is only recently that this type of test has been used to any large extent to study the resilient characteristics of granular materials.

Seed and Chan (7) investigated the effect of the duration of stress on the total deformation of soil specimens subjected to repeated loading. An increase in the duration of stress application, for intervals up to 2 min, resulted in an increase in the total deformation of the silty sand that they tested. From their data, it is also possible to show that the modulus of resilient deformation increases as the duration of load application decreases and that this increase is more pronounced for very short durations of load.

Haynes and Yoder (8) presented the results of undrained repeated-load triaxial-compression tests on gravel and crushed stone, similar to those used in the base

course of the special flexible pavement sections at the AASHO Road Test. Specimens of both the gravel and crushed stone were tested at dry densities corresponding to the average obtained in the field tests. The densities were obtained in the laboratory by impact compaction using a 5.5-lb weight falling from a 12-in. height. A 15-psi lateral pressure and a 55-psi deviator stress were used in all the tests. For the gravel, the modulus of resilient deformation was influenced both by gradation (i.e., percent passing the No. 200 sieve) and the degree of saturation, with an increase in degree of saturation causing an increase in resilience. On the other hand, for the crushed stone, the influence of gradation was small, and the degree of saturation for the range investigated (70 to 80 percent) appeared to be of minor importance.

Biarez (9) has presented results of cyclic-load triaxial-compression tests on a uniform sand (grain diameter 0.016 in.) in which the variation of the modulus of resilient deformation with mean normal stress was investigated. From the results obtained after several cycles of load, he concluded that the variation of the modulus with the mean normal stress may be stated as

$$E = K \cdot \sigma_m^n$$

where

E = the modulus of elasticity,

K = constant,

σ_m = mean normal stress = $\frac{\text{sum of principal stresses}}{3}$, and

n = exponent varying from 0.5 to 0.6.

Some repeated-load triaxial tests have been conducted by DeGraft-Johnson (10) on an air-dried, fairly rounded, well-graded gravel; in these tests the influence of void ratio and confining pressure were investigated. The most significant result of the investigation was the striking dependence of the modulus of resilient deformation on the confining pressure. For the range in conditions investigated, doubling the confining pressure resulted in a 100 percent increase in resilient modulus.

Trollope et al (11) have conducted a series of tests on sand in which an attempt was made to simulate parking conditions by subjecting soil specimens to slow, repeated cyclic loads. The effects of initial dry density, rate of deformation, lateral pressure and stress level were investigated on a poorly graded sand. The studies indicated that the modulus of the sand increased with a decrease in void ratio and an increase in rate of strain. In addition, the modulus increased with an increase in confining pressure, but was independent of the axial stress so long as a failure condition was not reached.

The Texas Transportation Institute has also investigated the behavior of granular materials in repeated loading. Based on the results of tests on partially saturated, well-graded aggregates, Dunlap (12) has suggested an equation of the form

$$M_Z = K_2 + K_3(\sigma_r + \sigma_\theta)$$

where

M_Z = the modulus of deformation measured in the direction of an applied stress, σ_Z,

K_2 = the modulus of resilient deformation for the unconfined condition,

K_3 = a constant of proportionality, and

σ_r and σ_θ = the radial and tangential stress respectively.

Coffman et al (13) have determined complex moduli for the granular materials representing both the subbase and base course at the AASHO Road Test. Over a limited range of water contents and densities, the complex modulus increased slightly with

TABLE 1

SUMMARY OF LABORATORY TRIAXIAL-COMPRESSION TESTS TO EVALUATE THE RESILIENT PROPERTIES OF GRANULAR MATERIALS

Reference	Material Investigated	Factors Investigated	Confining Pressure, psi	Deviator Stress, psi	Frequency and Duration	Number of Load Applications	Modulus of Resilient Deformation, psi
Seed and Chan (7)	Silty Sand	Duration of stress applications	14.7	23.5 and 36.0 36.0 36.0	20 per min for 1/3 sec, 2 min on, 2 min off, 20 min on, 20 min off	10,000	21,300 and 27,300 23,200 23,000
Haynes and Yoder (8)	AASHO base-course material adjusted gradation to 3/4-in. maximum size: 1. Gravel 2. Crushed stone	Percent of fines passing no. 200 sieve: 6.2, 9.1, 11.5. Degree of saturation: 70%, 85%, 100%	15.0	55	40 per min	100,000	28,000 - 63,000
University of California (10)	Niles aggregate, fairly rounded, 3/4" max. size, 5% passing, no. 200 sieve	Void ratio, confining pressure	14.2 and 28.4	20, 40 and 60	20 per min	10,000	16,700 - 54,500
Biarez (9)	Uniform sand, 0.016-in.-diam. particles	Variation of E with the applied mean normal stress	Mean normal stress: 2.2-145		Cyclic load (rate of deformation is not indicated)	~5	At σ_m = 2.2 psi-4300 At σ_m = 145 psi-71,000
Trollope, Lee and Morris (11)	Poorly graded, dry sand	Initial dry density (loose and dense); rate of deformation from 0.003 to 0.2 in. per min; lateral pressure at constant stress; effect of stress level at constant confining pressure	15 - 45	Stress level varied	Cyclic load, rate of deformation from 0.003 to 0.2 in. per min	~100	35,000 - 95,000
Texas Transp. Institute, Dunlap (12)	Graded material — 1 in. maximum size; 6% passing no. 200 sieve; molding water content, 5.5%	Variation of modulus with confining pressure	3 - 30	3.45 and 51.8	30 per min, duration 0.2 sec	130,000	30,000 - 160,000
Coffman et al (13)	AASHO base and subbase-factorial sections	Water content and dry density. Frequency.	Base - 14 Subbase - 9	Base 42 Subbase - 32	Creep-test results transformed through application of superposition principle to frequencies of 1 and 100 rad per sec	1	(Complex modulus) Subbase: 5-28,000 Base: 9-20,000

increased dry density and decreased slightly with increased water content for both base and subbase materials.

Hveem et al (14) have investigated the resilience characteristics of granular base and subbase materials using a modified stabilometer called the resiliometer. In this equipment, the deformation of a sample in repeated loading is measured as a volumetric displacement, termed the resilience value. They have presented data indicating that the resilience value at a given pressure decreases as the quality of the granular material increases. In addition, their data indicate an increase in resilience with an increase in water content for fine granular materials (e.g., silty sand).

A summary of the various investigations is given in Table 1. It will be noted that the values for resilient moduli of granular materials vary between 4,000 and 160,000 psi. In view of the wide range in values, it is desirable to discuss the factors which contribute to this variation and the relative influence of each.

The available data indicate that the resilient modulus of granular materials appears to depend on the following factors.

Duration of Stress Application and Rate of Deformation—The results of the triaxial repeated-loading tests on silty sand indicate that by decreasing the duration of the load application from 20 min to $\frac{1}{3}$ sec while keeping the other conditions constant, the modulus of resilient deformation increased from 23,000 to 27,000 psi, or about 18 percent. The results of the cyclic-load tests on dry sand indicate that the modulus of resilient deformation increased about 20 percent when the rate of deformation increased from 0.002 in. per min to 0.040 in. per min. Both investigations show that the modulus increases with a decrease in the duration of load applications, but that, in spite of the large range of values investigated, the change in the magnitude of the modulus of resilient deformation is relatively small.

Frequency of Load Application—The results of Coffman et al indicate that the higher the frequency of load application, the higher the modulus. These increases ranged from 50 to 100 percent, depending on water content and dry density.

Type of Aggregate and Percentage of Material Passing the No. 200 Sieve—The results presented by Haynes and Yoder indicate that gravels containing 6.2 and 11.5 percent passing the No. 200 sieve exhibited almost identical rebound. The relative densities (difference between field and loose densities divided by difference between maximum and loose densities) of the compacted materials prepared from these two gradations were essentially the same. The rebound of material containing 9.1 percent passing the No. 200 sieve was up to 20 percent greater than that for material with 6.2 or 11.5 percent passing the No. 200 sieve, and the relative density was about 5 percent lower. For the crushed stone, the values of rebound were almost the same for all three gradations in spite of differences in relative densities. These results may be summarized as:

Material Tested	Percent Passing No. 200 Sieve	Rebound Modulus (psi) for Saturation of		
		70%	80%	90%
Gravel	6.2	56,000	46,500	34,000
	9.1	—	40,000	31,000
	11.5	57,500	45,000	37,000
Crushed rock	6.2	42,000	39,000	—
	9.1	39,000	29,000	—
	11.5	39,500	33,500	—

Void Ratio—A limited number of tests carried out at the University of California indicated that two specimens with slightly different initial void ratios will reach the same void ratio after several hundred load repetitions. Trollope et al indicated, however, that the difference between the moduli of loose and dense sand can be as much as 50 percent.

Degree of Saturation—The repeated-load tests reported by Haynes and Yoder indicated that by increasing the degree of saturation of a gravel from 70 to 100 percent, the modulus of resilient deformation decreased to one-half its original value. Tests on crushed stone indicated that, within the range of 70 to 80 percent saturation, the values of the resilient modulus had a small random variation not exceeding 20 percent.

Confining Pressure—All tests in which the effect of confining pressure was investigated show the large influence of this factor on the resilient modulus; e.g., the tests performed at the Texas Transportation Institute indicated that the modulus could increase by as much as 500 percent by varying the confining pressure from 3 to 30 psi. Biarez's equation also suggests the importance of mean normal stress.

Stress Level—Trollope et al concluded that the resilient modulus was independent of the stress level as long as the stress did not cause excessive plastic deformation.

In spite of these effects, it would appear that the problem of laboratory evaluation of resilient moduli (or an approximate equivalent elastic modulus) of granular materials can be somewhat simplified. In preparing specimens for test, estimates must be made for the void ratio and expected degree of saturation. The rate of load application, although having an influence, is not of major importance—a reasonable loading rate consistent with moving traffic can be utilized. Frequency, on the other hand, may influence results significantly, and some indication of the frequency of load applications should be considered. A representative number of repetitions consistent with the field conditions should also be used. The major difficulty is to define the stress condition under which the resilient behavior of the material should be measured. Because this will vary widely in the pavement base course, selection of a representative stress condition presents a major problem.

Field Tests on Paving Materials

Field tests which have been used to determine resilient moduli of materials comprising the pavement section can be divided into (a) plate-load tests—static or slowly applied loads[1]; (b) Benkelman beam tests using a loaded truck; (c) vibratory tests; and (d) plate-load tests with loads of short duration repeated many times. Results of these tests have been summarized in Table 2[2]. Of particular interest are the results for untreated granular materials. As may be seen in Table 2, reported modulus values for these materials vary from 8,000 psi (Burmister) to as high as 200,000 psi (Heukelom and Klomp). This range is comparable to that obtained for the results of repeated-load tests in the laboratory.

This variation in modulus is somewhat surprising in that the modulus of granular materials would be expected to vary less than that of the other materials comprising the pavement section. The most probable explanation for this variability is the influence of confining pressure. Thus it would appear important to know fairly precisely the stresses induced in the pavement when estimating the resilient modulus of untreated aggregates.

Stress Distribution in Pavement Sections

Generally, in determining stress distribution in pavement sections, the pavement has been represented either by a single homogeneous semi-infinite elastic solid (Boussinesq), or by a series of layers assumed to be either plates or elastic solids

[1]Procedures according both to ASTM D 1195 and D 1196 would be considered in this category, even though D 1195 is listed as a repetitive-load test.

[2]Reference (6) contains a detailed summary of the data used in establishing Table 2.

TABLE 2

SUMMARY OF TEST METHODS TO DETERMINE THE MODULI OF IN-PLACE MATERIALS

General Test Category	Investigator	Type of Test	Test Location	Theory Used to Evaluate Moduli of Components	Criteria Used to Evaluate Moduli	Typical Moduli Values	
						Material	Modulus, psi
Plate Load Tests — Static Load	Burmister (15)	Rigid plate	Both at surface of subgrade and pavement section	Two-layer elastic solid (Burmister)	Variable; e.g., for WASHO subgrade — deformation resulting from 2nd application of 12.7-psi stress	WASHO subgrade: uncompacted compacted HYBLA Valley subgrade-compacted Subbase - (granular) Base and asphalt concrete	2,000 (avg.) 5,800 (avg.) 2,500 (avg.) 8,000 - 22,000 80,000 - 160,000
	Brown (16)	Rigid plate	At surface of pavement sections	Two-layer elastic solid (Burmister)	Total deformation of 0.2 in. for one application	Subgrade soils Base and asphalt concrete	3,000 - 16,000 7,500 - 21,000 10,000 - 15,000[a]
	Corps of Engineers (17,18)	Flexible plate	At surface of homogeneous test sections	Boussinesq	Total deformation for sustained stress	Clay silt Sand	5,000 - 25,000[b] 20,000 - 40,000[c]
Benkelman Beam	Walker et al (19)	Benkelman Beam	Deflection of component layers of in-service pavement	Boussinesq	Deflection under 18,000 lb axle load	Subgrade (A-1 to A-6 soils) Subbase (granular open graded) Base (waterbound macadam)	19,000 - 40,000 10,000 - 20,000 18,000 - 100,000
Vibratory (Dynamic) Tests	Heukelom and Klomp (20)	Heavy vibrator and light electrodynamic vibrator	On surface of pavement or at surface of any components	Elastic plate on elastic solid or the assumption that transmitted waves are shear waves	Dynamic deflection with heavy vibrator — phase velocity with light electrodynamic vibrator	Soft clay Stiff clay, sand Clay gravel Granular base Asphalt concrete (@ 10° to 20° C)	7,000 28,000 56,000 40,000 - 200,000 300,000 - 1,000,000
	Nijboer and Metcalf (21)	Light electrodynamic vibrators	On surface of section under investigation	Wave propagation in layered elastic solids	Phase velocity	AASHO subgrade: Before frost After frost AASHO subbase AASHO base	21,000 8,500 ~105,000 420,000
	Jones (22)	Light electrodynamic vibrators	On surface of section under investigation	Wave propagation in layered elastic solids	Phase velocity	Sand subbase Wet mix slag base Subgrade (range in soil types) Asphalt concrete (B.S. 594)	~8,500 14,000 - 65,000 3,000 - 60,000 200,000 - 500,000
Plate Load Tests — Repeated Load	Odemark (23)	Rigid plate cyclic load	At surface of test pavements	Odemark	Elastic deformation after 4 repetiions of load	Sand (subgrade) Dry sand (subgrade) Clay Sand (base) Gravel (base) Crushed stone (base) Asphalt concrete	~10,500 ~ 4,000 250 - 400 3,500[d] 3,500[d] - 13,500 3,700[d] - 24,000 140,000
	Dehlen (24)	Rigid plate cyclic load	At various levels in pavement	Odemark and two-layer elastic solid	Slope of load vs. deformation curve — 4th load cycle	Subgrade (variable) Aggregate subbase Crushed rock base	5,000 (avg.) 15,000 35,000
	Seed et al (25)	Rigid plate cyclic or repeated load	At surface of homogeneous section of modeling clay	Boussinesq	Resilient deformation after varying numbers of load repetitions	Plasteline modeling clay (similar to saturated clay)	1,300 - 2,800

(a) Majority of data.
(b) At depth, results indicated a modulus equal to 25,000 psi.
(c) At depth, results indicated a modulus equal to 40,000 psi.
(d) These values were obtained on a clay subgrade (E = 250-400 psi) and indicate that the strength of the subgrade influences the density and hence the modulus which can be obtained in the overlying material. This point has also been more recently documented by Heukelom and Klomp.

(26, 27). A summary of investigations concerned with determining the applicability of these theories to predicting actual stress distributions indicates the following:

1. The stresses throughout a uniform clay resulting from surface loads can reasonably be determined by assuming a stress distribution according to Boussinesq. This

stress distribution also gives a fairly good estimate of stresses at greater depths in homogeneous sand layers (17, 18).

2. In a layered structure, when the ratio of the modulus of the upper layer to that of the lower layer approaches unity, the Burmister and Boussinesq solutions produce the same results, e.g., the tests with sand asphalt on sand reported by Trollope et al (11).

3. The distribution of stresses within layered structures can be estimated by Burmister's solution if the upper layers consist of concrete or soil cement. When they consist of untreated granular materials and/or asphalt concrete, on the other hand, the evidence is somewhat contradictory. McMahon and Yoder (28) indicate that the distribution of stresses is not as dependent on modular ratio (a ratio of 10 was used in the analysis) as predicted by Burmister's analysis, although a definite reduction of stress at the base-subgrade interface below that predicted by Boussinesq was observed. However, Vesic (29) found that the pattern of stresses predicted by Boussinesq was more adequate than layered-system-theory results for predicting the stress distribution in pavements, even though modular ratios of 4 were indicated by static tests on the pavement components (30, 31).

It would appear from these results that either the Burmister theory is not applicable to layered pavements consisting of asphalt concrete or that the moduli used in making these comparisons were not correct. It is possible that the modular ratio of 10 used by McMahon and Yoder and the ratio of 4 used by Vesic may be too large when considering the behavior of untreated granular bases resting on compressible subgrades. In addition, implicit in the Burmister theory is the assumption that the modulus is constant in the upper layer. Recent data would suggest, in the case of untreated materials, that this may also be incorrect.

To determine the extent to which the Boussinesq or Burmister patterns of pressure distribution occur in pavements, both the effective modulus of untreated granular material and its variation within the pavement should first be established.

From the information presented, a number of points have become apparent and can be summarized as follows:

1. The behavior of granular materials comprising the pavement section should be measured under conditions of stress which are representative of the actual conditions existing in pavements, since the magnitude of the stress influences the resilient behavior of the material.
2. Laboratory repeated-load triaxial tests would appear to provide a satisfactory means of determining the resilient characteristics of untreated granular materials.
3. Results of investigations to determine the extent to which present theories of pressure distribution are applicable to asphalt-concrete pavements containing granular bases are somewhat contradictory. Great care should be taken in selecting the modular ratios when using Burmister's analysis of layered systems; a Boussinesq distribution may be a very close approximation and it is much easier to compute.

Ideally, the solution to the problem of predicting transient pavement deflections would be obtained through studies of suitably instrumented pavements subjected to actual vehicle loads, since it is necessary for materials comprising the pavement section to be subjected to a number of repetitions of load prior to the measurement of the response. This approach has the advantage that the paving materials have been "conditioned" (i.e., the deformation under loads is comprised primarily of elastic deflection rather than a combination of comparatively large plastic or irrecoverable deformation and a smaller amount of elastic or resilient deformation). The stresses generated in the various materials comprising the structural section are those resulting from representative vehicular loads, and the time of loading (under moving wheel loads) is realistic. Initially this approach, because of the broad scope, has many difficulties, such as control of materials, size and costs. Ultimately, however, for application of techniques developed from other procedures, this type of investigation must be accomplished.

Another approach, at a more modest level of effort, is the use of the repeated-load plate test on carefully controlled field test sections. The requirements of specific numbers of load repetitions, and stresses of the same order of magnitude as those produced by loads on tires, are met by this type of test. By using suitable theories and criteria of failure, the results of this type of test could also be used in design.

Unfortunately, the use of the plate-load test for design purposes has the same disadvantage as other in situ measurements in that it can be used to evaluate the properties of the paving materials only at the time the test is conducted. Because the properties of these materials are susceptible to changes during the pavement lifetime, the testing conditions are not necessarily the most critical conditions which can occur during this time. Other disadvantages of the plate-load test are the length of time spent in performing the tests and the high cost relative to small-scale laboratory tests. Therefore, it is desirable to be able to predict the resilient deformations of the different pavement layers from laboratory test results. If this could be achieved, the critical material properties could be reproduced in the laboratory, and the resilient modulus expected from plate-load test measurements for these same conditions could be produced. Thus, the primary purpose of this investigation is to establish the possibility of predicting pavement deflections in prototype structures from the results of repeated-load laboratory tests on individual materials comprising the pavement section, with particular emphasis on the role of untreated granular materials.

LABORATORY REPEATED-LOAD TESTS ON GRANULAR MATERIALS

Emphasis in this section will be on determining the resilience characteristics of a well-graded gravel in repeated-load triaxial-compression tests, since this is the material used in the prototype tests described in a subsequent section. To illustrate, however, that the characteristic resilient behavior defined by the type of test described in this section is applicable to other granular materials, a brief indication of such behavior will also be presented for a uniform sand and representative base and subbase materials obtained from two in-service pavements in California.

Material Description

The gravel used for the prototype pavement tests was a well-graded, subrounded material from Pleasanton, California, with a grain-size distribution as shown in Figure 1.

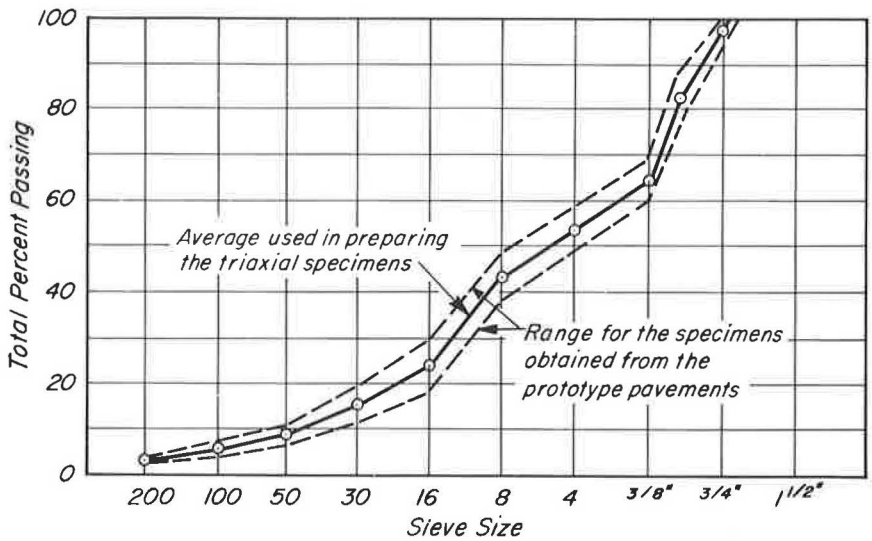

Figure 1. Grading curve, gravel base.

These results were the average obtained from analyses of several specimens taken from successive 2-in. layers of the base course of the pavements; the gradation was within the California specification limits for a Class 2 aggregate base. The specific gravity of the material retained on the No. 4 sieve was 2.75, and that of the material passing the No. 4 sieve was 2.65. Routine strength tests on the material indicated an angle of internal friction of 55 deg at a void ratio of 0.31, corresponding to the average in-place density of 139 lb/cu ft, an average CBR value of 103 and an average R value of 85. This material was tested in the air-dry condition both in the laboratory and in the field.

Equipment

A piston capable of applying comparatively large loads for short durations was necessary for the tests on granular material, particularly since triaxial specimens up to 6 in. in diameter were required for aggregate with maximum size particles up to $\frac{3}{4}$ in. or $1\frac{1}{2}$ in. (sizes approaching those used in actual base courses). The loading piston developed to meet these requirements is shown in Figure 2; it was also used to apply repeated loads to the plates in the field tests on the prototype pavements.

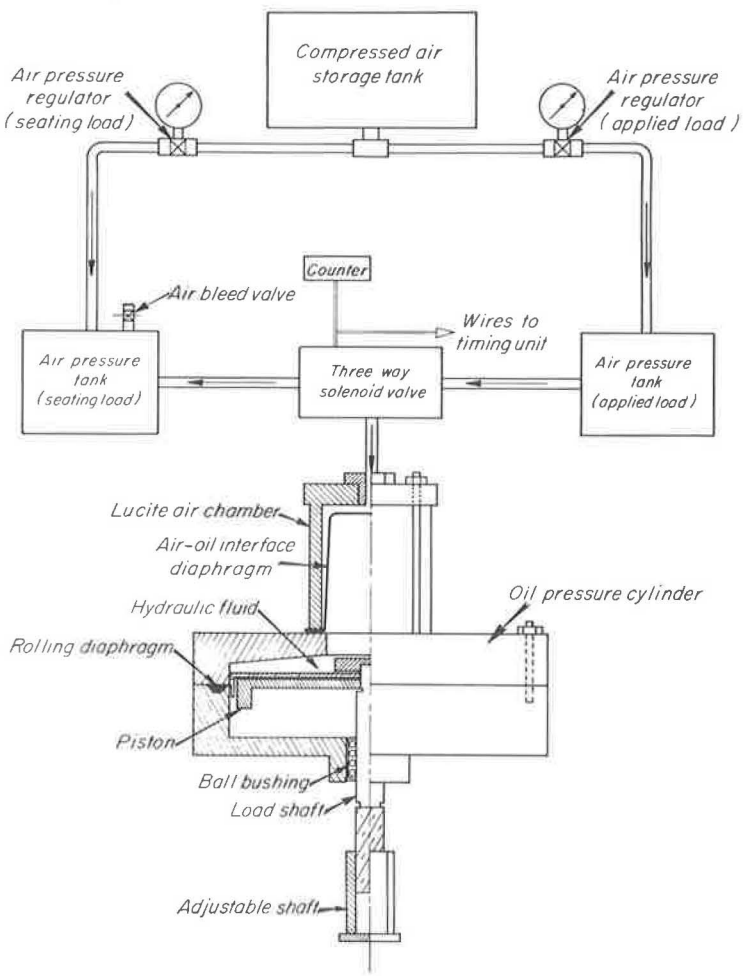

Figure 2. Large loading piston and control mechanism.

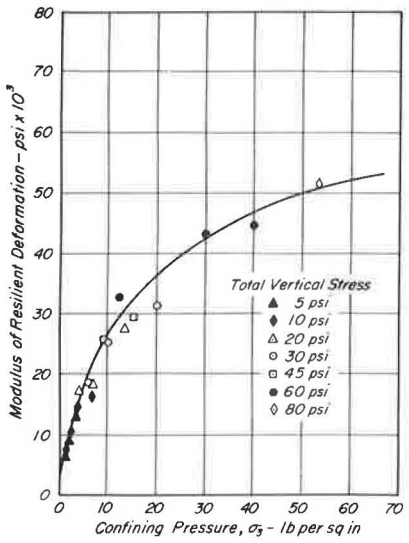

Figure 3. Relationship between modulus of resilient deformation and confining pressure for dry gravel.

The loading system was operated by compressed air stored in separate tanks at the required pressures for the seating load and the peak or applied load. By using a three-way solenoid valve, the appropriate pneumatic pressure was supplied through a bellofram seal to oil above the main piston. A ball-bushing guide was provided to reduce friction and a neoprene rolling-diaphragm seal was utilized to minimize friction and to prevent loss of oil. The volume of air between the piston and the three-way valve was reduced to a minimum to provide a rapid buildup of pressure during each load pulse. The peak load applied to the specimen was varied by regulating the air pressure, as recorded by the pressure gage. Any desired load up to 5,000 lb can be obtained. During calibration, the load was applied both statically and dynamically, and the two calibration curves were identical.

Triaxial cells capable of testing specimens up to 6 in. in diameter were used, although the majority of tests were performed with a cell in which specimens 3.9 in. in diameter and about 8 in. in height could be tested.

Procedure

For the tests on the dry gravel, the samples were prepared to the desired dry density (139 lb/cu ft) by vibratory compaction, because this method minimized puncturing of membranes and crushing or degradation of the aggregate. Each sample was prepared inside a forming jacket mounted on the base of the triaxial cell attached to a table supported by rubber springs. Vibrations were then induced by compacting the specimens in two equal layers for 15 sec under a 15-lb weight. When compacting the upper layer, the cap of the specimen was inserted to obtain a flat horizontal layer.

A range in confining pressures from 1 to 53.3 psi was used for the repeated-load tests. Confining pressures up to about 11 psi were obtained by vacuum inside the membrane; for larger confining pressures, air pressure was used in the triaxial cell outside the membrane. Deviator stresses ranging from 1.7 to 40.0 psi were applied with the hydraulic-pneumatic piston at a frequency of 20 applications per minute and with a load duration of 0.1 sec. Generally, the repeated loading was continued for at least 10,000 stress applications.

Test Results for Gravel

The influence of applied stresses on the modulus of resilient deformation for dry gravel is shown in Figure 3. It will be noted the majority of tests were conducted at low confining pressures, since the change in modulus with confining pressure is greatest in this range.

Principal stress ratios used in these tests (between 1.5 and 5.0) were lower than the principal stress ratio at failure under a steadily increasing load application (approximately 11). However, one specimen was tested at a principal stress ratio of 10. At the beginning of this test and for about 800 load repetitions, essentially the same modulus was obtained as would be predicted from Figure 3. After this number of load applications, the plastic deformation increased rapidly with additional load applications, and failure occurred at approximately 1,000 load repetitions. Thus, this test would

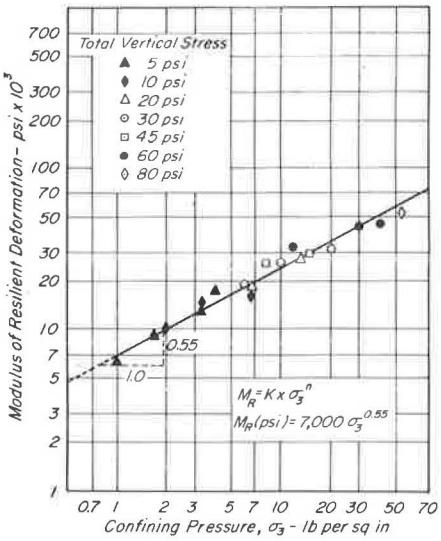

Figure 4. Relationship between modulus of resilient deformation and confining pressure for dry gravel.

appear to indicate that the relationship obtained is valid for all magnitudes of deviator stress (for the range of confining pressures investigated), as long as failure does not occur.

These results emphasize the importance of properly accounting for the actual magnitude of the confining pressure and its variation with depth in untreated bases, so that a realistic measure of the resilient characteristics of these materials throughout the layers in which they are used can be obtained. For example, for this gravel, a variation of confining pressure from 1.0 to 53.3 psi resulted in an increase in modulus from 7,000 to 50,000 psi. It will be noted that the largest increase occurs in the low pressure range, i.e., 0 to 10 psi.

The data shown in Figure 3 can be more conveniently utilized by plotting the results as shown in Figure 4. In this figure, it will be noted that a linear relationship between the logarithm of resilient modulus and the logarithm of the confining pressure is obtained; thus, the modulus M_R can be expressed by an equation of the form

$$M_R = K \cdot \sigma_3^n \qquad (1)$$

where

K = material constant determined experimentally (7,000 for gravel),

σ_3 = confining pressure, and

n = material constant determined experimentally (0.55 for gravel).

The form of this equation is similar to that presented by others; e.g., Jakobson (32) has shown theoretically that for spherical particles the exponent n in Eq. 1 has a value of $\frac{1}{3}$.

The data can also be analyzed in terms of the sum of the principal stresses. From this analysis an alternative form of the equation for resilient modulus has been developed as follows:

$$M_R = K' \cdot \theta^{n'} \qquad (2)$$

where

θ = sum of the principal stresses ($\sigma_1 + \sigma_2 + \sigma_3$), and

K' and n' = experimentally determined coefficients.

The resulting plot of the data in this form is shown in Figure 5. Although Eq. 2 has not been used in conjunction with the theories presented in this paper to predict pavement deflections, it has the potential for use in analyses such as that presented by Cumming and Gerrard (33). In addition, it has the advantage from a theoretical viewpoint that it is a valid tensorial relationship, whereas Eq. 1 in terms of σ_3 is not.

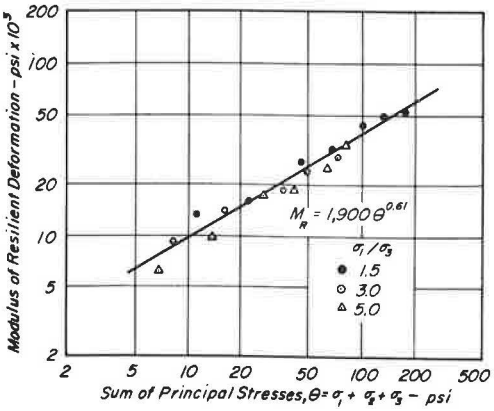

Figure 5. Relationship between modulus of resilient deformation and the sum of principal stresses for dry gravel.

Test Results for Other Materials

Although not used in the analysis of prototype pavements presented here, modulus vs confining-pressure data, such as those shown in Figure 4, have been developed for other granular materials. To emphasize that Eq. 1 would appear to be a reasonable way to represent the dependence of resilient modulus on confining pressure for a range in granular materials, data are presented in Figures 6, 7, and 8 for 4 other untreated granular materials; the data are plotted in the same form as that used in Figure 4. All of the results were obtained at the same frequency and duration of loading as the data for the gravel.

Figure 6 shows the test results for a dry, rounded, uniform sand (essentially all of the material passed the No. 16 sieve and was retained on the No. 100 sieve) from Monterey, California, compacted to a density of 101 lb/cu ft.

In Figure 7, data are presented for tests on recompacted, disturbed samples of granular base obtained from an in-service pavement near Gonzales, California. This material was compacted in the laboratory to a dry density and water content representing in situ conditions, and in this instance the degree of saturation was of the order of 60 percent.

Similar data are presented in Figure 8 for laboratory-compacted samples of both base and subbase materials from another in-service pavement near Morro Bay, California. Both materials were compacted to densities approaching those in situ and to a degree of saturation of approximately 60 percent, which was the lower limit of values measured at the time of sampling. The scatter in the data for the base course may be due in part to the fact that samples from four different locations in the pavement were used to develop the data, and no attempt was made to separate the points according to location. For the subbase material (a fine sand), a line with a slope equal to 0.33 was drawn through the available data.

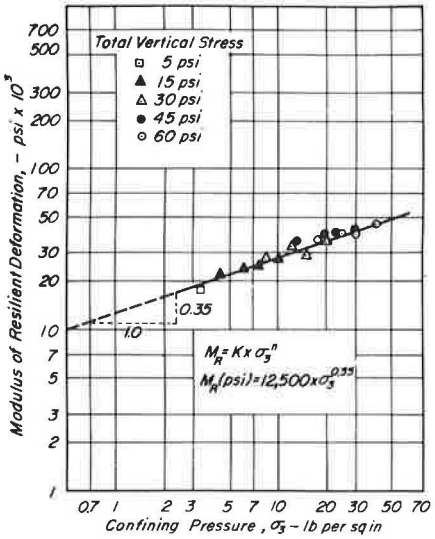

Figure 6. Relationship between modulus of resilient deformation and confining pressure for uniform sand.

Table 3 gives a summary of the coefficients K and exponents n obtained for the various materials tested in this investigation and emphasizes that the resilience characteristics of granular materials vary considerably and thus should be determined for each pavement section investigated.

In general, the data presented in this section substantiate the form of the equation relating resilient modulus and confining pressure developed for the untreated gravel. The data also emphasize the large variation which can occur in the resilience

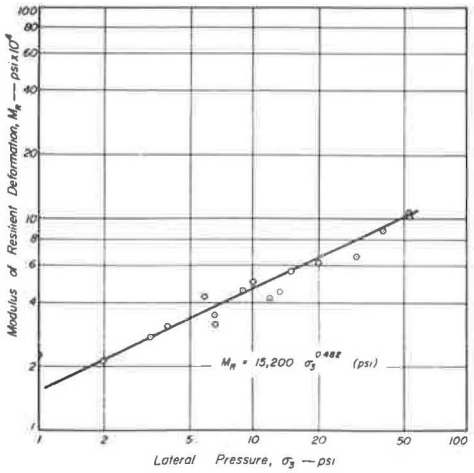

Figure 7. Relationship between modulus of resilient deformation and confining pressure, laboratory-prepared specimens of untreated base course; Gonzales By-Pass.

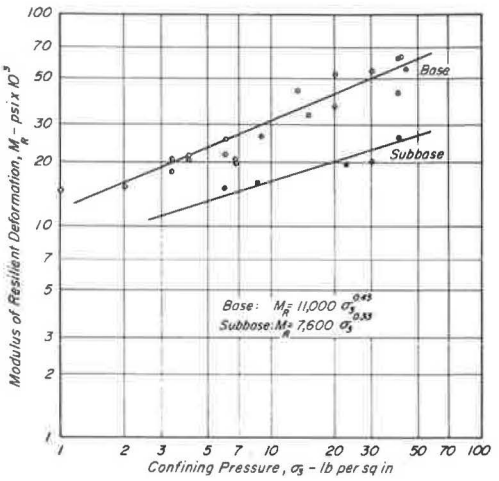

Figure 8. Relationship between modulus of resilient deformation and confining pressure, laboratory-prepared specimens of untreated base and subbase; Morro Bay pavement.

characteristics of granular materials depending on the confining pressure, a factor which plays an important role in defining the behavior of these materials in the pavement section.

TRANSIENT DEFLECTIONS IN TWO-LAYER PROTOTYPE PAVEMENTS

To investigate the resilience characteristics of the untreated gravel base course under field loading conditions, a series of tests was performed on prototype pavement sections.

The test area was paved with a layer of asphalt concrete approximately 4 in. thick. For each field test, a section 8 by 8 ft in plan was cut from the asphalt-concrete paved area. These dimensions were chosen so that the boundary conditions would have little influence on the test results. Within this 8-ft square section, the test pits were excavated to the desired depth. Final trimming of the pit was done by hand to obtain a reasonably smooth horizontal surface. The entire excavated area was then covered with a polyethylene sheet to prevent change in water content of the natural soil due to

TABLE 3

SUMMARY OF RESILIENCE DATA FOR UNTREATED AGGREGATES

Type	Degree of Saturation (%)	Constants in Eq. 1	
		K	n
Gravel	0	7,000	0.55
Uniform sand	0	12,500	0.35
Base from Gonzales	~60	15,200	0.48
Base from Morro Bay	~60	11,000	0.45
Subbase from Morro Bay	~60	7,600	0.33

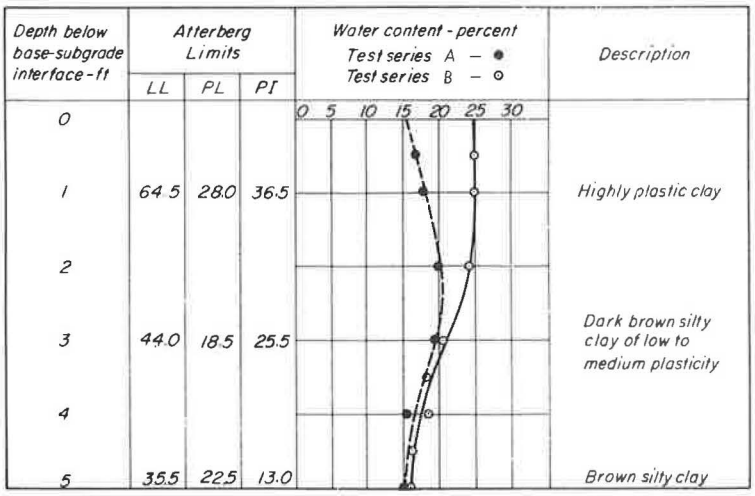

Figure 9. Subgrade characteristics.

either evaporation or absorption and to control the condition of the base course. Within this pit, a particular test pavement was constructed and tested as described in the following sections.

Six tests were performed on the following pavement sections:

1. Test Series A—subgrade comparatively dry: (a) 8-in. base, 8-in. diameter plate; (b) 8-in. base, 12-in. diameter plate; (c) 12-in. base, 8-in. diameter plate; and (d) 12-in. base, 12-in. diameter plate.
2. Test Series B—subgrade comparatively wet: (a) 8-in. base, 8-in. diameter plate; and (b) 8-in. base, 12-in. diameter plate.

A summary of the subgrade characteristics for these tests is shown in Figure 9.

Equipment

Steel plates ranging from 8 in. to 30 in. in diameter were used to apply the load to the components of the pavement section. Load was applied to the plates by means of

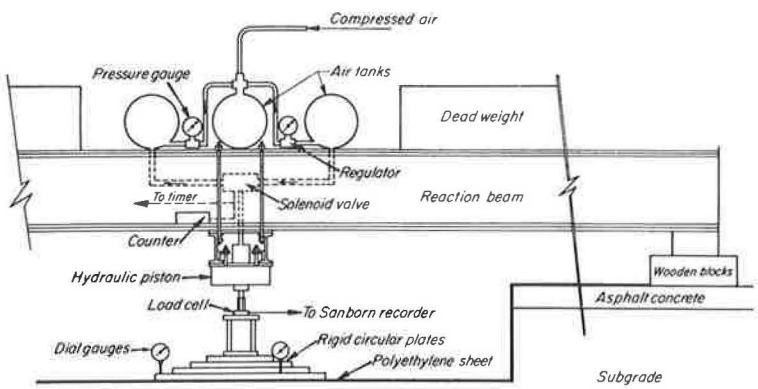

Figure 10. Repeated-plate-load test installation for test at surface of subgrade.

the same loading piston described in the previous section. As noted earlier, this piston is capable of applying loads up to 5,000 lb. A loading frequency of 20 applications per minute and loading duration of about 0.1 sec were used for the field tests. The magnitude of the loads and the shape of the load traces were constantly checked by a load cell, and were recorded on a Sanborn strip-chart recorder.

The loading piston was connected to a frame fastened to a reaction beam. The relative positions of the piston and the frame could be adjusted to center the shaft of the piston with respect to the center of the loaded plate, so as to avoid eccentricity which might result in subsequent tilting of the plate. Reaction for the load piston was provided by a steel beam loaded with either concrete cylinders or water tanks. The steel beam could be raised or lowered according to the thickness of the test section. Deflections of the pavement section were measured from a reference beam 20 ft in length, stiffened laterally to prevent sway. A schematic view of the test section set up for a test at the surface of the subgrade is shown in Figure 10.

Procedures

For the tests reported here, repeated loads were applied at the surface of the subgrade and on top of two thicknesses (8 and 12 in.) of the untreated base. Load was applied to the subgrade through a series of rigid circular plates, 18, 24, and 30 in. in diameter. Even though the subgrade was hand trimmed, it was not possible to obtain a perfectly smooth horizontal surface, and the plates were placed on a thin layer of hydrostone (maximum thickness of 0.1 in.). At least 1,000 repetitions of a particular magnitude of stress were applied. Deformations were measured by three dial gages attached to the reference beam and located at 120-deg intervals around the edge of the plate. The resilient deformation was taken to be the average of the three dial readings.

After testing the subgrade, the base courses were placed and compacted in 2-in. lifts by vibratory compaction. When the desired thickness had been constructed, repeated-load plate tests were performed using 12- and 8-in. diameter plates.

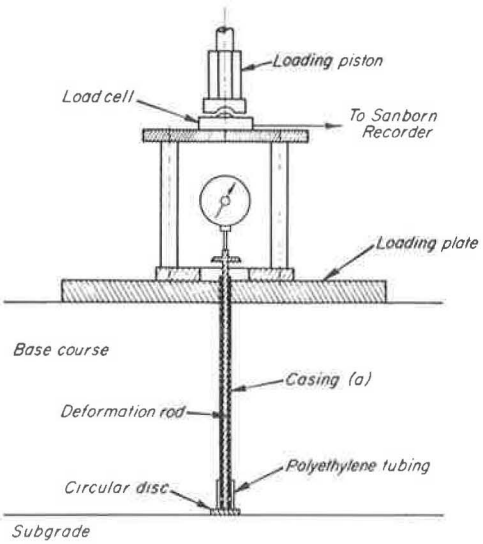

Figure 11. Device that measures deflections of individual layers of the pavement.

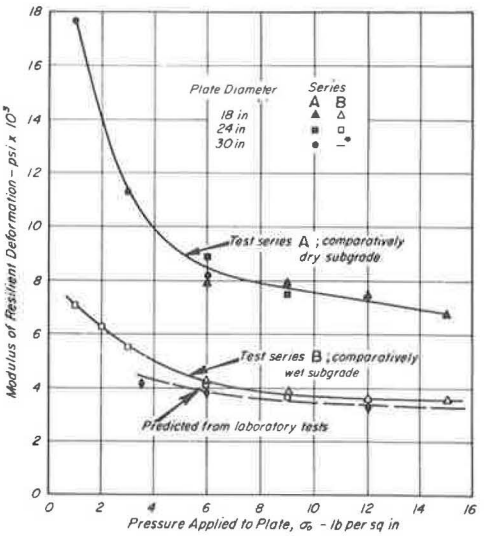

Figure 12. Relationship between resilient modulus of the subgrade determined by repeated-plate-load tests and applied pressure.

TABLE 4

RESILIENT MODULI DETERMINED FROM LABORATORY REPEATED-LOAD COMPRESSION TESTS

Laboratory Test, Stress σ_d (psi)	Stress in Plate σ_o Corresponding to σ_d (psi)	Resilient Modulus (psi)
1.0	3.5	4150
1.7	6.0	3900
3.5	12.0	3300
5.2	18.0	3200

Each stress was repeated several thousand times in the plate-load tests; after a few hundred repetitions, however, the plastic deformation generally did not increase appreciably with number of repetitions and the resilient deformation approached a constant value. Thus, the resilient deformation at 1,000 load repetitions was considered suitable for evaluating the resilient characteristics of the various layers.

Deformations of the components were measured independently (Fig. 11). The resilient deformation of the aggregate layer was evaluated by subtracting the resilient deformation of the subgrade from the total resilient deformation beneath the plate. Deformations were determined by measuring the movement of a small rigid disc 1 in. in diameter and ¼ in. thick resting on the subgrade (Fig. 11). The disc was welded to an adjustable vertical rod passing through the center of the loaded plate; measurements were taken on a smooth, flat, circular plate ½ in. in diameter, attached to the top of the rod.

To insure that this vertical rod moved freely with respect to the base course, it was placed in a thin steel casing with gaps to allow for deformation (Fig. 11). The friction between the inner rod and the outer casing was eliminated by placing a thin layer of grease in the annulus. When the inner rod was displaced, a gap between the plate in contact with the subgrade and the outer casing was formed, into which sand grains or fines tended to penetrate; this situation was avoided by covering the gap with thin polyethylene tubing.

Test Results

Subgrade—A summary of the plate-load tests performed directly on the surface of the subgrade for the two test series is shown in Figure 12. Comparison of the resilient modulus data for series A with that for series B illustrates the influence of water content near the surface of the subgrade on its resilient behavior.

The moduli shown in Figure 12 were determined using the equation for a rigid plate:

$$E = 1.18 \frac{\sigma_o \cdot r}{\Delta} \qquad (3)$$

where

E = modulus of elasticity (in this case resilient modulus) of the material,

σ_o = pressure applied to surface of plate,

r = radius of the plate, and

Δ = resilient deflection of plate.

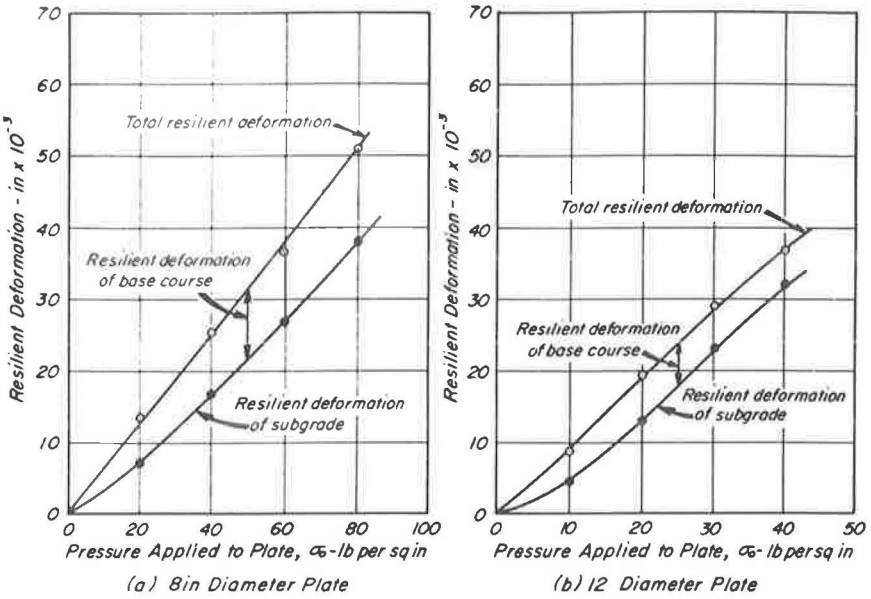

Figure 13. Relationship between applied pressure and resilient deformation of components of a two-layer system consisting of the natural subgrade and 8 in. of base; test series A.

Also shown in Figure 12 are moduli determined from repeated-load triaxial-compression tests (25) on specimens trimmed from undisturbed samples obtained at a 6-in. depth below the subgrade surface at the conclusion of test series B. The laboratory specimens were subjected to as many as 100,000 repetitions of deviator stresses ranging from 1.0 to 5.2 psi in undrained compression tests conducted using a frequency of 20 stress repetitions per minute and a duration of loading of 0.1 sec. Moduli of deformation were determined from these tests as the ratio of the repeated stress to the induced resilient strain.

To plot the moduli from the laboratory tests in Figure 12, the relation between pressures applied in the plate-load test and the stresses used in the undrained triaxial-compression tests (25) was utilized (i.e., $\sigma_d = 0.29\sigma_o$, where σ_d is the deviator stress in the repeated-load test and σ_o is the corresponding plate pressure). For convenience, the comparable pressures are summarized in Table 4. The moduli predicted from the laboratory tests follow the same trends as those observed in test series B. Since the test specimens were obtained 6 in. below the surface where the water contents are highest, the laboratory-determined moduli would be expected to give slightly lower values than the field tests. The comparison, however, is extremely encouraging and lends support to the use of the repeated-load triaxial-compression test as a means for testing fine-grained subgrade materials.

Because the field plate-load tests at the surface of the subgrade covered a wider range in applied stress (particularly in the low stress range) than would be accomplished with available laboratory repeated-load equipment, the relationships between resilient modulus and applied stress developed from the field tests have been used in the analyses of the prototype pavement behavior. It should be noted, however, that, with suitable equipment, laboratory tests would provide results equally suitable for use, as evidenced by the comparisons between field and laboratory values shown in Figure 12.

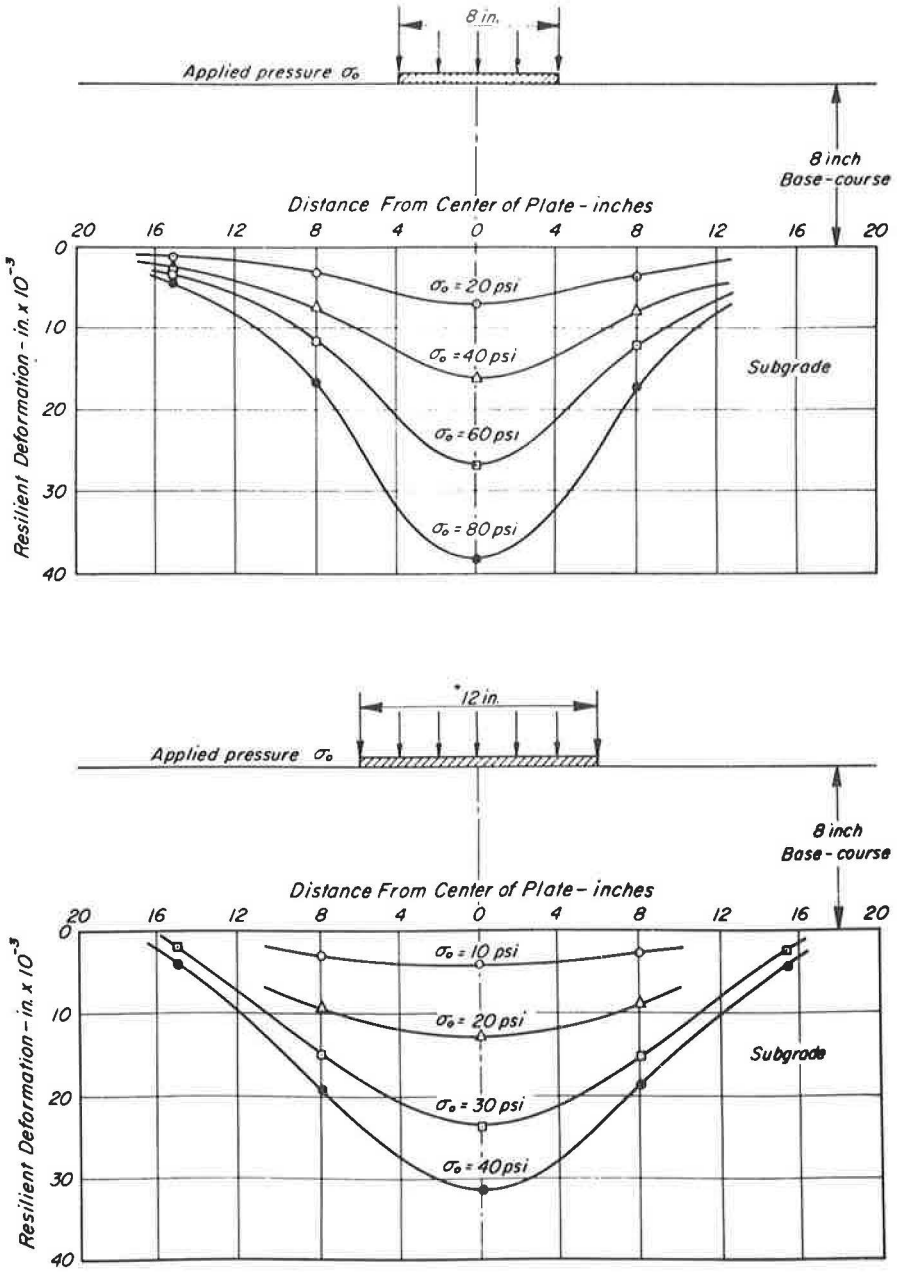

Figure 14. Radial variation of resilient deformation at base-subgrade interface for repeated-plate-load tests at surface of 8-in. base; test series A.

Two-Layer System—Results of the tests at the surface of the two-layer systems are shown in Figures 13 through 17. Figures 13 and 14 illustrate the patterns of resilient deformations at the surface of an 8-in. layer and at the surface of the subgrade in test series A, due to surface loads applied by 8- and 12-in. diameter plates. As noted in Figure 14, deformations at the surface of the subgrade were measured at

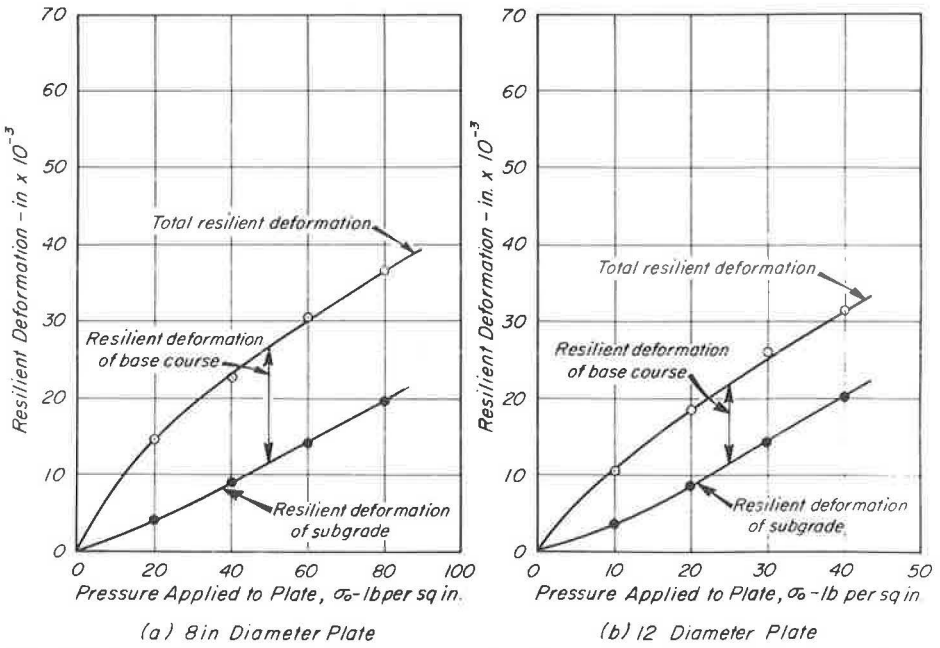

Figure 15. Relationship between applied pressure and resilient deformation of components of two-layer system consisting of the natural subgrade and 12 in. of base; test series A.

radial distances of 8 and 16 in. as well as directly under the center of the plate. Similar data are shown in Figures 15 and 16 for tests at the surface of a 12-in. aggregate layer, also for test series A.

Figure 17 shows the relationship between resilient deformations of the subgrade and base course and applied pressure for 8- and 12-in. diameter plate tests conducted on a test section involving an 8-in. gravel base in test series B.

Evaluation

While the emphasis in this paper is on the behavior of granular materials, the tests on the subgrade shown in Figure 12 illustrate certain points worthy of note:

1. These data indicate that the resilient modulus is dependent on applied stress and varies in the same manner as shown by Seed et al (25) for laboratory repeated-load tests on subgrade soils. At stresses less than 10 psi, such as can be expected in the subgrades of well-designed asphalt-concrete pavements, the variation is considerable. Thus it is evident that, to estimate the modulus of the subgrade, the stresses within the subgrade must be known.
2. The data also demonstrate the influence of water content on the resilient modulus of the subgrade and emphasize the importance, when predicting pavement deflections, of considering the changes in subgrade water content that are likely to occur during the life of the pavement. These results also indicate the inadequacy of the plate-load test since it is only capable of measuring the soil conditions at time of test—which is generally not the most critical state that the material will attain.

For the tests at the surface of the two-layer systems, the data indicate the following factors.

Influence of Applied Pressure on Resilient Deformation of Base Courses—The test results indicate a comparatively large increase in the deformation of the base course when the pressure at the surface is increased from 0 to about 10 psi (see Fig. 15). A smaller increase, on the other hand, is obtained with an increase from 10 to 20 psi.

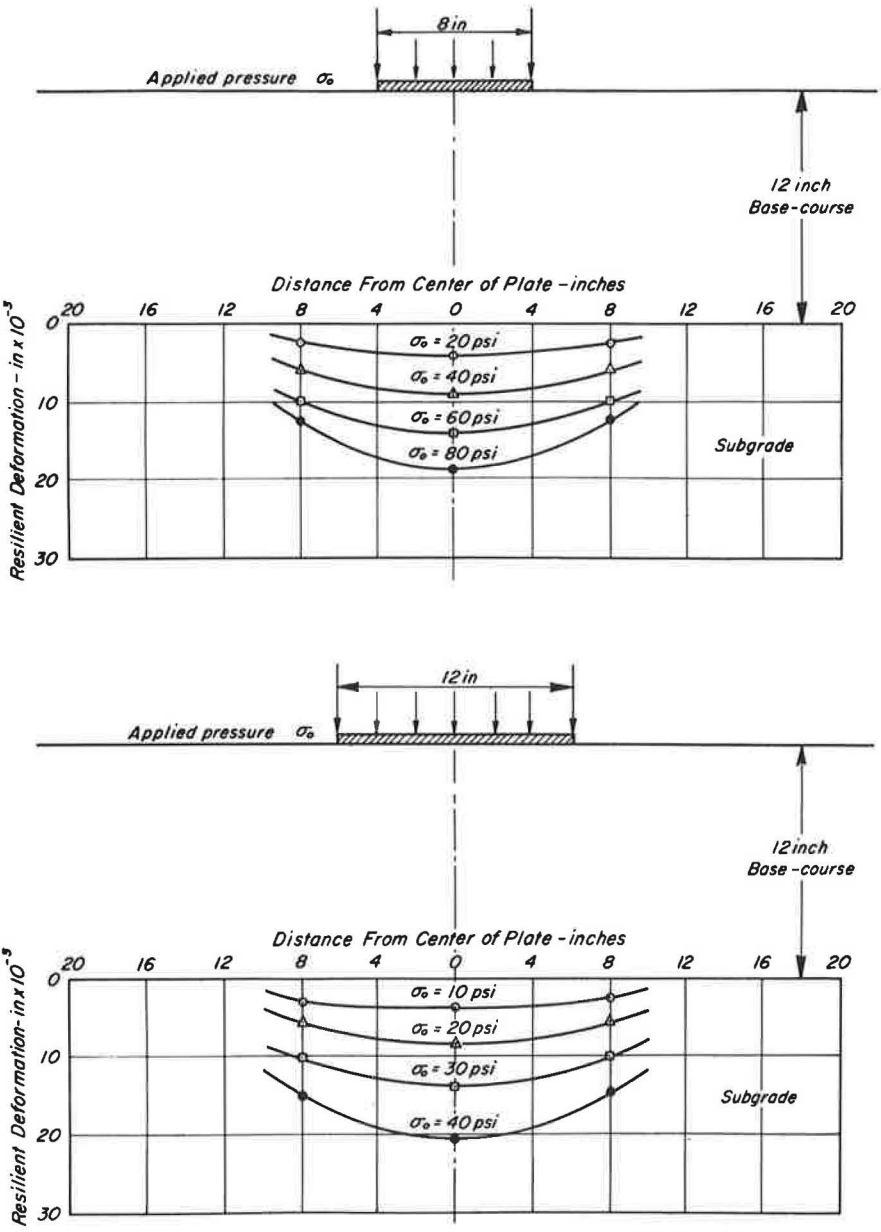

Figure 16. Radial variation of resilient deformation at base-subgrade interface for repeated-plate-load tests at surface of 12-in. base; test series A.

Because the rate of increase in resilient deformation is less than the rate of increase in applied stress, it can be concluded that the average modulus of resilient deformation of this material increases with applied pressure; this is consistent with the observed laboratory behavior reported previously.

Influence of Applied Pressure on the Resilient Deformation of the Subgrade—The resilient deformation of the subgrade measured at the base-subgrade interface increases gradually up to an applied pressure of 10 psi. When the pressure on the plate

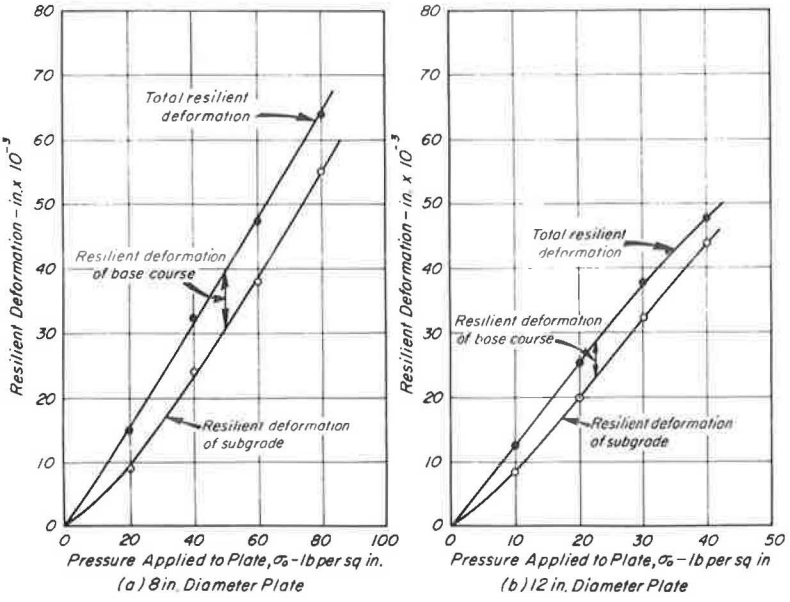

Figure 17. Relationship between applied pressure and resilient deformation of components of a two-layer system consisting of the natural subgrade and 8 in. of base; test series B.

reaches between 20 and 30 psi (e.g., Figs. 13 and 15), the resilient deformation of the subgrade increases more rapidly and almost linearly with the applied pressure. This trend indicates that the subgrade modulus is largest at low applied stresses and decreases until a level of 20 to 30 psi is reached, whereupon the modulus remains almost constant. This variation in modulus with applied pressure follows a trend similar to that obtained when testing the subgrade alone (Fig. 12).

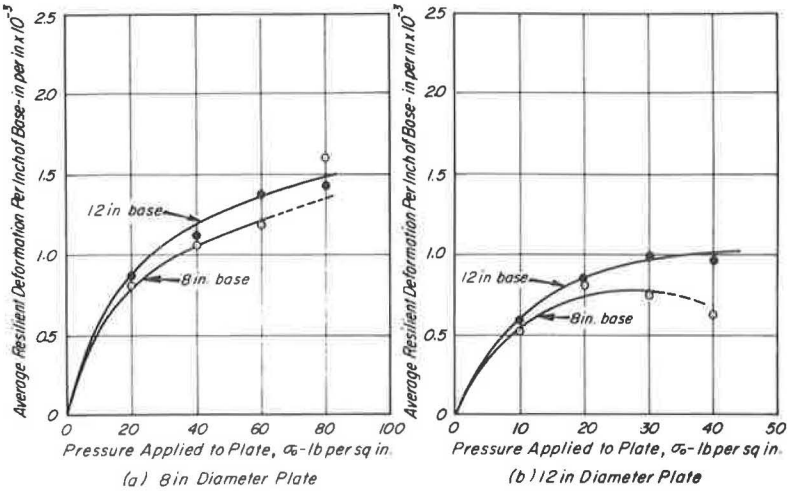

Figure 18. Relationship between applied pressure and resilient deformation per inch of base course; test series A.

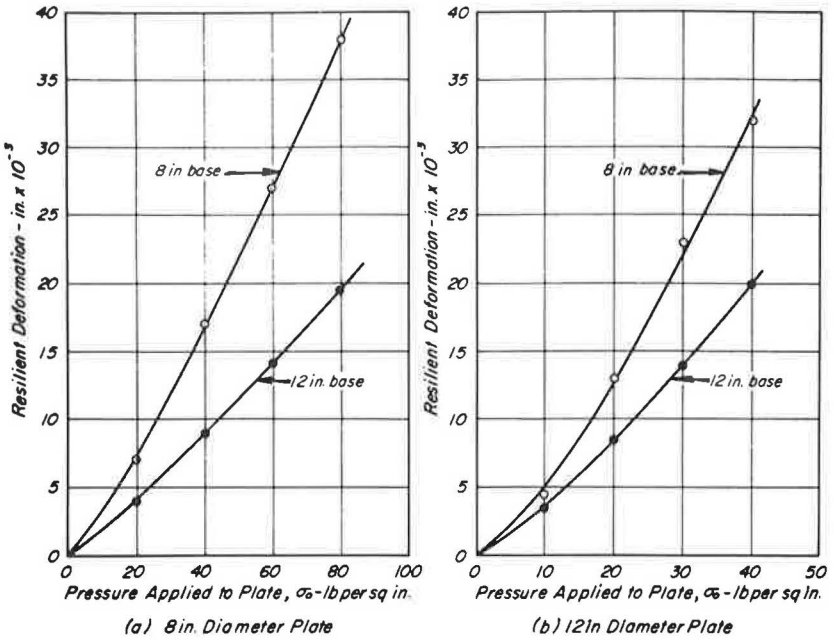

Figure 19. Relationship between applied pressure, resilient deformation of subgrade and base thickness; test series A.

Influence of Thickness of Base Course on Its Resilient Deformation—Although the influence of thickness of base can be obtained from a comparison of Figures 13 and 15, a more direct comparison is shown in Figure 18. In this figure, notice that the resilient deformation per inch of base is larger for the 12-in. base than for the 8-in. base. This pattern is in accord with data obtained in the laboratory, in that the average stress

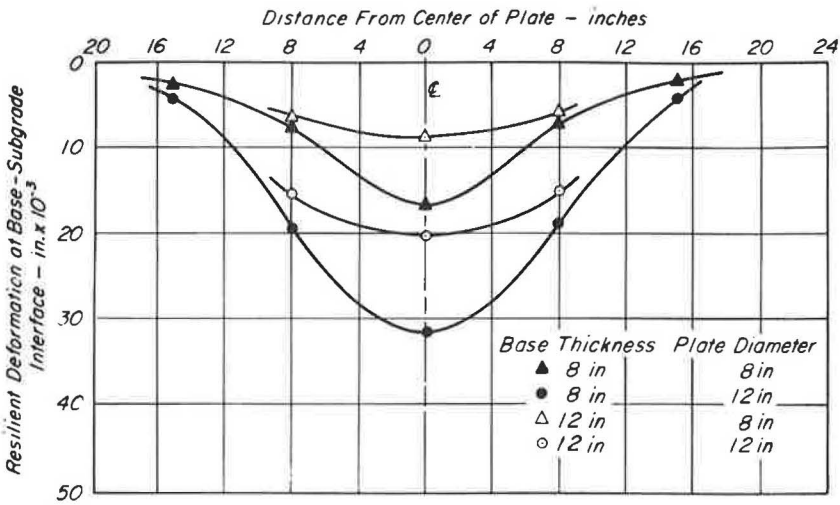

Figure 20. Influence of thickness of base on the radial variation of resilient deformation at the base-subgrade interface; test series A.

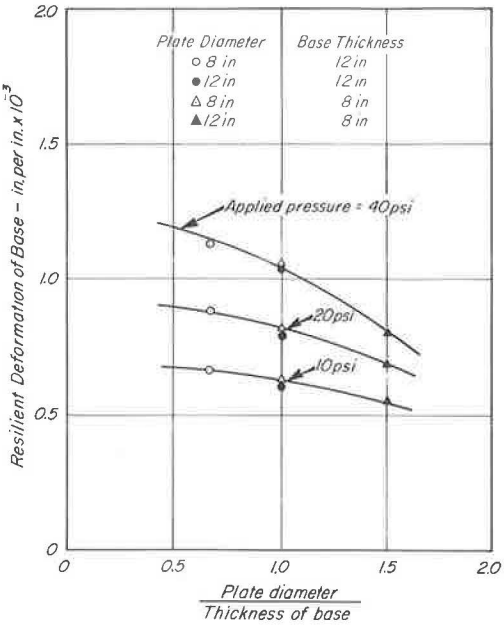

Figure 21. Relationship between the ratio of plate diameter to base thickness and the resilient deformation per inch of base; test series A.

induced in the base by a specific plate size and pressure increases as the thickness of the base decreases; thus, the modulus of resilient deformation of the aggregate increases and consequently reduces the resilient deformation.

Influence of Base Thickness on the Resilient Deformation of the Subgrade—A decrease in resilient deformation of the subgrade with increase in the base thickness is shown in Figure 19. This occurs because an increase in base thickness increases the "load spreading" capacity of the base, thereby reducing the subgrade stresses, and with reduced stress the subgrade modulus is higher; both contribute to a reduced resilient deformation. The influence of base-course thickness on the pattern of resilient deformation at the base-subgrade interface is shown in Figures 14 and 16. For comparison, the various deformation patterns corresponding to an applied stress of 40 psi have been replotted in Figure 20. The influence of the thicker base on the magnitude and distribution of the subgrade deflection is readily apparent.

Influence of Plate Diameter on the Resilent Deformation of the Base Course—The influence of plate diameter on the resilient deformation of the base course is shown in Figure 21. This figure shows the resilient deformation per inch of base as a function of the ratio of the plate diameter to base thickness. For a large ratio of plate diameter to base thickness, the confining effect is larger and the resilient deformation is correspondingly lower. It will also be noted that the resilient deformation per inch of base is essentially constant for the 8- and 12-in. bases when the ratio of plate diameter to base thickness is the same.

Influence of Plate Diameter on the Resilient Deformation of the Subgrade—For the same base thickness, the stresses induced at the subgrade-base interface are higher as the plate diameter is increased. This is shown in Figure 20 (by the increased resilient deformation) and is explained by the fact that, because of the higher stresses in the subgrade, correspondingly lower resilient moduli are developed, both of these factors leading to increased resilient deformations.

Influence of Change in Subgrade Water Content on the Resilient Deformation of the Base—A comparison of test results from series A and B for the two conditions of loading are shown in Figure 22. No significant or consistent difference is noted in the resilient deformation of the base course due to change in water content of the subgrade. These data also indicate the effectiveness of the plastic sheet in maintaining the base course in a dry condition.

Influence of Change in Water Content of the Subgrade on Its Resilient Deformation—The influence of the water content of the subgrade on tests performed at the surface of the subgrade has already been noted (Fig. 12). This influence is also important when considering the results of tests on layered systems. Figure 22 indicates that, for the change in water content which occurred from test series A to test series B, the resilient deformation of the subgrade increased on the order of 40 percent.

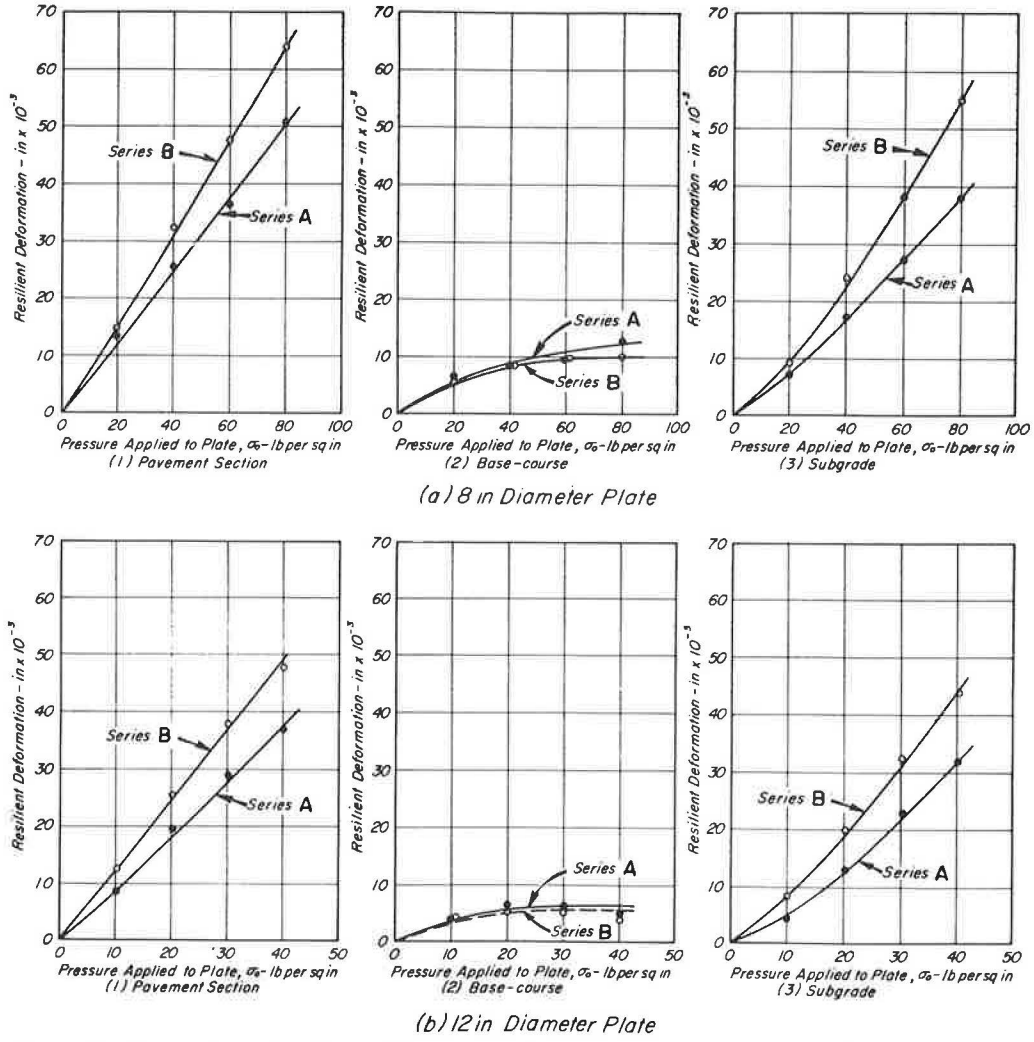

Figure 22. Comparison of resilient deformations of pavement components in two-layer system in test series A and B; 8-in. base.

PREDICTION OF DEFLECTIONS IN TWO-LAYER SYSTEMS

To predict the resilient deformation of an untreated-aggregate base course, both the resilient moduli and the stresses within the layer of material must be ascertained. As has already been noted, the modulus of resilient deformation of base-course materials is dependent on stress and, as seen in Figure 4, can be related to confining pressure. Because the vertical and horizontal stresses induced in a pavement by a wheel load vary both vertically and horizontally, the resilient modulus within the base will vary accordingly. However, no workable theoretical solution of pavement stresses and deflections which accounts for the variation of modulus in vertical and horizontal directions is available at the present time. Thus, the variation in modulus must be taken into consideration through simplifying assumptions.

In the following analyses, it will be assumed that the modulus of resilient deformation of the base course underneath the loading plate is constant along a horizontal plane (see Appendix). Variation of the modulus in the vertical direction can be approximated by subdividing the base course into several horizontal layers, each of which is assumed to have a constant modulus throughout its thickness. The modulus of each horizontal layer may then be determined by calculating the lateral stresses in the layer, resulting from the applied load and the weight of the pavement, and selecting the corresponding modulus from the results of repeated-load triaxial tests (relating the resilient modulus to confining pressure).

Proposed Analysis

Stresses and deflections in pavements can be analyzed by assuming that the materials behave like uniform elastic materials (Boussinesq), or like layered elastic materials (Burmister). In the latter case, approximate ratios of the moduli of the layer components must be determined.

McMahon and Yoder (28) and Sowers and Vesic (30) have shown that the stresses measured in two-layer systems consisting of an untreated base course overlying a compressible soil (similar to the two-layer systems analyzed in this study), are very similar to those predicted by Boussinesq's analysis for stress distribution; results of the analyses shown in subsequent sections also support this conclusion. Therefore, it has been considered appropriate to assume, for the two-layer system, that the lateral and vertical stresses are equal to those determined by the Boussinesq theory of stress distribution.

With this assumption, the proposed procedure to estimate the resilient deformations of the system consisting of an untreated granular base and subgrade can be briefly summarized as follows:

1. To compute the modulus of resilient deformation of the base course, the horizontal normal stresses resulting from the applied load can be estimated using the expression developed from the Boussinesq solution and presented by Ahlvin and Uhlery (34):

$$\sigma_H = \sigma_o [2\nu A + C + (1 - 2\nu) F] \quad (4)$$

where

σ_H = lateral pressure,

σ_o = uniform pressure at the surface of the base course[3],

ν = Poisson's ratio, and

A, C and F = functions depending on the depth and offset of the element under consideration relative to the center of the plate—determined from tables presented by Ahlvin and Uhlery (34).

The stresses are computed along a vertical line offset from the center of the plate at a distance equal to 0.7 times the radius of the plate[4] and for values of Poisson's ratios of 0.35 and 0.50, since it appears that the values for granular materials lie between these two limits so long as the deformations are small.

The lateral confining pressure caused by the weight of the material above a particular point can be determined by assuming that it is equal to the earth pressure at rest and,

---

[3]The computed values are based on a uniform surface pressure applied to a circular area, whereas the measured values are obtained from rigid-plate tests. Computations which have been made for a few of the conditions analyzed in the report show that there is, at the most, a ± 20 percent change in the deflection pattern under the plate for the flexible as compared to the rigid loaded area.

[4]This distance divides the contact area into two equal parts.

in the case of granular materials, the coefficient of earth pressure at rest, K_o, is assumed to be 0.5. This stress, when added to the lateral stress induced by the applied load, is considered as the controlling stress in defining the resilient modulus of the granular material at this point.

2. The variation in horizontal normal stress with depth can then be used to determine the variation of the modulus of resilient deformation of the base course with depth from the results of repeated-load triaxial tests at appropriate confining pressures.

3. The vertical stresses under the center of the plate induced in the subgrade by an applied load are calculated to a depth of 4 radii from the surface, on the assumption of a Boussinesq stress distribution.

4. The variation in vertical normal stress with depth in the subgrade can be used to determine the variation of the modulus of resilient deformation of the subgrade from repeated-plate-load tests on the subgrade under various vertical stresses or from repeated-load triaxial tests on the subgrade material with a range in deviator stresses (6), as seen in Figure 12.

5. The variation of resilient modulus with depth can be considered by dividing the base course and subgrade into several horizontal layers, each having a constant modulus equal to the average modulus over the thickness of each layer.

6. Deflection factors, presented by Ahlvin and Uhlery (34), can be used to compute the compression of a layer of any thickness at any depth. The deflection of a particular layer along a vertical axis through the center of the plate can be determined from the expression

$$w_{z_1} - w_{z_2} = \sigma_o \frac{1+\nu}{E} r \left[(z_1 A_1 - z_2 A_2) + (1-\nu)(H_1 - H_2)\right] \quad (5)$$

where

w_{z_1} = deflection at top of layer,

w_{z_2} = deflection at bottom of layer,

E = average modulus of the layer,

A and H = functions whose values depend on the location of the point under consideration, and

z = depth in multiples of the radius of the loaded area.

Subscript 1 refers to the upper surface of the layer and subscript 2 to the lower surface.

7. The compression of the individual layers comprising the base course can then be added to give the total deformation of the base course; the deformations of the subgrade can be computed in the same manner.

Example

As an example, an analysis is presented for a 12-in. base course loaded with a 12-in. diameter rigid plate. Confining pressures and the corresponding moduli at points on a vertical line 0.7 rad from the center of the plate have been tabulated in Table 5 for a Poisson's ratio of 0.50. A similar computation was also made for Poisson's ratio of 0.35.

In this table notice that, although the confining pressure contributed by the weight of the base is relatively small in the upper portion, it is a major contributor in the lower portion of the base, especially when the surface pressure is low. The variation in modulus with depth corresponding to the computed confining pressures is shown in Figure 23; the results are typical of the trend obtained in all cases. The modulus of resilient deformation at the surface of the base is several times that at the bottom of the base, the rate of change with depth depending on thickness of the base, plate diameter and applied pressure. In addition, also note that the resilient modulus at the bottom of the base is approximately the same as that of the subgrade (5,000 to 10,000 psi).

TABLE 5

VARIATION OF CONFINING PRESSURE AND CORRESPONDING RESILIENT MODULUS WITH DEPTH IN UPPER LAYER OF TWO-LAYER SYSTEM[a]

Depth (in.)	Confining Pressure Due to Weight of Pavement (psi)	Applied Pressure							
		1		10		20		30		40	
		Confining Pressure (psi)		Confining Pressure (psi)	Resilient Modulus (psi)	Confining Pressure (psi)	Resilient Modulus (psi)	Confining Pressure (psi)	Resilient Modulus (psi)	Confining Pressure (psi)	Resilient Modulus (psi)
0	0.040	0.650		6.54	20,000	13.04	29,000	19.54	34,500	26.04	39,500
2	0.120	0.315		3.27	13,500	6.42	19,500	9.57	24,500	12.72	28,500
4	0.200	0.175		1.95	10,000	3.70	14,500	5.45	18,000	7.20	21,000
6	0.280	0.105		1.33	7,500	2.38	11,500	3.43	14,000	4.48	16,000
8	0.360	0.065		1.01	6,500	1.66	9,000	2.31	11,000	2.96	13,000
10	0.440	0.042		0.86	5,500	1.29	8,000	1.70	9,000	2.12	10,500
12											

[a]System consists of 12 in. of gravel and the natural subgrade; load applied to a 12-in. diameter plate; stresses were obtained from tables prepared by Ahlvin and Uhlery for a value of Poisson's ratio equal to 0.5. Corresponding moduli were obtained from Figure 3.

Figure 23. Variation of modulus of resilient deformation with depth in base course of two-layer system consisting of 12 in. of gravel base and the natural subgrade, 12-in. diameter plate.

By dividing the base course into 6 equal layers and using the moduli determined in Table 5, the deformation of each layer can be obtained from Eq. 5, as shown in Table 6 for a Poisson's ratio of 0.5. The total deflection of the base course is obtained by summing the deflections of the individual layers.

A comparison of the resilient deflections of the base course computed in this way for values of Poisson's ratio equal to 0.5 and 0.35 with those observed in the field tests is shown in Figures 24 and 25 for 8- and 12-in. thick gravel layers.

TABLE 6

RESILIENT DEFORMATION OF 12-IN. BASE LOADED WITH 12-IN. DIAMETER PLATE (ν = 0.5)

Layer	Resilient Deflection, in. $\times 10^{-3}$			
	At Pressure of 10 psi	At Pressure of 20 psi	At Pressure of 30 psi	At Pressure of 40 psi
From 0 to 2 inches	$\frac{10 \times 9 \times .07}{20,000} = .31$	$\frac{20 \times 9 \times .07}{29,000} = .435$	$\frac{30 \times 9 \times .07}{34,500} = .550$	$\frac{40 \times 9 \times .07}{39,500} = .64$
2 - 4	$\frac{10 \times 9 \times .105}{13,500} = .70$	$\frac{20 \times 9 \times .105}{19,500} = .972$	$\frac{30 \times 9 \times .105}{24,500} = 1.160$	$\frac{40 \times 9 \times .105}{28,500} = 1.39$
4 - 6	$\frac{10 \times 9 \times .115}{10,000} = 1.03$	$\frac{20 \times 9 \times .115}{14,500} = 1.423$	$\frac{30 \times 9 \times .115}{18,000} = 1.720$	$\frac{40 \times 9 \times .115}{21,000} = 1.97$
6 - 8	$\frac{10 \times 9 \times .110}{7,500} = 1.32$	$\frac{20 \times 9 \times .110}{11,500} = 1.720$	$\frac{30 \times 9 \times .11}{14,000} = 2.120$	$\frac{40 \times 9 \times .11}{16,000} = 2.48$
8 - 10	$\frac{10 \times 9 \times .090}{6,500} = 1.24$	$\frac{20 \times 9 \times .09}{9,000} = 1.800$	$\frac{30 \times 9 \times .09}{11,000} = 2.210$	$\frac{40 \times 9 \times .09}{13,000} = 2.49$
10 - 12	$\frac{10 \times 9 \times .06}{5,500} = .98$	$\frac{20 \times 9 \times .06}{8,000} = 1.350$	$\frac{30 \times 9 \times .06}{9,000} = 1.800$	$\frac{40 \times 9 \times .06}{10,500} = 2.06$
Total Resilient Deformation, in. $\times 10^{-3}$	5.60	7.76	9.56	11.03

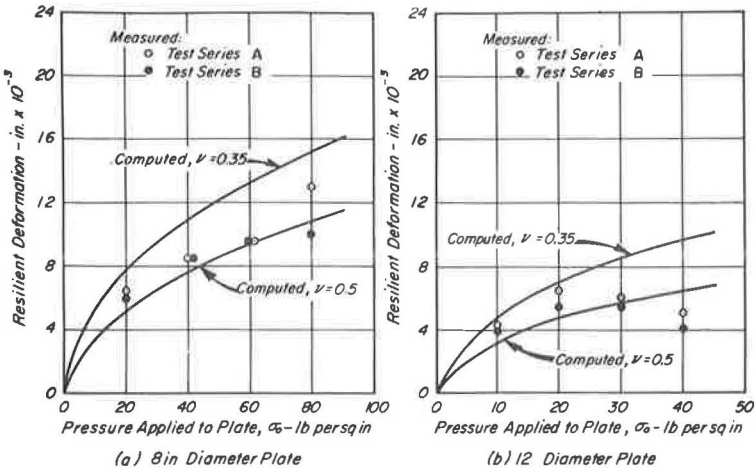

Figure 24. Comparison between computed and measured resilient deformations of base course in a two-layer system consisting of 8 in. of base and the natural subgrade; test series A and B.

These figures indicate that the resilient deformations of the base course computed for a Poisson's ratio of 0.35 are about 40 percent higher than those computed for a Poisson's ratio of 0.50. It has been suggested (35) that, for a homogeneous material, the resilient deflection under a plate load for a material with a Poisson's ratio of 0.35 would be about 17 percent higher than when Poisson's ratio was 0.50. However, the change in confining pressure due to a change in Poisson's ratio, and the corresponding change in resilient modulus, were not considered in this latter analysis. A low value of Poisson's ratio creates lower confining pressures and correspondingly decreases the modulus of resilient deformation. When this factor is considered, the increase in

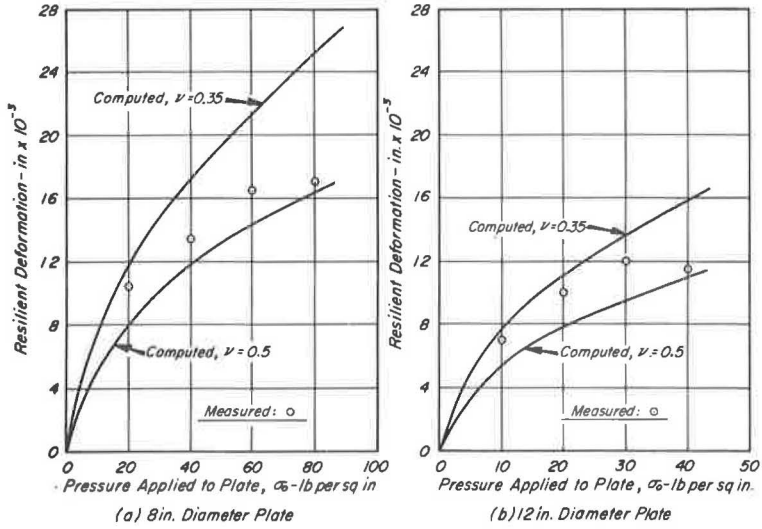

Figure 25. Comparison between computed and measured resilient deformations of base course in a two-layer system consisting of 12 in. of base and the natural subgrade; test series A.

TABLE 7

DETERMINATION OF RESILIENT DEFORMATION IN SUBGRADE—12-IN. THICK BASE, 12-IN. DIAMETER PLATE AND 20-PSI APPLIED PRESSURE

Depth from the Surface of the Pavement (in.)	Vertical Stress (psi)	Corresponding Modulus of Resilient Deformation[a] (psi)	Resilient Deformation in Layer Between Indicated Depths (in. × 10^{-3})
12	5.70	8,000	1.71
15	3.98	8,900	1.11
18	2.92	10,000	1.30
24	1.74	13,400	3.27
			Σ = 7.40

[a]From Figure 12.

resilient deflection due to a change in Poisson's ratio from 0.5 to 0.35 will change from 17 percent to 40 percent.

The measured resilient deformations of the base course fall, in general, within the range of resilient deformations predicted, although at high stresses for the 8-in. base-course tests the measured deflections are somewhat lower than those predicted; this difference may be due to the fact that at the higher stresses the plastic deformation was continuously increasing with number of load applications.

In general, the results of this approximate analysis using the results of repeated-load triaxial tests agree reasonably well with the measured resilient deflections in plate-load tests, especially if Poisson's ratios of 0.40 to 0.45 are assumed in the computations.

A similar analysis has been used for determining the resilient deformation of the subgrade. For example, the deformations in this material under a 12-in. base course

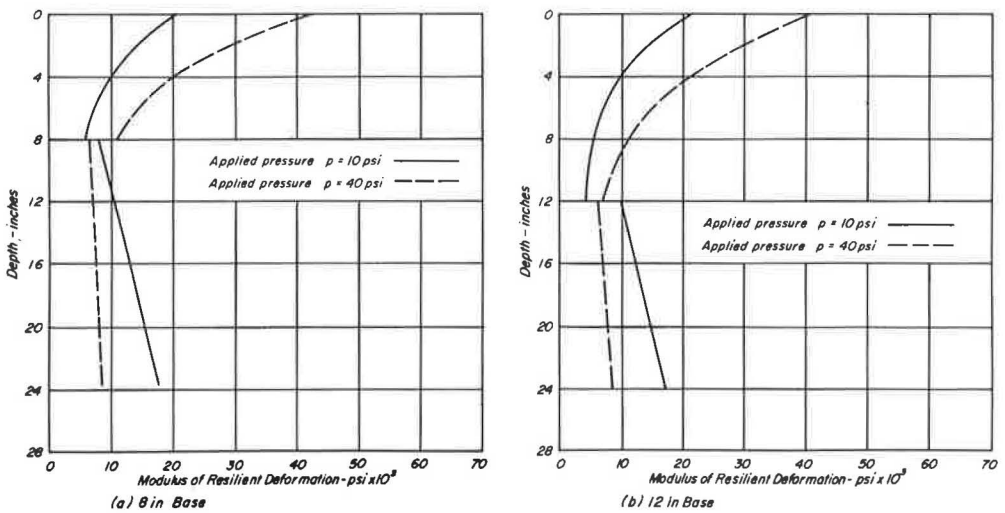

Figure 26. Variation of resilient modulus with depth beneath the center of a 12-in. diameter plate in two-layer systems (ν_{base} and $\nu_{subgrade}$ assumed equal to 0.35 and 0.5, respectively); test series A.

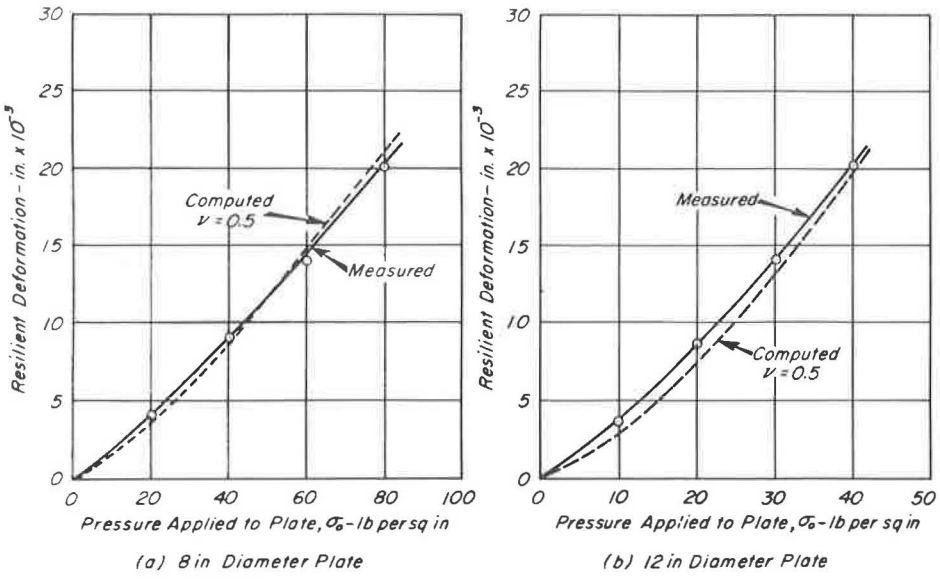

Figure 27. Comparison between measured and computed subgrade deflections for two-layer system consisting of 12 in. of base and the natural subgrade; test series A.

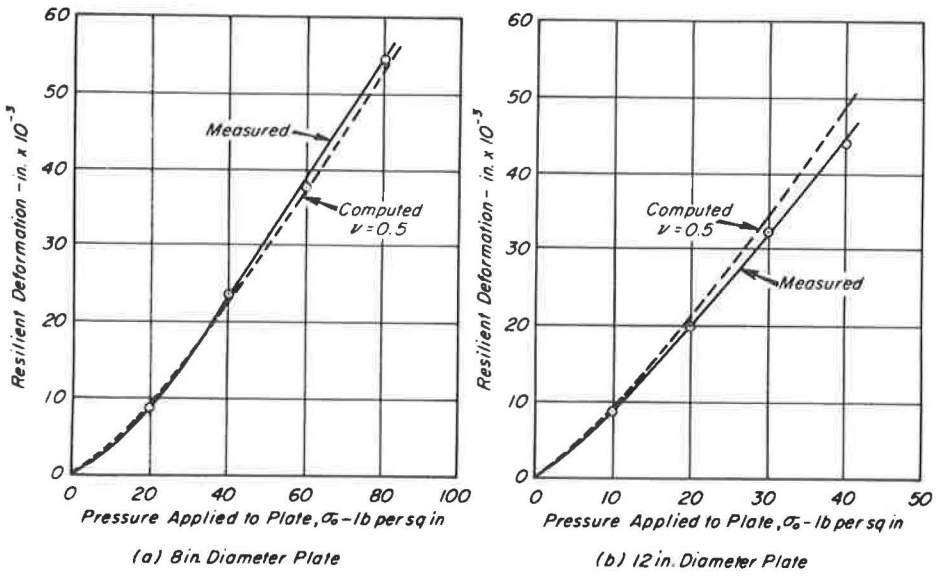

Figure 28. Comparison between measured and computed subgrade deflections for two-layer system consisting of 8 in. of base and the natural subgrade; test series B.

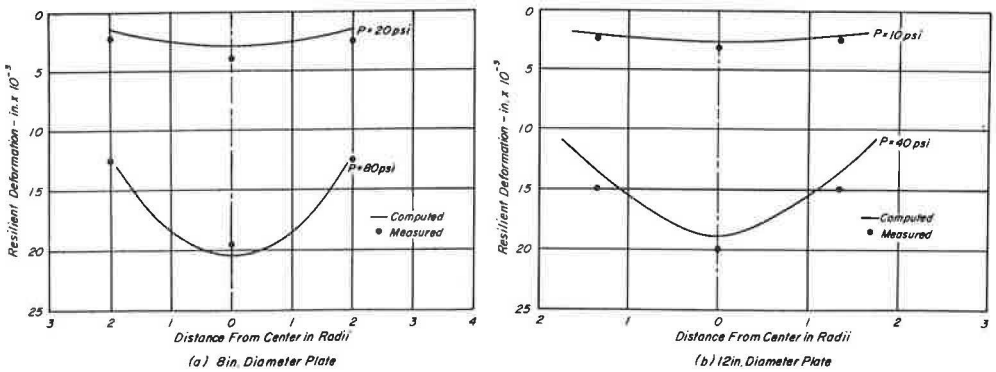

Figure 29. Comparison between computed and measured resilient deformations at the base-subgrade interface for two-layer systems consisting of 12 in. of base and the natural subgrade; test series A.

loaded by a 12-in. diameter rigid plate with an applied pressure of 20 psi are given in Table 7. For convenience, the subgrade has been divided into four layers, and the vertical stress at the top of each layer estimated from the tables prepared by Ahlvin and Uhlery. The moduli of resilient deformation corresponding to these vertical stresses were in turn estimated from Figure 12 (test series A). Deformations were then computed from Eq. 5 with a value for Poisson's ratio of 0.5.

The moduli for the subgrade determined in this way together with those obtained previously for the base course are plotted in Figure 26 to illustrate the variation in

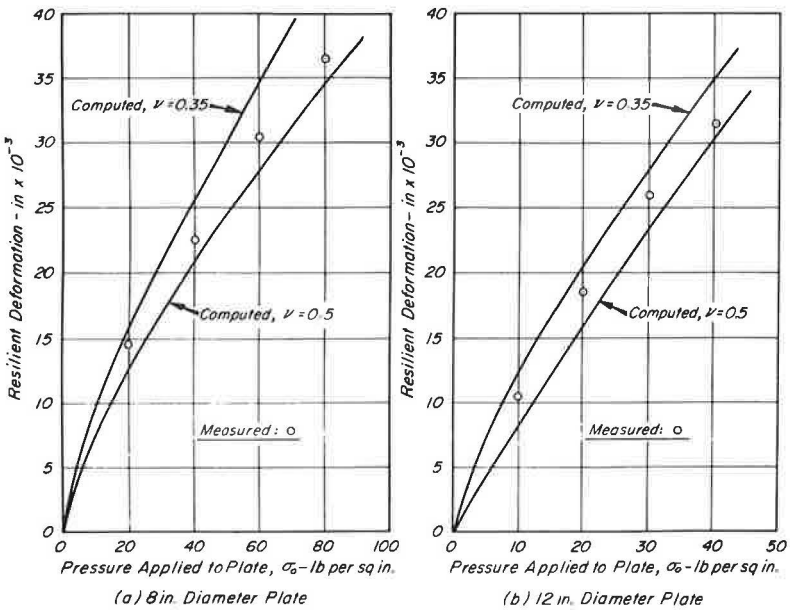

Figure 30. Comparison between computed and measured total resilient deformation for two-layer system consisting of 12 in. of base and the natural subgrade; test series A.

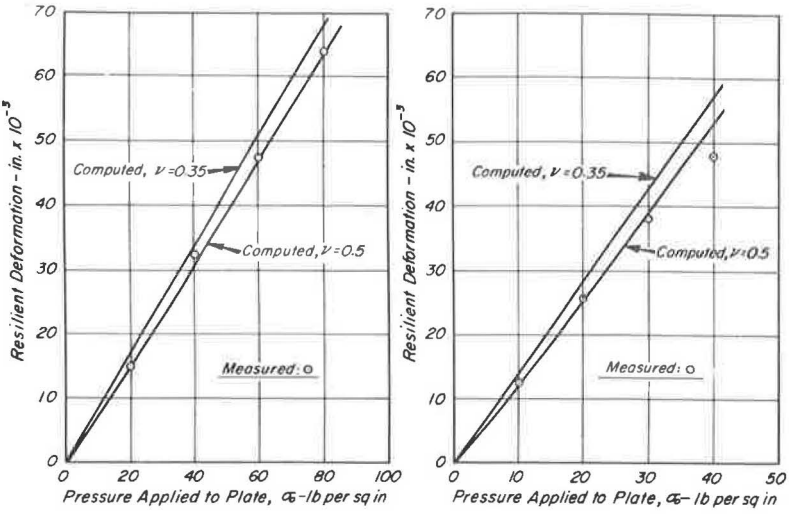

Figure 31. Comparison between computed and measured total resilient deformation for two-layer system consisting of 8 in. of base and the natural subgrade; test series B.

base-course and subgrade moduli with depth for the above conditions. It will be noted that the ratio of the modulus of the base to that of the subgrade at the interface of the two layers varies from approximately 0.4 to 1.75, depending on the surface pressure.

Comparisons between computed and measured deflections directly below the center of the plate at the surface of the subgrade are shown in Figures 27 and 28. The computed values are based on a value for Poisson's ratio equal to 0.5 and moduli determined from Figure 12. Excellent agreement is indicated for both 8- and 12-in. diameter plates.

In a similar manner, the variation of deflection at the top surface of the subgrade has been computed along a radial line, using Eq. 5. The values obtained are compared to those determined from the field tests in Figure 29; again, good agreement is indicated.

Comparisons between the computed total resilient deformations and the corresponding measured deformation are presented in Figures 30 and 31. The computed values in this case were obtained by adding the resilient deformations shown in Figures 24 and 25 for the gravel to those shown in Figures 27 and 28 for the subgrade. The predicted and measured values, as shown in these figures, are again in reasonably close agreement.

These results would indicate that the resilient deformations of two-layer systems consisting of untreated granular base and compressible subgrade soils can be reasonably predicted from the results of laboratory repeated-load triaxial-compression tests by the proposed analysis.

SUMMARY

This investigation was undertaken because of the interest in deflections under load as a measure of pavement performance, and the need for a procedure whereby pavement deflections could be predicted in advance from suitable laboratory tests.

The deflections of interest are essentially elastic in the sense that they are completely recoverable (for all practical purposes) on unloading and appear to be

approximately proportional to load. However, in order that these deformations should not be confused with elastic deformation in the classical sense, they have been termed resilient deformations.

It would appear that one of the major difficulties in predicting resilient pavement deflections is the lack of knowledge concerning the resilient behavior of untreated granular materials; hence, the major portion of this paper has been devoted to a discussion and definition of the factors influencing the resilience characteristics of these materials. It has involved the measurement of the resilient behavior of representative granular materials in the laboratory, the measurement of deflections of prototype pavements composed of one of these materials (a well-graded, partially crushed gravel) in the field, and the relating of the laboratory test results to the observed deflections of the prototype pavements.

One of the major factors influencing the resilience characterisitcs of granular materials has been the magnitude of the applied stress. Since stresses due to load vary in both the vertical and horizontal directions in a pavement section, this influence of stress on resilience should properly be accounted for in order to adequately predict the deformation characteristics of the pavement section. Accordingly, an evaluation of existing methods for computing stress distributions was also prepared. This evaluation was based on analyses for elastic media, since it is the transient recoverable deflections due to passage of the wheel load which are of interest.

Essentially two methods are available: Boussinesq considered stresses and displacements in a uniform system, whereas Burmister considered a layered system. The evaluation indicated that the actual distribution of stress in pavements constructed of untreated granular materials is most closely approximated by the Boussinesq analysis. Accordingly, approximate values for deflections in these structures may be obtained by using the Boussinesq theory and the modifications suggested by Vesic to account for the variability in deformation characteristics (as measured by resilient moduli) of the granular material. This method has been used to analyze the results of tests performed on the two-layer systems studied in this investigation.

CONCLUSIONS

1. The results of repeated plate-load tests at the surface of the subgrade indicate that the modulus of resilient deformation of clay soils varies extensively with the applied pressure and water content. The resilient modulus of the subgrade soil used in the test program decreased rapidly in the range of stress between 1 and 10 psi (which is the range to be expected in the subgrade of well-designed pavements); the modulus had an effectively constant value at a stress of the order of 10 psi and over. The test results also indicated that the rate of change in modulus with stress is dependent on water content. As the water content increased, the rate of change in modulus with stress decreased. When comparing the results of two series of tests conducted with the subgrade at different water contents, the resilient modulus was reduced to about one-half the initial value as the subgrade became wetter. This change emphasizes the importance of allowing for possible variations in the modulus of the subgrade due to environmental changes during the pavement lifetime.

2. The resilient deformation of an untreated base course depends on (a) confining pressure—the average modulus of resilient deformation increases with the confining pressure; (b) thickness of base—the resilient deformation of the base increased as the thickness of base increased from 8 to 12 in.; and (c) plate diameter—when the surface pressure remained constant, the resilient deformation of the base course decreased as the diameter of the plate increased from 8 to 12 in. The resilient deformation per inch of thickness of base decreased as the ratio of plate diameter to thickness of base increased.

3. A general statement concerning the relative contribution of the base and subgrade to the total resilient deformation of a two-layer pavement section cannot readily be made on the basis of data obtained from the field tests. It appears that, because the modulus of the base increases and that of the subgrade decreases as the applied stress

increases, the resilient deformation of the subgrade becomes relatively more significant at higher magnitudes of surface-pressure applications.

4. Results of repeated-load triaxial-compression tests on dry granular materials indicate a unique relationship between the modulus of resilient deformation and the confining pressure (σ_3) so long as a shear failure does not occur. A similar relationship appears also to be valid in terms of the sum of the principal stresses.

The modulus of resilient deformation of the dry materials varies with the effective confining pressure or the sum of the principal stresses according to the equations

$$M_R = K \cdot \sigma_3^n \quad \text{and} \quad M_r = K' \cdot \theta^{n'}$$

which indicates that the modulus can vary considerably over the range of stresses usually encountered in pavements.

5. The results of repeated-load tests on subgrade and base-course materials clearly show that the resilient moduli vary with stresses. When the stresses at the top and bottom of the base course are very different (i.e., when the base is loaded directly), the resilient modulus at the top of the course may be as much as four times the resilient modulus at the bottom. For the conditions used in this study, the ratio of the moduli of the base course to that of the subgrade at the interface between the two layers varied from 0.4 to about 1.75.

6. The resilient deformations computed by the proposed method from the results of repeated-load triaxial-compression tests for two-layer structures were in reasonably good agreement with the resilient deformations measured in the prototype pavements. Thus, it would appear that the results of repeated-load tests on paving materials can be used within the framework of available theories to predict transient pavement deflections.

ACKNOWLEDGMENTS

This work was sponsored by AASHO in cooperation with the U.S. Bureau of Public Roads, and was conducted in the National Cooperative Highway Research Program which is administered by the Highway Research Board of the National Academy of Sciences—National Research Council. The authors wish to acknowledge the support provided by the Institute of Transportation and Traffic Engineering of the University of California in the form of shop and office staff and facilities, and by the California Division of Highways. Thanks are due to the County of Contra Costa, California, for providing personnel to construct the asphalt-concrete pavement surface and to the Kaiser Sand and Gravel Company for supplying the gravel used in the base courses of the prototype pavements. The authors especially wish to acknowledge the assistance of Masaru Nishi and Chin-Yung Chang who assisted in the development of the test results.

REFERENCES

1. Hveem, F. N. Pavement Deflections and Fatigue Failures. HRB Bull. 114, pp. 43-87, 1955.
2. Monismith, C. L. Symposium on Pavement Behavior as Related to Deflection, Part II—Significance of Pavement Deflections. Proc. AAPT, Vol. 31, pp. 231-253, 1962.
3. Monismith, C. L. Asphalt Mixture Behavior in Repeated Flexure. Rept. No. TE 65-9, Univ. of California, Berkeley, Nov. 1965.
4. State of California, Division of Highways. The Development of a Resilience Design Procedure for Flexible Pavements. Materials and Research Dept. Final Research Rept. No. M&R 431618-2, April 1966.
5. Seed, H. B., and Monismith, C. L. Moderators' Summation of Session V, Strength Evaluation of Pavement Structure Elements. Proc. Internat. Conf. on the Structural Design of Asphalt Pavements, 1962, Univ. of Michigan, pp. 1009-1011, 1963.

6. Seed, H. B., Mitry, F. G., Monismith, C. L., and Chan, C. K. Prediction of Pavement Deflections from Laboratory Repeated Load Tests. Rept. No. TE 65-6, Univ. of California, Berkeley, Oct. 1965.
7. Seed, H. B., and Chan, C. K. Effect of Duration of Stress Application on Soil Deformation Under Repeated Loading. Proc. Fifth Internat. Conf. on Soil Mech. and Found. Eng., Vol. 1, pp. 340-345, 1964.
8. Haynes, J. H., and Yoder, E. J. Effects of Repeated Loading on Gravel and Crushed Stone Base Course Materials Used in the AASHO Road Test. Highway Research Record 39, pp. 82-96, 1963.
9. Biarez, J. Contribution a l'Etude des Proprietes Mecaniques des Sols et des Materiau Pulverulents. D. Sc. thesis. Univ. of Grenoble, France, 1962.
10. DeGraft-Johnson, J. Unpublished Research Report. Soil Mechanics and Bituminous Materials Laboratory, Univ. of California, Sept. 1962.
11. Trollope, D. H., Lee, I. K., and Morris, J. Stresses and Deformation in Two Layer Pavement Structures Under Slow Repeated Loading. Proc. Australian Road Research Board, Vol. 1, Part 2, pp. 693-721, 1962.
12. Dunlap, W. A. A Report on a Mathematical Model Describing the Deformation Characteristics of Granular Materials. Tech. Rept. No. 1, Texas Transportation Institute, Texas A&M Univ., 1963.
13. Coffman, B. S., Kraft, D. C., and Tamayo, J. A Comparison of Calculated and Measured Deflections for the AASHO Road Test. Proc. AAPT, Vol. 33, pp. 54-91, 1964.
14. Hveem, F. N., Zube, E., Bridges, R., and Forsyth, R. The Effect of Resilience-Deflection Relationship on the Structural Design of Asphaltic Pavements. Proc. Internat. Conf. on the Structural Design of Asphalt Pavements, 1962, Univ. of Michigan, pp. 649-666, 1963.
15. Burmister, D. M. Applications of Layered System Concepts and Principals to Interpretations and Evaluations of Asphalt Pavement Performances and to Design and Construction. Proc. Internat. Conf. on the Structural Design of Asphalt Pavements, 1962, Univ. of Michigan, pp. 441-453, 1963.
16. Brown, P. P. Analysis of Flexible Airfield Pavements by Surface Plate-Loading. Proc. Internat. Conf. on the Structural Design of Asphalt Pavements, 1962, Univ. of Michigan, pp. 680-685, 1963.
17. U. S. Army Engineer Waterways Experiment Station. Investigations of Pressures and Deflections for Flexible Pavements, Report No. 1. Homogeneous Clayey Silt Test-Section. Tech. Memo. 3-323, Vicksburg, Miss., 1951.
18. U. S. Army Engineer Waterways Experiment Station. Investigations of Pressures and Deflections for Flexible Pavements, Report No. 4. Homogeneous Sand Testing Section. Tech. Memo. 3-323, Vicksburg, Miss. 1954.
19. Walker, R. D., Yoder, E. J., Spencer, W. T., and Lowry, R. Significance of Layer Deflection Measurements. HRB Bull. 321, pp. 63-81, 1962.
20. Heukelom, W., and Klomp, A. J. G. Dynamic Testing as a Means of Controlling Pavements During and After Construction. Proc. Internat. Conf. on the Structural Design of Asphalt Pavements, 1962, Univ. of Michigan, pp. 667-679, 1963.
21. Nijboer, L. W., and Metcalf, C. T. Dynamic Testing at the AASHO Road Test. Proc. Internat. Conf. on the Structural Design of Asphalt Pavements, 1962, Univ. of Michigan, pp. 713-721, 1963.
22. Jones, R. Following Changes in the Properties of Road Bases and Subbases by the Surface Wave Propagation Method. Civil Engineering and Public Works Review, Part I, May 1963, and Part II, June 1963.
23. Odemark, N. Investigations as to the Elastic Properties of Soils and Design of Pavements According to the Theory of Elasticity. Meddelande 77, Statens Väginstitut, Stockholm, 1949.
24. Dehlen, G. L. An Investigation of Flexure Cracking on a Major Highway. Proc. Internat. Conf. on the Structural Design of Asphalt Pavements, 1962, Univ. of Michigan, pp. 812-820, 1963.
25. Seed, H. B., Chan, C. K., and Lee, C. K. Resilience Characteristics of Subgrade Soils and Their Relation to Fatigue Failures in Asphalt Pavements.

Proc. Internat. Conf. on the Structural Design of Asphalt Pavements, 1962, Univ. of Michigan, pp. 611-636, 1963.
26. Burmister, D. M. The General Theory of Stresses and Displacements in Layered Soil Systems. Jour. Appl. Phys., Vol. 16, No. 2, pp. 89-96; Vol. 16, No. 3, pp. 126-127; Vol. 16, No. 5, pp. 296-320, 1945.
27. Whiffin, A. C., and Lister, N. W. The Application of Elastic Theory to Flexible Pavements. Proc. Internat. Conf. on the Structural Design of Asphalt Pavements, 1962, Univ. of Michigan, pp. 499-521, 1963.
28. McMahon, T. F., and Yoder, E. J. Design of a Pressure Sensitive Cell and Model Studies of Pressures on a Flexible Pavement Subgrade. HRB Proc., Vol. 39, pp. 650-682, 1960.
29. Vesic, A. B. Discussion presented at Session III. Proc. Internat. Conf. on the Structural Design of Asphalt Pavements, 1962, Univ. of Michigan, pp. 283-290, 1963.
30. Sowers, G. F., and Vesic, A. B. Stress Distribution Beneath Pavements of Different Rigidities. Proc. Fifth Internat. Conf. on Soil Mech. and Found. Eng., Vol. 2, pp. 327-332, 1961.
31. Sowers, G. F., and Vesic, A. B. Vertical Stresses in Subgrades Beneath Statically Loaded Flexible Pavements. HRB Bull. 324, pp. 90-123, 1962.
32. Jakobson, B. Some Fundamental Properties of Sand. Proc. Fourth Internat. Conf. on Soil Mech. and Found. Eng., London, Vol. 1, pp. 167-171, 1957.
33. Cumming, D. A., and Gerrard, C. M. Computation of Stresses on Pavements. Proc. Australian Road Research Board, Vol. 2, Part 2, pp. 729-743, 1964.
34. Ahlvin, R. G., and Uhlery, H. H. Tabulated Values for Determining the Complete Pattern of Stresses, Strains, and Deflections Beneath a Uniform Circular Load on a Homogeneous Half Space. HRB Bull. 342, pp. 1-13, 1962.
35. Peattie, K. R., and Jones, A. Surface Deflections of Road Structures. Proc. Symposium on Road Tests for Pavement Design, 1962, Lisbon, Portugal, pp. VIII, 1-30.

Appendix

ANALYSIS OF ASSUMPTION OF CONSTANT MODULUS IN THE HORIZONTAL PLANE FOR TWO-LAYER SYSTEMS

In the paper, two-layer systems consisting of untreated granular material and the natural subgrade were analyzed by dividing the base course into a series of horizontal layers. To simplify this analysis, the variation of the resilient modulus in the horizontal direction was assumed negligible with respect to that in the vertical direction. This assumption was based on the results of analyses, examples of which are shown in Figures 32 and 33.

In these figures, contours of resilient moduli have been plotted to show their variation in both the horizontal and vertical directions. Moduli were determined from the results of the repeated-load triaxial-compression tests using the sum of horizontal stresses resulting from the applied load and the weight of the pavement. Thus it would appear that the assumption of a constant modulus in a horizontal plane under the loaded area is justified.

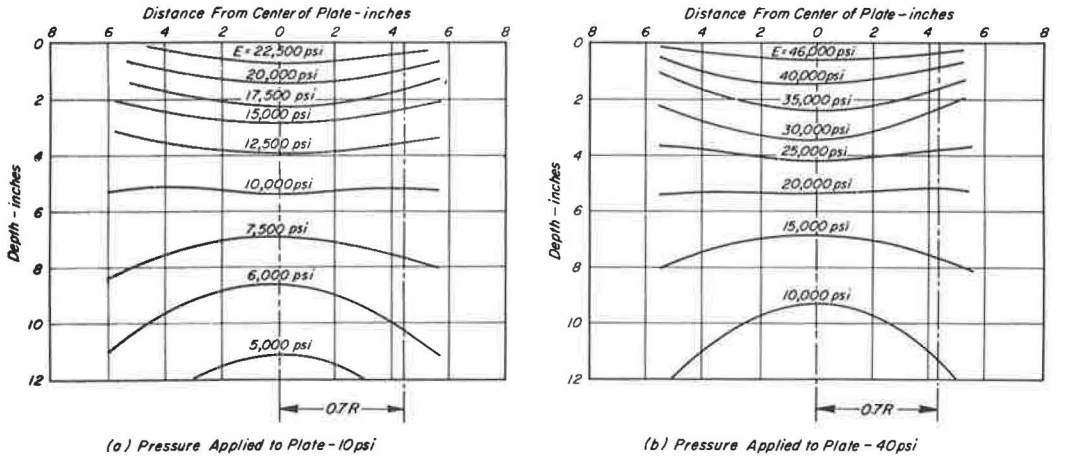

Figure 32. Variation of modulus of resilient deformation under 12-in. diameter plate in 12-in. thick base (σ_o = 20 psi, ν = 0.5, K_o = 0.5).

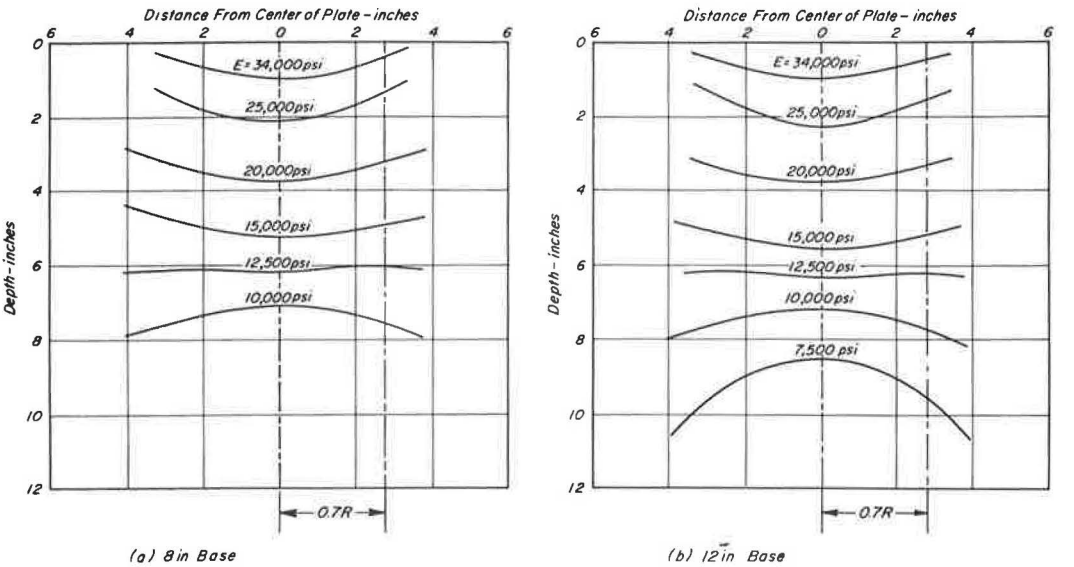

Figure 33. Variation of modulus of resilient deformation under 8-in. diameter plate in both 8- and 12-in. thick base courses (σ_o = 20 psi, ν = 0.5, K_o = 0.5).

Monte Carlo Simulation of Pile Performance

B. B. SCHIMMING and W. A. GARVEY
Respectively, Associate Professor and Research Assistant, Department of Civil Engineering, University of Notre Dame

The study of the interaction of engineered foundations with the earth as a probabilistic environment is the basic theme of this investigation. The effect of statistically variable soil deposits on foundation design parameters is of primary concern.

In particular, the Monte Carlo simulation technique is discussed and applied to a specific example. The replacement of analytical inference with observation via simulation is emphasized. The example presented consists of the prediction of design variables such as mean length, etc., for friction piles driven into a two-layer soil deposit overlying rock. The strength of the soil and depth to rock are treated as stochastic variables. The importance of the size of the sample required for a competent simulation is discussed.

•THE earth, quite literally, is the base for all civil engineering structures. Paradoxically, the most prevalent material the engineer deals with is also the most complex. Confronted with a typical nonlinear, anisotropic, nonhomogeneous and stratified soil deposit, a strategic retreat is often made into a linear, isotropic homogeneous theory.

Equally important but sometimes ignored is the extent to which the actual configuration of the subsurface deposits are known. By definition, samples of the foundation environment are taken and with the aid of geological principles, estimates are made of the shape and size of the deposits encountered. A deterministic conclusion is reached from sampling a probabilistic environment. Quite obviously the output is not justified by the input.

What is required is the study of the interaction of a foundation with the so-called probabilistic environment of the earth's crust. The discussion and application of a particularly powerful technique for this type of study comprises the subject of this paper.

SIMULATION

Simulation in the context of this paper essentially means that a controlled representation of reality is utilized in order to obtain information about the behavior of a system. Observation of the behavior of the system replaces the inference associated with analysis because the system is simply too complicated to permit inference to work.

Simulation of problems involving stochastic variables utilizes the aptly named Monte Carlo techniques. The first practical problems treated by the Monte Carlo method were connected with the design of atomic weapons at Los Alamos during World War II. "In these problems nature was directly modeled in its probabilistic aspects and many problems in particle diffusion were solved" (1).

The Monte Carlo method is not limited to probabilistic simulation. The principle can be extended to difficult mathematical problems arising from deterministic problems

Paper sponsored by Committee on Mechanics of Earth Masses and Layered Systems and presented at the 46th Annual Meeting.

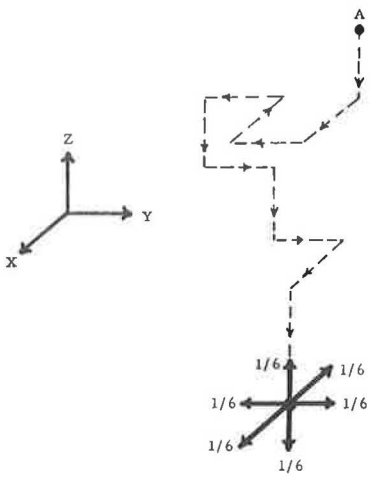

Figure 1.

by finding analogous problems in probability leading in their analysis to formally identical mathematical equations and then solving the probability problems by sampling experiments.

In order to demonstrate the mechanics of the Monte Carlo probabilistic simulation procedure, an easily visualized problem (Fig. 1), has been chosen for discussion. A colloidal particle or ion, A, finds itself in an environment where it is a victim of Brownian motion. This simply means that it suffers collisions with other particles that cause it to trace a rather haphazard or random path. The path can be simulated in the following manner: At any particular location in a three-dimensional space there are 6 possible directions of motion the particle can assume as a result of a collision. If any one of these directions is as likely as another (i.e., they are completely random), then the probability of any particular path is $\frac{1}{6}$. To initiate the "random walk," a choice must be made for the direction of the first step. This is accomplished by generating a random number which dictates the consequence of the first collision. For example, if a die is rolled, and each of the 6 numbers on the die correspond to one of the 6 possible directions, then the result of the roll will determine the particle direction. If the process is repeated each time the particle arrives at a new destination, the history of a particular walk can be traced.

It is important to note that this trace is probably not the actual course taken by the real particle. However, if a large number of walks are simulated and the average behavior statistically examined, then reality can be statistically predicted. Also of importance is the awareness of the nature of the technique. The outcome of a large number of simple computations are observed. Labor replaces sophistication in the interest of describing reality which is usually not digestable by elegance. Thus, a digital computer is practically a necessity.

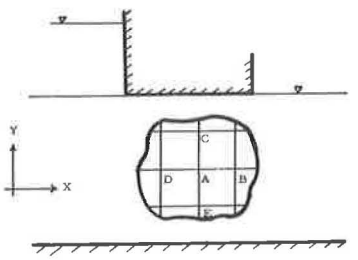

1. POTENTIAL FUNCTION DESCRIPTION:

$$\frac{\partial^2 \phi}{\partial x^2} + \frac{\partial^2 \phi}{\partial y^2} = 0$$

in finite difference notation

$$\phi_A = 1/4\ (\phi_B + \phi_C + \phi_D + \phi_E)$$

2. PROBABILITY OF A PARTICLE PERFORMING A RANDOM WALK ARRIVING AT A

$$P_A = 1/4\ (P_B + P_C + P_C + P_E)$$

Figure 2.

The use of the Monte Carlo technique as an analog for solving deterministic problems is probably best known in the soil mechanics area for seepage applications.

As shown in Figure 2, the finite difference approximation to the Laplacian describing the potential function for flow in a porous medium is the same as the probability equation describing the likelihood that a particle moving randomly will arrive at point A in terms of its probability of arriving at B, C, D and E. Thus, by sampling a large number of random walks on a grid overlying the flow regime, the probability and hence potential distribution can be obtained. A complete description of this application is given by Scott (2).

PILE FOUNDATION SIMULATION

An almost classic case of the interaction of an engineering design with a probabilistic environment is the driving of piles into soil which can only be statistically described.

If a large project involving a number of different foundation requirements is in the preliminary design stages, the feasibility of pile foundations will probably be involved. If the exact location of the piles is not established, only a probabilistic answer can be given for the response of the interaction of the piles and the statistically variable soil mass.

The first step in the analysis involves a quantitative description of the probabilistic character of the soil. As shown in Figure 3, a two-layer system overlying an irregular rock layer has been chosen for consideration. Three different soil types are present in each layer. The probabilities listed over the strength distribution of each type indicate their relative prevalence. For example, soil A, with P = 0.3 was encountered in 30 percent of the borings, soil B, 40 percent of the time, etc. Now, within each soil type there is a strength distribution as dictated by the bar chart. Again, examining soil A, 30 percent of the samples had a shear strength of approximately 0.06, 20 percent had a strength of 0.16, etc. The sum of these probabilities must of course equal 1.0, as is also the case for the probability of occurrence of different soil types in each layer.

The bar chart at the bottom of Figure 3 gives the distribution of rock depths encountered—20 percent of the borings found rock at 22 ft, 10 percent at 26 ft, etc. The flatness of the distribution points to a gradual slope of the rock surface over the site.

With the statistical features of the soil deposit established, it is now possible to commence the simulation. The simulation sequence is schematically outlined in Figure 4.

A location for driving the first simulated pile is in a sense chosen by generating a random number that states which soil type is encountered. Various subroutines are available for generating random numbers on the digital computer. Of the integers 0

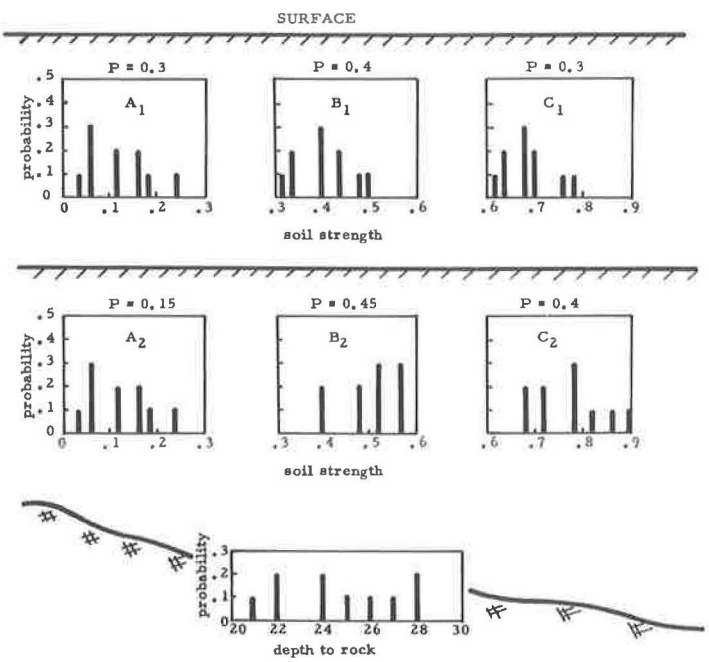

Figure 3.

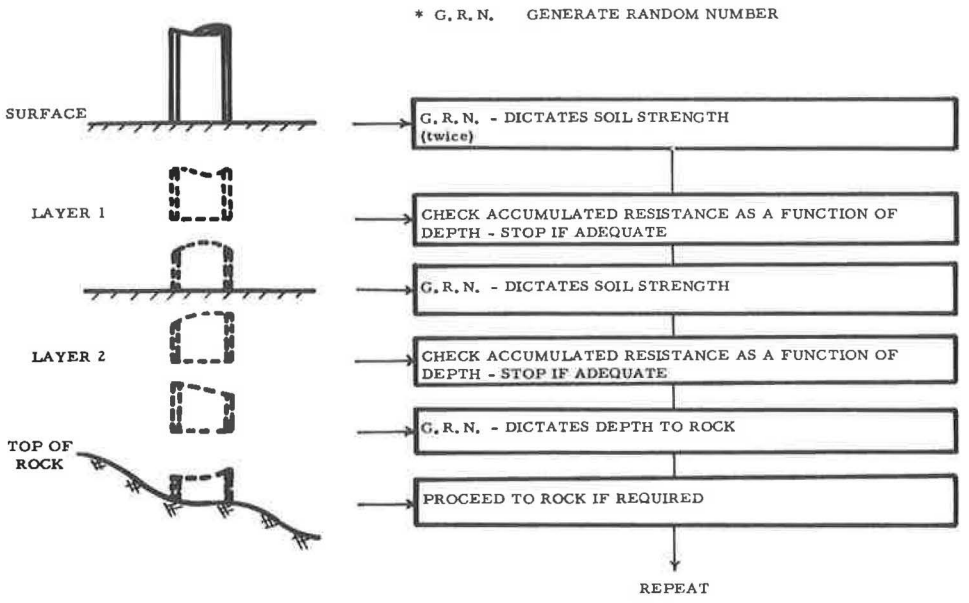

Figure 4.

to 9 inclusive, the choice of 0, 1 or 2 would correspond to soil A_1; 3, 4, 5 or 6 would correspond to soil B_1; and 7, 8 or 9 to soil C_1. Once the soil type is established, a second random number is generated which picks the particular strength encountered, i.e., 0 would mean a strength of 0.04 for soil A_1, 1, 2 or 3 a strength of 0.06, 4 or 5 a strength of 0.12, and so on.

The simulated driving can now be started. As the pile penetrates the top layer, the accumulated resistance along the perimeter is checked at 1-ft intervals for accommodation of the applied column load. If adequate resistance is not accrued when the bottom of the first layer is reached, the soil type encountered in the second layer must be chosen. The random number generation and decision-making is repeated using the strength distribution in layer 2. If at a depth of 20 ft (top of rock), sufficient skin friction has not developed to support the column load, the depth to the rock surface at the simulated location is again determined by random sampling. This provides sufficient information to determine the final pile length. The behavior of a second pile is now simulated by repeating the entire process as described for the first pile.

The question now arises as to how many simulated piles should be driven to adequately sample the soil-pile interaction. Figure 5 shows the mean pile length as a function of number of simulations for various column loads. It is readily apparent that 100 samples would have been adequate for engineering purposes. However, caution should be exercised regarding general conclusions about this limited sample size. The extent of sampling required is related to the complexity of the phenomenon under study. A much larger sample would have probably been required for a soil environment with more "branches" in the probabilistic tree diagram. It appears that the most direct approach to this question is to examine a variable of interest as a function of sample size in order to locate where the response stabilizes. This is especially true when using a digital computer.

For design purposes, the pile variables are conveniently plotted as a function of column load. The mean pile length as a function of column load is shown in Figure 6. As can be seen, there is an increase in length of approximately 5 ft as the column load is increased from 25 to 40 tons with less than a 2-ft increase for an increase from 40 to 100 tons. The effect of the undulating rock surface is thus quite vividly portrayed. Up to approximately 40 tons, most of the piles do not reach rock; however, for column loads greater than 40, the majority do bear on rock.

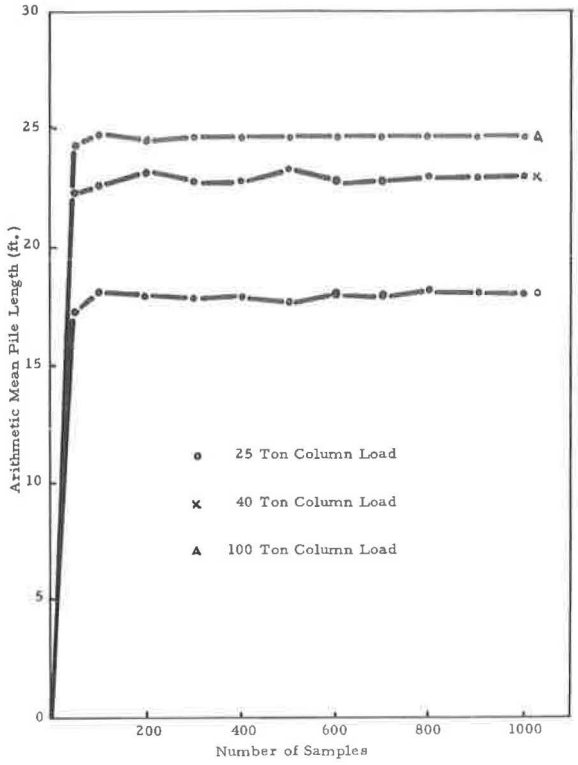

Figure 5.

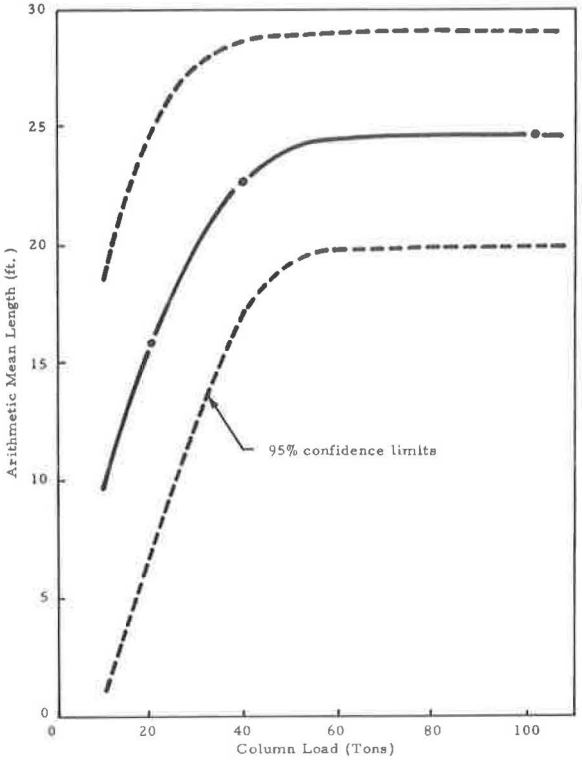

Figure 6.

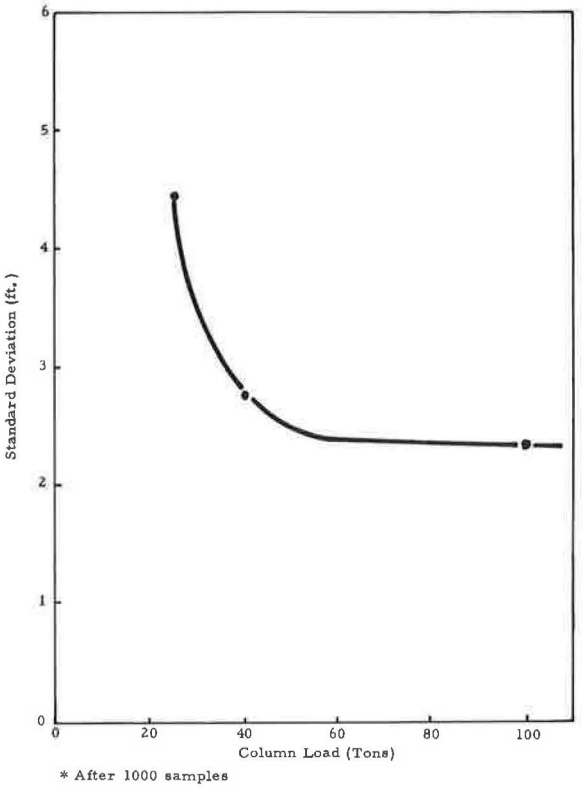

Figure 7.

It would appear that in conjunction with the structural requirements, this type of chart would greatly facilitate the decision as to whether or not to consider pile foundations.

Also of interest to the designer would be the variations in pile length as measured by the standard deviation for different column loads (Fig. 7). At the 25-ton column load the variation in strength of the soil results in a 4.5-ft standard deviation; however, again as the column load is increased and more piles bear on rock the standard deviation decreases as there is less variation in elevation of the rock surface than in soil strength.

CONCLUSIONS

A number of other variables such as elapsed driving time, etc., could have been presented for the particular problem under consideration. However, the purpose of this paper has been to explain and demonstrate the use of the Monte Carlo simulation technique rather than solve a particular problem.

As a technique such as probabilistic simulation is developed by workers in related disciplines, the profession of civil engineering becomes obligated to explore potential areas of application. As typified by this presentation, there is no excuse to ignore some of natures realities as new methods become available.

REFERENCES

1. Marshall, A. W. Symposium on Monte Carlo Methods. John Wiley and Sons, New York, 1956.

2. Scott, R. F. Principles of Soil Mechanics. Addison-Wesley Publishing Co., 1963.
3. Parzen, E. Modern Probability Theory and Its Applications. John Wiley and Sons, New York, 1960.
4. Chorafas, D. N. Systems and Simulation. Academic Press, 1965.
5. The Monte Carlo Method. National Bureau of Standards Applied Math. Series, No. 12, 1951.
6. Ackoff, R. L. Progress in Operations Research. Vol. 1, John Wiley and Sons, New York, 1961.
7. Beckenbach, E. F. Modern Mathematics for the Engineer. McGraw-Hill Book Co., New York, 1961.
8. Churchman, C. W., Ackoff, R. L., and Arnoff, E. L. Introduction to Operations Research. John Wiley and Sons, New York, 1957.

Stresses and Deflections in Stabilized Soil Layers

BILLY J. HARRIS and JOAKIM G. LAGUROS
Respectively, National Science Foundation Fellow and Associate Professor of Civil Engineering, University of Oklahoma

The improvement of the engineering properties of three highly plastic clayey soils resulting from stabilization with portland cement, hydrated lime and conjunctively with sodium hydroxide was measured in terms of strength beneficiation. The 28-day unconfined compressive strengths rose to the 120- to 750-psi range and the static modulus of elasticity assumed values from 1.1×10^3 to 1.9×10^4 psi.

These results imply that when similar stabilization responses are established, the soil used as a base resembles a semirigid beam resting on a subgrade behaving like an elastic foundation. To determine the stresses in the stabilized soil base, a new method is suggested whereby use is made of Westergaard's plate theory and Winkler's beam-on-elastic foundation model. First the stresses induced by a surface point load are calculated, assuming that the plate theory holds true. Then the Winkler model is applied to a section of the base having a finite beam length equal to the width of the pavement and an unknown beam width b_e. The stress is calculated in terms of the width b_e. By equating the two stresses, the equivalent beam width is established.

Graphs and tables of stresses are presented for a 10,000-lb wheel load at 75-psi tire pressure with various combinations of modulus of elasticity, subgrade reaction and layer thickness. A set of deflection parameters was calculated and compared to a set of PCA field data. The theoretical results are in agreement with the experimental data.

THE stresses induced in the constituent layers of a pavement by surface loads have been the subject of experimental and theoretical research for many years. The extensive use of modified soil such as lime or cement stabilized soil in pavement structures makes the determination of these stresses more difficult because such modified soils characteristically fall into the category of semirigid materials. Recently, it has been suggested (4) that, in addition to the classical Boussinesq and Burmister method, the deflection-beam method may be used to analyze the stresses and deflections in stabilized soil layers. The study reported here is directed to the theoretical evaluation of this method and to proving that certain field measurements (6) are in agreement with this theory.

STRENGTH CHARACTERISTICS OF STABILIZED SOILS

Three poorly reactive clayey soils were stabilized with portland cement, hydrated lime and conjunctively with sodium hydroxide to give optimum results (5). The unconfined compressive strength and the modulus of elasticity of the soil mixes were measured after 28 days of curing and a 24-hour immersion. The data given in Table 1

Paper sponsored by Committee on Strength and Deformation Characteristics of Pavement Sections and presented at the 46th Annual Meeting.

TABLE 1

STRENGTH CHARACTERISTICS OF SOIL MIXES

Specimen No.	Type of Mix	Unconfined Compressive Strength (psi)	Ave. E_{sc} (psi)
1[a]	North Carolina clay—kaolinite	0	—
1A	North Carolina clay + 12% portland cement	400	9.0×10^3
1B	North Carolina clay + 12% portland cement + 0.5% NaOH	450	9.4×10^3
1C	North Carolina clay + 6% lime	120	2.1×10^3
1D	North Carolina clay + 6% lime + 1.5% NaOH	150	2.1×10^3
2[b]	Illinois clay—illite	0	—
2A	Illinois clay + 12% portland cement	750	9.3×10^3
2B	Illinois clay + 12% portland cement + 0.25% NaOH	760	9.9×10^3
2C	Illinois clay + 6% lime	130	1.2×10^3
2D	Illinois clay + 6% lime + 0.25% NaOH	180	1.1×10^3
3[c]	Texas clay—montmorillonite	0	—
3A	Texas clay + 12% portland cement	420	9.4×10^3
3B	Texas clay + 12% portland cement + 0.25% NaOH	680	19.0×10^3
3C	Texas clay + 6% lime	300	8.8×10^3
3D	Texas clay + 6% lime + 0.25% NaOH	320	8.9×10^3

[a]Series 1 compacted to 97.2 pcf density at 25.7 percent optimum moisture.
[b]Series 2 compacted to 111.4 pcf density at 18.0 percent optimum moisture.
[c]Series 3 compacted to 102.5 pcf density at 22.6 percent optimum moisture.

suggest that stabilization increased the shearing strength of these soils substantially, placing them in the class of semirigid materials.

THEORETICAL CONSIDERATIONS

Structural Analysis

Using the deflection beam method, it has been hypothesized (4) that a stabilized soil base acts as a finite beam on the subgrade or subbase which is assumed to respond like an elastic foundation. This analogy lends itself to simple solutions and presents a method for analytically predicting the stresses and deflections in the pavement layers. Although at first observation a pavement layer presents itself as a plate, in actuality it may be approximated to a beam on an elastic foundation so long as appropriate widths are employed. This hypothesis and assumption become more realistic especially when the plate is thick, as is the case in uncracked, thick, stabilized soil bases, and the surface loads are considered concentrated point loads above thin wearing surface courses (overlays). For example, using references (10) and (7), it can be shown that plate stresses are less than simply supported beam stresses by a factor approximately equal to the ratio of beam length to beam width. For instance, considering that a plate 12 ft on a side is subjected to a bending stress of 50 psi under a load, the same load will produce a bending stress of 600 psi in a one-way simply supported beam of unit width and 300 psi in a two-way beam of unit width. Furthermore, since bending moments are quite localized and effective beam lengths are short, it is possible to calculate the "equivalent beam" which carries the same stresses as those of a plate and determine the equivalent beam width. In the calculations, the data assumed and used are as follows:

1. The surface wearing course is thin, has no stiffness, and does not spread the load.
2. The stabilized soil base is free of structural cracks.
3. No stresses occur from other effects such as temperature and moisture.
4. Stabilized soil base modulus of elasticity values are 8,000, 12,000 and 20,000 psi.
5. Base thicknesses are 12, 18 and 24 in.
6. Subgrade reaction coefficients are 50, 100 and 200 pci.
7. Unit load is 10,000 lb at a tire pressure of 75 psi.

Plates

Timoshenko, realizing that thin plate theories are inadequate to help in the calculation of moments under concentrated loads, referenced the relationship established by Westergaard (11). Thus, when $\mu = 0.15$, the interior stress, σ_i, is given by:

$$\sigma_i = \frac{0.316P}{h^2}\left[4 \log_{10}\left(\frac{\ell}{b}\right) + 1.069\right] \quad (1)$$

where

$b = \sqrt{1.6a^2 + h^2} - 0.675h$;

a = radius of area of load contact, in.;

$\ell = \sqrt[4]{\frac{Eh^3}{12(1 - \mu^2)k}}$; and

k = subgrade reaction coefficient, pci.

Assuming a unit load of 10,000 lb at a tire pressure of 75 psi, the value of a is $\sqrt{\frac{10,000}{75\pi}} = 6.51$ in. and from the expression $b = \sqrt{67.8 + h^2} - 0.675h$, the values of b are 6.47, 7.65, and 9.20 in. corresponding to h values of 12, 18 and 24 in. The term ℓ is tabulated by Yoder (12) for concrete at $\mu = 0.15$ and $E = 4 \times 10^6$ psi. The values may be converted to stabilized soil by a factor determined as follows:

$$\ell\,(\text{soil}) = A_1 \cdot \ell\,(\text{concrete}), \text{ where } A_1 = \sqrt[4]{\frac{E\,(\text{soil})}{4 \times 10^6}}$$

TABLE 2

MAXIMUM STRESSES AT UNIT LOAD BY WESTERGAARD THICK PLATE THEORY[a]

E (psi)	k (pci)	h (in.)	ℓ(conc.) (in.)	ℓ(stab. soil) (in.)	$\frac{\ell}{b}$	$\log_{10}\frac{\ell}{b}$	$4 \log_{10}\frac{\ell}{b}$	$1.069 + 4 \log_{10}\frac{\ell}{b}$	$\frac{0.316P}{h^2}$ (psi)	σ_i (psi)
8,000	50	12	58.59	12.40	1.908	0.281	1.124	2.193	21.95	48.1
		18	79.41	16.80	2.196	0.342	1.368	2.455	9.75	24.0
		24	98.54	20.85	2.27	0.356	1.424	2.493	5.48	13.7
	100	12	49.27	10.42	1.603	0.206	0.824	1.893	21.95	41.6
		18	66.78	14.12	1.847	0.266	1.064	2.133	9.75	20.8
		24	82.86	17.50	1.902	0.280	1.120	2.189	5.48	12.0
	200	12	41.43	8.75	1.346	0.129	0.516	1.585	21.95	34.8
		18	56.16	11.90	1.556	0.192	0.768	1.837	9.75	17.9
		24	69.68	14.74	1.603	0.205	0.820	1.889	5.48	10.4
12,000	50	12	58.59	13.72	2.11	0.324	1.296	2.365	21.95	52.0
		18	79.41	18.60	2.43	0.386	1.544	2.613	9.75	25.5
		24	98.54	23.05	2.505	0.399	1.596	2.665	5.48	14.6
	100	12	49.27	11.52	1.77	0.248	0.992	2.061	21.95	45.2
		18	66.78	15.63	2.045	0.311	1.244	2.313	9.75	22.6
		24	82.86	19.40	2.11	0.324	1.296	2.365	5.48	13.0
	200	12	41.43	9.69	1.49	0.173	0.692	1.761	21.95	38.7
		18	56.16	13.16	1.72	0.236	0.944	2.013	9.75	19.6
		24	69.68	16.32	1.775	0.249	0.996	2.065	5.48	11.3
20,000	50	12	58.59	15.60	2.40	0.380	1.52	2.589	21.95	56.8
		18	79.41	21.10	2.76	0.441	1.764	2.833	9.75	27.6
		24	98.54	26.20	2.85	0.455	1.82	2.889	5.48	15.8
	100	12	49.27	13.12	2.02	0.306	1.224	2.293	21.95	50.3
		18	66.78	17.78	2.325	0.367	1.468	2.537	9.75	24.8
		24	82.86	22.05	2.40	0.380	1.520	2.589	5.48	14.2
	200	12	41.43	11.02	1.70	0.230	0.92	1.989	21.95	43.6
		18	56.16	14.95	1.955	0.291	1.164	2.233	9.75	21.75
		24	69.68	18.55	2.020	0.306	1.224	2.293	5.48	12.6

[a]Unit load is 10 kips @ 75 psi.

Thus, for the stabilized soil E values of 8,000, 12,000, 20,000 and 100,000 psi, the corresponding A_1 values obtained are 0.2115, 0.234, 0.266 and 0.707.

Calculations for maximum stresses based on Westergaard's plate equation for the desired range of E, k, and h values are given in Table 2. To illustrate the influence of E and k on maximum stresses, selected data from Table 2 are plotted in Figures 1 and 2. Figure 1 shows the effect of subgrade reaction coefficient for a fixed E of 12,000 psi. In Figure 2, the maximum stress is plotted vs E for each of the three base thicknesses of 12, 18 and 24 in. The subgrade reaction coefficient is 100 pci. In both illustrations, it is noted that as the base thickness increases, the effect of E and k decreases.

Beams

The classical problem of beams on elastic foundations is treated by several well-known texts. Included among these are Seeley and Smith (8), Timoshenko (9) and Hetenyi (3). Gazis (2) outlined a procedure for analyzing finite beams on elastic foundations by using finite difference iterations. Dodge (1), summarizing much of the work of Timoshenko and Hetenyi, developed influence functions for beams of constant elastic properties.

Due to the relatively short deflection zone, the infinite beam assumption is adequate for interior calculations. The development of the formulation begins with the well-known basic beam bending equation:

$$\frac{d^4y}{dx^4} = \frac{q}{EI} \tag{2}$$

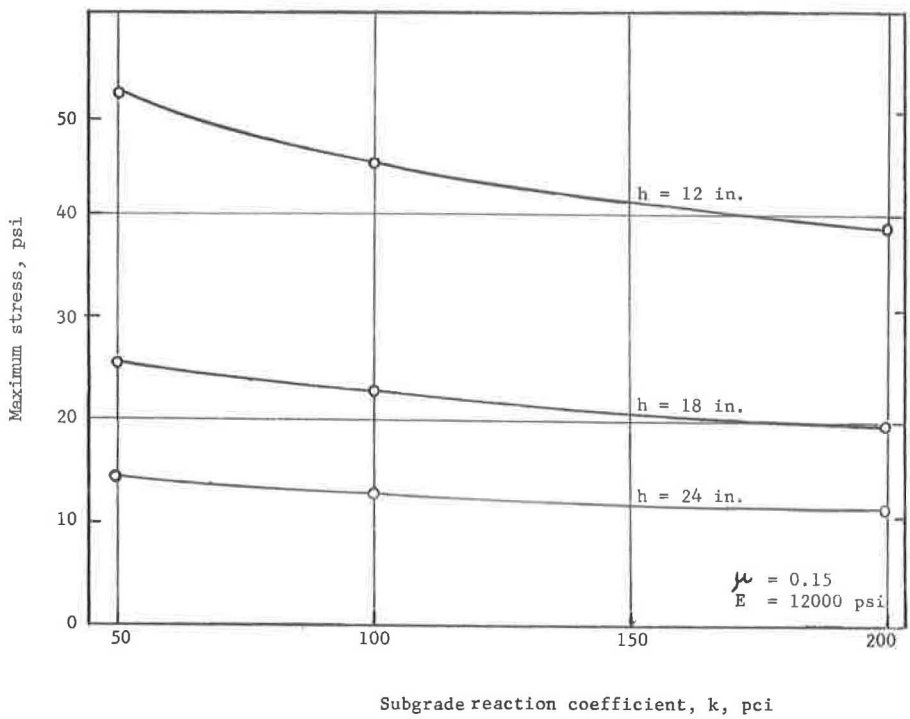

Figure 1. Maximum stress based on plate theory.

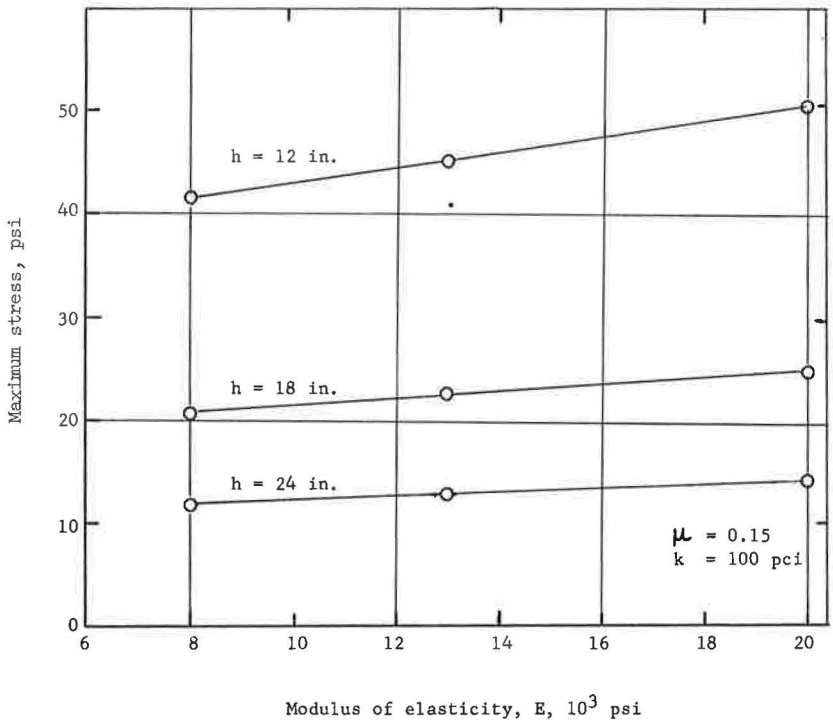

Figure 2. Maximum stress based on plate theory.

The general solution of the governing differential equation is expressed as:

$$y = e^{\beta x}(A\cos\beta x + B\sin\beta x) + e^{-\beta x}(C\cos\beta x + D\sin\beta x) \qquad (3)$$

where the "characteristic" of the system is:

$$\beta = \sqrt[4]{\frac{kb_e}{4EI}} = \sqrt[4]{\frac{3k}{Eh^3}} \qquad (4)$$

where

b_e = equivalent beam width,
k = subgrade reaction coefficient in pci, and
I = equivalent beam moment of inertia.

The coordinate system is referenced to the load point. Four boundary conditions are necessary to determine the constants in Eq. 3. These are:

$x = \infty$	$y = 0$
$x = \infty$	$y'' = 0$
$x = 0$	$y' = 0$
$x = 0 + \Delta$	$V = -EIy''' = -P/2$

The boundary conditions lead to the following values of the constants:

$$A = B = 0$$
$$C = D = P/(8\beta^3 EI)$$

The final deflection equation then becomes:

$$y = \frac{P}{8\beta^3 EI} e^{-\beta x} (\cos \beta x + \sin \beta x) \tag{5}$$

Recalling that

$$\beta = \sqrt[4]{\frac{kb_e}{4EI}}$$

it follows that

$$y = \frac{P\beta}{2kb_e} e^{-\beta x} (\cos \beta x + \sin \beta x) \tag{6}$$

and

$$M = -EIy'' = -\frac{P}{4\beta} e^{-\beta x} (\sin \beta x - \cos \beta x) \tag{7}$$

If

$$\phi = e^{-\beta x} (\cos \beta x + \sin \beta x)$$

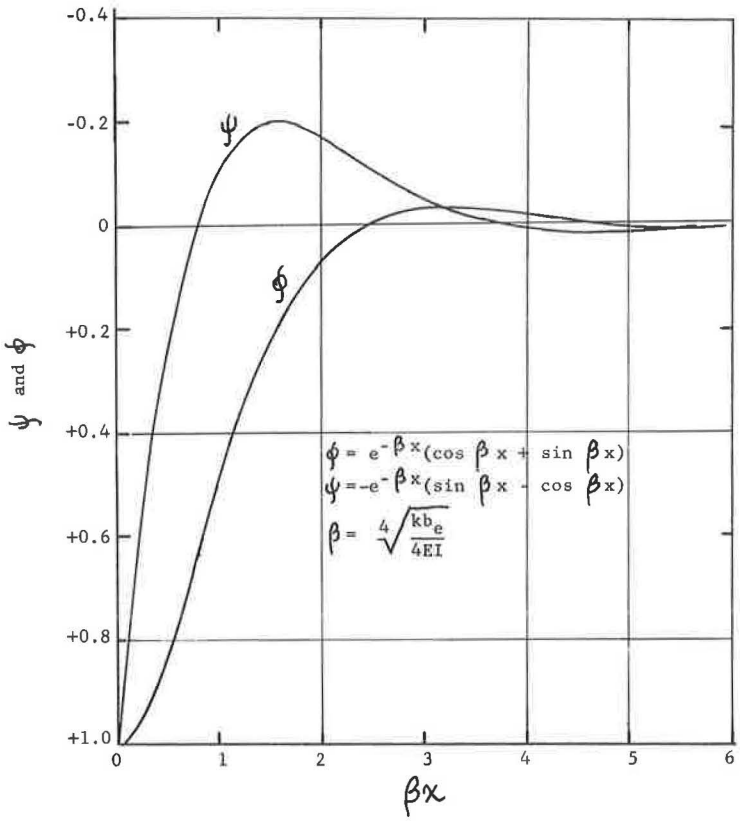

Figure 3. Functions of the beam equation.

and

$$\psi = -e^{-\beta x}(\sin \beta x - \cos \beta x)$$

then

$$y = \frac{P\beta}{2kb_e}\phi \tag{8}$$

and

$$M = \frac{P}{4\beta}\psi \tag{9}$$

Values of ϕ and ψ are shown in Figure 3. The moment is shown to experience an inflection point at $\beta x = 0.8$. This points out the very small zone of the beam experiencing significant moments. Moment effects are shown to have practically vanished at $\beta x = 3.0$.

Beam stresses may be determined from the relationships

$$\sigma = \frac{Mc}{I} = \frac{6M}{b_e h^2} = \frac{1.5 P \psi}{b_e h^2 \beta} \tag{10}$$

$$\sigma_{max} = \frac{1.5 P}{b_e h^2 \beta} \tag{11}$$

Calculations of beam stresses are given in Table 3 where σ_{max} is expressed in terms of beam width, b.

TABLE 3

MAXIMUM STRESSES AT UNIT LOAD BY BEAM ON ELASTIC FOUNDATION THEORY[a]

E (psi)	k (pci)	h (in.)	$\frac{3k}{E} \times 10^3$ (1/in.)	$\frac{3k}{Eh^3} \times 10^8$ (1/in.^{4})	$\beta = \sqrt[4]{\frac{3k}{Eh^3}} \times 10^2$ (1/in.)	$h^2\beta$ (in.)	$\sigma_{max} b_e$† (lb/in.)	b_e* (in.)	b_e/h	$X_{lim} = \frac{3}{12\beta}$ (ft)	$\frac{X_{lim}}{h}$
8,000	50	12	18.75	1085.0	5.74	8.266	1815	37.7	3.14	4.36	4.36
		18	18.75	321.5	4.23	13.71	1094	45.6	2.53	5.91	3.94
		24	18.75	135.6	3.41	19.64	752	54.9	2.29	7.33	3.66
	100	12	37.50	2170.0	6.84	9.85	1523	36.7	3.06	3.66	3.66
		18	37.50	643.0	5.04	16.33	919	44.1	2.45	4.96	3.31
		24	37.50	271.3	4.06	23.39	641	53.4	2.22	6.16	3.08
	200	12	75.0	4339.0	8.12	11.70	1281	36.8	3.07	3.08	3.08
		18	75.0	1286.0	6.00	19.43	772	43.2	2.40	4.17	2.78
		24	75.0	543.0	4.83	27.85	538	51.7	2.16	5.17	2.59
12,000	50	12	12.5	723.4	5.19	7.47	2008	38.7	3.22	4.82	4.82
		18	12.5	214.3	3.83	12.41	1209	47.4	2.63	6.53	4.35
		24	12.5	90.4	3.08	17.74	846	58.0	2.14	8.11	4.06
	100	12	25.0	1446.8	6.17	8.88	1689	37.4	3.12	4.05	4.05
		18	25.0	428.7	4.55	14.74	1018	45.1	2.51	5.50	3.67
		24	25.0	180.8	3.67	21.14	710	54.6	2.28	6.81	3.41
	200	12	50.0	2893.0	7.34	10.57	1417	36.6	3.05	3.40	3.40
		18	50.0	857.0	5.40	17.51	856	43.7	2.43	4.62	3.09
		24	50.0	361.0	4.36	25.13	596	52.7	2.19	5.73	2.86
20,000	50	12	7.5	434.0	4.56	6.57	2280	40.1	3.34	5.48	5.48
		18	7.5	128.6	3.36	10.89	1375	49.8	2.77	7.44	4.95
		24	7.5	54.3	2.72	15.67	957	60.6	2.53	9.19	4.59
	100	12	15.0	868.1	5.43	7.82	1918	38.1	3.18	4.61	4.61
		18	15.0	257.2	4.00	12.96	1157	46.6	2.59	6.25	4.16
		24	15.0	108.5	3.23	18.60	806	56.8	2.37	7.44	3.72
	200	12	30.0	1736.0	6.45	9.18	1614	37.0	3.09	3.88	3.88
		18	30.0	514.0	4.76	15.42	972	44.5	2.47	5.25	3.49
		24	30.0	217.0	3.84	22.09	679	53.8	2.24	6.51	3.26

[a]Unit load = 10 kips @ 75 psi.
†1.5 P/h^2.
*$\sigma_{max} b_e/\sigma_i$ of Table 2.

Equivalent Beam Relationships

Stresses due to a 10,000-lb wheel load are given in Table 2 using the plate theory and a 75-psi tire pressure. Stresses due to the same load, but assuming a beam of width b, are given in Table 3. By equating these stresses, it is possible to solve for a beam width, b_e, which will produce stresses due to a point load on the beam that will closely approximate the behavior of a true plate. Equivalent widths, b_e, are listed in Table 3. The variation of equivalent width is shown in Figure 4 where the dimensionless ratio b_e/h is plotted vs base modulus of elasticity, E, for thicknesses of 12, 18 and 24 in. and for k values of 50, 100 and 200 pci.

To establish a limit as to the distributive effects of a point load, the distance $\beta x = 3.0$ was calculated for the desired range of variables and listed in Table 3 as the dimensionless term x_{lim}/h. As pointed out earlier, the moment actually decreases substantially away from the load to an inflection point a distance of $0.8/\beta$ away. This inflection may be determined by multiplying the x_{lim}/h value by 0.267. For a depth of 24 in., the inflection point is approximately equal to the depth. The significance of this fact is that the influence of additional wheels on the stresses under a particular wheel load is negligible except for two wheels together, as in the case of dual tires on a single axle.

In dual wheel loadings, the stresses are obtained simply by adding the stresses resulting from separate applications of Eq. 10 with values from Figure 3. The following example is used to illustrate the method.

Wheel load: 10,000 lb dual, 16-in. spacing;

Base thickness: 18 in.;

Base E: 12,000 psi; and

Subgrade k: 100 pci.

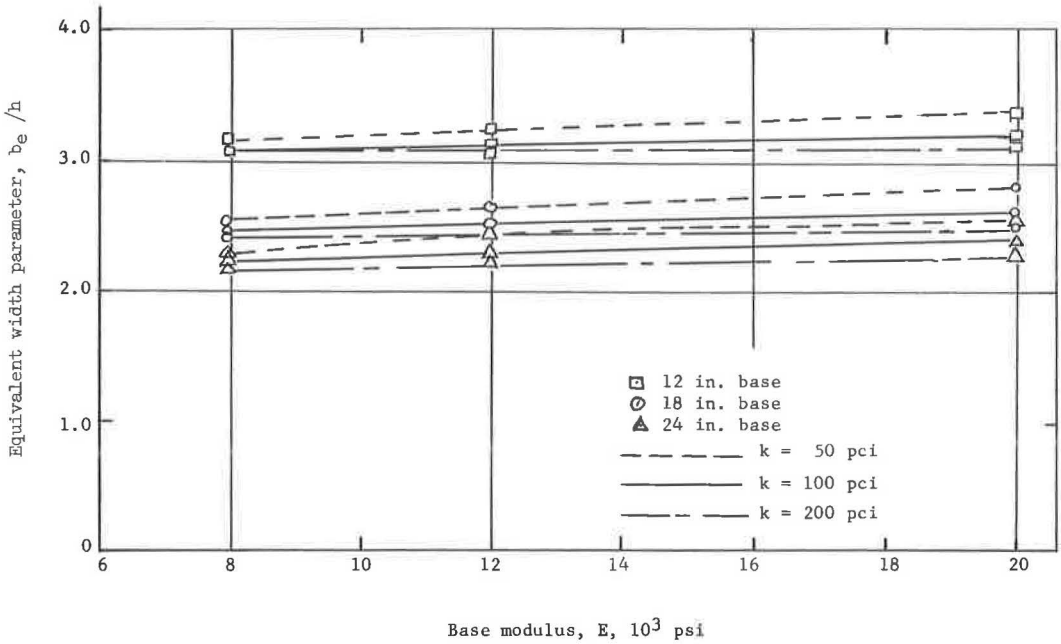

Figure 4. Effect of modulus of elasticity on equivalent width parameter at P = 10,000 lb, tire pressure = 75 psi, and $\mu = 0.15$.

The stress under one wheel is calculated by employing Eq. 10:

$$\sigma = \frac{1.5\,P\,\psi\,(0)}{b_e\,h^2\beta} + \frac{1.5\,P\,\psi\,(16'')}{b_e\,h^2\beta}$$

From Table 3, $\beta = 0.0455$ in.$^{-1}$ Thus, $\beta x = 0.0455 \times 16 = 0.728$. Using $\beta x = 0.728$, from Figure 3, $\psi = 0.05$. From Figure 4, $b_e = 2.5h$. Then,

$$\sigma = \frac{1.5\,(5000)\,(1.0)}{2.5\,(18)^3\,(0.0455)} + \frac{1.5\,(5000)\,(0.05)}{2.5\,(18)^3\,(0.0455)}$$

$$\sigma = 11.9 \text{ psi}$$

It is noted that the influence of one wheel on the stress under the other wheel is only 5 percent in this case. This might seem a little unrealistic, but it is actually a characteristic of solutions of beams and plates on elastic foundations. A very conservative estimate of stresses under dual-wheel combinations could be obtained by translating the dual wheel to an equivalent single-wheel load (12).

Comparisons with PCA Experiments

Recent experimental studies by PCA (6) on load-deflection characteristics of soil-cement pavements gave the parameter relationship shown in Figure 5 and reflected in the equation:

$$\frac{y^k}{P} = \alpha\left(\frac{a}{h}\right)^{\gamma}$$

where α and γ are constants. On a log-log plot, α corresponds to the ordinate on the best-fit line for an abscissa of $a/h = 1$ and γ is the slope of the best-fit line. The best-fit line for the PCA soil-cement load-deflection tests is shown in Figure 5. These tests were performed on cement-stabilized soils with an elastic modulus E (determined by sonic methods) varying from 570×10^3 to 1400×10^3 psi. Compressive strengths ran as high as 675 psi. These values indicate that the soil-cement bases tested were quite rigid, whereas some of the data in Table 1 cover relatively weaker soils for which the beam method is essentially intended. It is expected that elastic modulus values of such weaker base materials would not exceed 20×10^3 psi. To substantiate the validity of the equivalent beam method, the load deflection characteristics were plotted in Figure 5 using E values of 8×10^3, 12×10^3 and 20×10^3 psi, for various values of a/h. The resulting plot is a family of curves having essentially the same slope as the PCA reference line with the least E giving a line further removed from the PCA "best fit." In addition, Figure 5 shows a point reflecting the data obtained when $E = 500 \times 10^3$ psi. The characteristic plot for $E = 1000 \times 10^3$ psi is coincident with the PCA reference line, a further evidence of the applicability of the beam method.

Other Load-Pressure Ratios

As pointed out in the original assumptions, a unit load of 10,000 lb at a tire pressure of 75 psi was taken as a standard for the method presented. The ratio of load to tire pressure is a significant parameter in determining effective load radius, b, used in the plate stress Eq. 1. The ratio of tire load to pressure used herein was 10,000/75 = 133.3. For other load-pressure ratios, the resulting base stresses and deflections may be in error. Table 4 will serve as a guide to assess the probable error when using the equivalent beam widths of this report for load-pressure ratios other than 133.3.

The data in Table 4 indicate the percent difference in equivalent width with different load-pressure ratios. As noted, the equivalent width decreases as the load-pressure ratio decreases. The maximum percent decrease occurs for E, h, and k values of

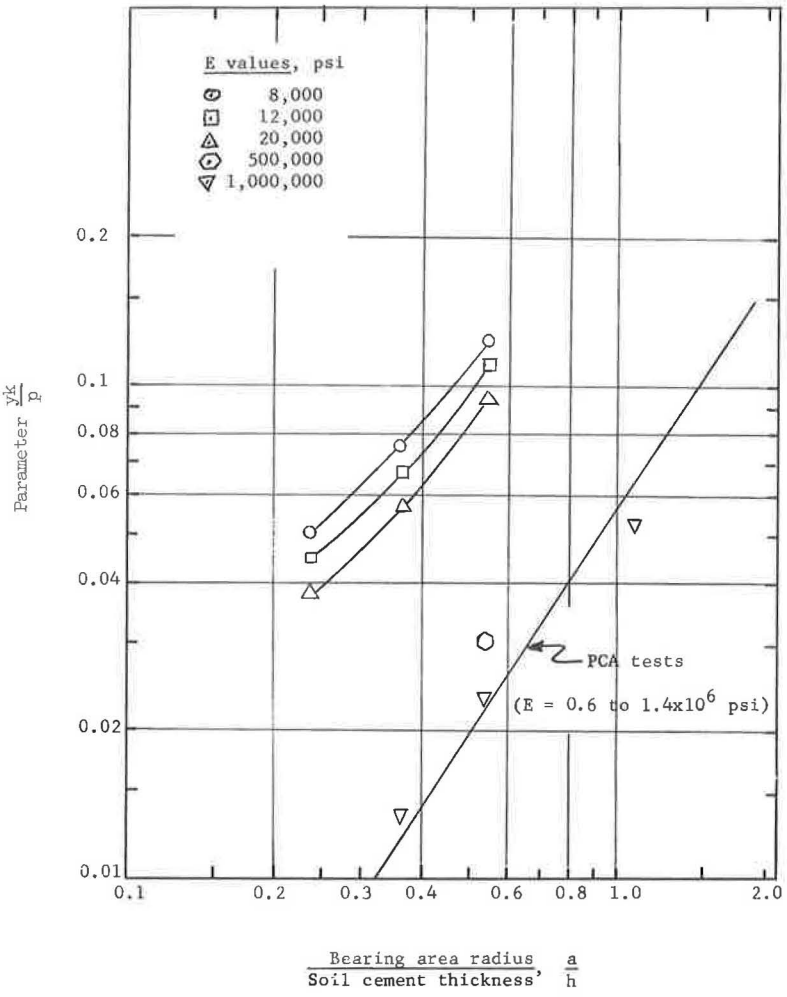

Figure 5. Load deflection relationships.

8,000 psi, 12 in., and 200 pci. The Nominal Percent Decrease represents the middle values for parameters E, h, and k of 12,000 psi, 18 in., and 100 pci. The Minimum Percent Decrease occurs for E, h, and k values of 20,000 psi, 24 in., and 50 pci.

Realizing the limitations and approximations of any analytical approach to predicting stresses in materials having such widely varying physical properties as stabilized soils, it appears practical to merely decrease equivalent beam width by the percentage determined by interpolation of Table 4.

TABLE 4

DECREASE OF EQUIVALENT WIDTH

Load-Pressure Ratio	Max. Percent Decrease	Nominal Percent Decrease	Min. Percent Decrease
133.3	0	0	0
100.0	10.7	4.3	3.0
66.7	21.2	8.6	5.1

CONCLUSIONS

Equivalent beam approximations to stabilized soil layers on elastic foundations afford very useful and expedient solutions in the determinations of stresses and deflections in these layers. The beam method calculations of load deflection are in good agreement with actual test results reported by PCA.

REFERENCES

1. Dodge, A. Influence Functions for Beams on Elastic Foundations. Proc. ASCE, Jour. Struct. Div., Vol. 90, Paper 4002, pp. 63-102, Aug. 1964.
2. Gazis, D. C. Analysis of Finite Beams on Elastic Foundations. Proc. ASCE, Jour. Struct. Div., Vol. 84, Paper 1722, pp. 1-18, July 1958.
3. Hetenyi, M. Beams on Elastic Foundation. Univ. of Michigan, Ann Arbor, 1946.
4. Laguros, J. G. Lime-Stabilized Soil Properties and the Beam Action Hypothesis. Highway Research Record 92, pp. 12-20, 1965.
5. Laguros, J. G. Response Differences in the Stabilization of Clayey Soils. Paper presented at the 2nd Highway Research Symposium, Rio de Janeiro, Sept. 1966.
6. Nussbaum, P. J., and Larsen, T. J. Load Deflection Characteristics of Soil-Cement Pavements. Highway Research Record 86, pp. 1-14, 1965.
7. Sechler, E. E. Elasticity in Engineering. John Wiley and Sons, New York, 1952.
8. Seeley, F. B., and Smith, J. O. Advanced Mechanics of Materials. John Wiley and Sons, 2nd edition, New York, 1952.
9. Timoshenko, S. Strength of Materials. Part II, Van Nostrand, 3rd edition, New York, 1956.
10. Timoshenko, S., and Woinowsky-Krieger, S. Theory of Plates and Shells. McGraw-Hill Book Co., 2nd edition, New York, 1959.
11. Westergaard, H. M. Stresses in Concrete Pavements Computed by Theoretical Analysis. Public Roads Magazine, Vol. 7, No. 2, pp. 25-35, 1926.
12. Yoder, E. J. Principles of Pavement Design. John Wiley and Sons, New York, 1959.

A Simple Method for Obtaining Undisturbed Soil Samples for CBR Determination

I. S. UPPAL, RESHAM SINGH, and S. R. BAHADUR, P. W. D. Building and Roads Research Laboratory, Chandigarh, India

A simple arrangement for collecting undisturbed soil samples for determining the CBR value of road bases and subgrades has been developed by making use of hard steel core cutters of the same internal dimensions as the standard CBR molds. The percent-area ratio of the core cutters is 8.5. The method for collecting undisturbed samples by the new arrangement has been explained and illustrated and the results compared with in situ test results.

•THE California Bearing Ratio Test (CBR) is a comparative measure of the shearing resistance of a soil under controlled density and moisture conditions. It is widely used with empirical curves for designing flexible pavements. CBR is expressed as a percentage of the unit load required to force a piston of 3 sq in. surface area (1.954 in. diameter) into the soil at a rate of 0.05 in. per minute, divided by the unit load required to force the same piston the same depth at the same rate into a standard sample of crushed stone.

$$\text{CBR} = \frac{\text{test unit load}}{\text{standard unit load}} \times 100$$

The CBR used in design is the 0.1 or 0.2-in. penetration value, whichever is greater. For most soils, the 0.1-in. penetration value is the greater. Unless it is certain that the soil will not accumulate moisture after construction, CBR tests are performed on soaked samples. This test can be performed in the laboratory as well as at the actual work site.

EQUIPMENT AND PROCEDURE FOR CBR TEST

In the laboratory method, the soil to be tested is compacted at a certain moisture to the desired dry density in special cylindrical molds. These CBR molds have an internal diameter of 6 in. and an internal height of 7 in., with a detachable perforated base which can be fitted at either end. A displacer disk 2 in. deep and 5.93 in. in diameter provides a specimen exactly 5 in. long.

For testing CBR, the mold (after soaking if necessary) is placed on the base of a loading frame provided with a screw jack, and the standard plunger (having a circular cross section of 3 sq in.) is placed in the center of the specimen and load is applied by working the screw jack. Penetration of the plunger in the soil specimen and the force applied are indicated on the dial gages fixed on the apparatus. A complete setup of the equipment is shown in Figure 1.

Although CBR tests on laboratory compacted specimens are usually performed to obtain information which will be used for design purposes, the field test is considered more reliable for determining the load carrying capacity of in-place material. When a field test is performed on materials that during the life of the pavement may undergo

Paper sponsored by Committee on Exploration and Classification of Earth Materials.

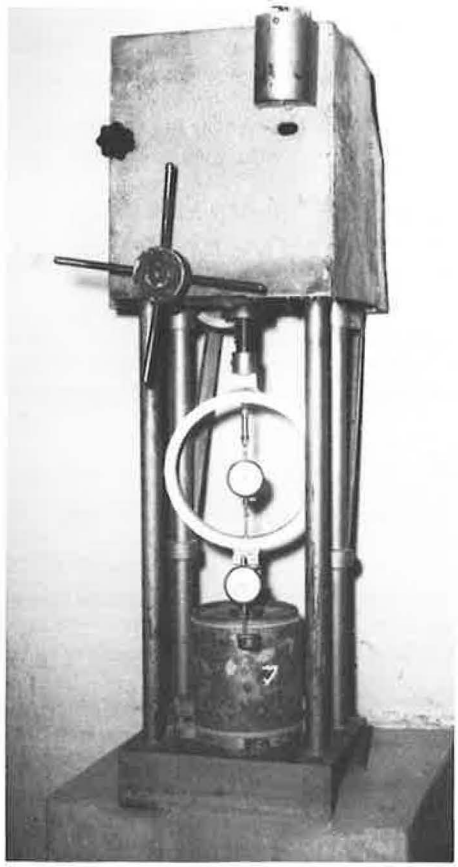

Figure 1.

moisture content changes, undisturbed samples of the field compacted material are tested in the laboratory.

EQUIPMENT FOR IN-PLACE FIELD TEST

A loaded truck has been found to be a convenient form of reaction load for testing CBR in situ. A screw jack is fitted to the back of the truck and the load is applied by working it in the same way as in the laboratory method. The dial gage for recording penetration is fixed with an independent long datum bar which is supported at ends on two stands. No specimen molds are required in this case. The test is done directly on the ground after it has been leveled. The general arrangement for this test is shown in Figure 2.

Drawbacks of the In Situ Test

The CBR in situ test has certain drawbacks which are briefly listed as follows:

1. During the test, the vibrations produced by the heavy traffic disturb the datum bar and thus the penetration value and the corresponding load cannot be measured accurately.
2. Test pits hinder the traffic particularly when the CBR is done under soaked conditions; the soaking has to be continued for at least 4 days. This is likely to cause accidents.

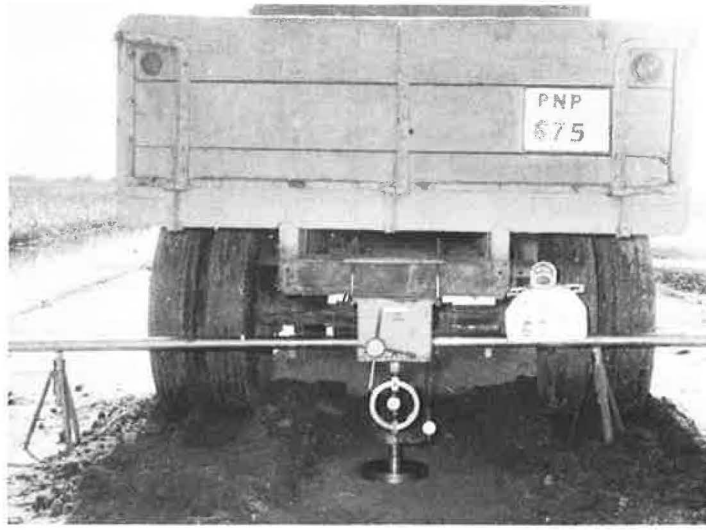

Figure 2.

3. Pits are likely to be disturbed by some external activities during soaking.
4. In situ soaking is done from the top to the bottom without any surcharge effect, whereas in actual practice the worst conditions of the subgrade below pavement are reached due to the rise of subsoil water.
5. In actual practice, the subgrade absorbs moisture under pavement surcharge and therefore the CBR value under in situ soaking may give a low value which in turn may be misleading.
6. A uniform soaking in situ is not possible and a proper check on soaking cannot be maintained if CBR values of many miles of road are to be determined.
7. For testing a pit under natural conditions and after soaking, the loaded truck has to go twice to the site. This makes the test very expensive and cumbersome.

In order to overcome these drawbacks, undisturbed samples of the field compacted material are obtained and tested in the laboratory for moisture conditions simulating those expected in the field. The testing equipment and arrangement are as shown in Figure 1.

METHOD OF OBTAINING UNDISTURBED SAMPLES

According to the presently accepted procedure of taking undisturbed samples, the standard CBR mold is used with a sampling collar having a sharp cutting edge. The ground surface is smoothed and the mold, with the sampling collar fixed at the bottom and the extension collar fixed at the top, is pressed into the soil with moderate pressure. Then a trench is excavated around the mold and the mold is pressed down firmly over the soil chunk. The soil is trimmed from the sampling collar with a knife by cutting downward and outward to avoid cutting into the sample. The trench is excavated deeper and the procedure is repeated until the soil is well into the extension collar. The sample is then cut off at the bottom of the mold with a knife, shovel or saw and removed from the hole. The extension and sampling collars are removed and the soil trimmed to the end of the mold on both sides. In order to get a specimen exactly 5 in. long, 2 in. of excess length can be removed by either scraping or pushing out, using the displacer disk and jack arrangement (Fig. 5a).

STUDY OBJECTIVE

This process of obtaining an undisturbed sample is, however, very laborious and time consuming. Besides, it needs elaborate and expensive equipment like a CBR mold, extension collar and sampling collar with cutting edge. In this age of rapid development when many miles of new roads have to be constructed and even greater lengths of old roads have to be reconditioned, a need for quicker and cheaper methods

TABLE 1

COMPARISON OF RESULTS OF DENSITY OF NATURAL GROUNDS AND AFTER TAKING UNDISTURBED SAMPLES WITH CORE CUTTERS NEAR THE SAME POINTS

Test Pit	Moisture (%)	Density of Natural Ground (gm/cc)	Density in Core Cutter (gm/cc)	Level of Natural Ground from Top Edge of Core Cutter (cm)			
				Core Cutter Half Filled		Core Cutter Nearly Filled	
				Inside	Outside	Inside	Outside
1	6.6	1.48	1.53	6.7	6.8	1.2	1.1
				7.5	7.3	1.6	1.4
				7.2	7.2	1.3	1.2
				7.4	7.5	1.3	1.2
2	17.5	1.52	1.52	7.4	7.6	1.3	1.4
				7.4	7.5	1.6	1.6
				7.8	7.9	1.5	1.55
				7.6	7.4	1.55	1.55
3	6.9	1.53	1.52	8.1	8.1	1.7	1.5
				8.3	8.1	1.6	1.4
				8.0	7.9	1.7	1.5
				8.3	8.2	1.8	1.7
4	18.1	1.45	1.48	—	—	2.3	2.2
						2.6	2.5
						2.3	2.2
						2.6	2.4

TABLE 2

COMPARISON OF CBR VALUES OBTAINED IN SITU AND ON UNDISTURBED SAMPLES TAKEN BY CORE CUTTER FROM NEAR THE SAME POINTS—AT NATURAL MOISTURE CONTENT

Test Pit	Dry Density (gm/cc)	Natural Moisture (%)	CBR	CBR of Undisturbed Sample in Core Cutter	CBR of Undisturbed Sample After Transfer to CBR Molds	Soil Characteristics		
						LL	PI	SC
1	1.60	14.4	5.1 5.9	4.5 —	— 5.5	39.0 —	19.5 —	8.2 —
2	1.60	11.4 7.3	9.8 19.3	7.6 —	— 14.8	36.7 —	18.4 —	10 —
3[a]	1.55	9.55	15.3 14.1	13.0 —	— 15.6	37.0 —	18.5 —	11.0 —
4	1.5	18.1	3.1	3.7	5.8	38.0	19.0	9.4
5	1.55	11.1	8.7	12.7	15.3	38.0	19.0	9.4
6	1.65	8.5	24.7	25.3	—	36.7	18.4	10.5
7	1.58	14.1	14.6	14.6	—	36.7	18.4	10.5
8[b]	1.8	9.3	21.9 19.1	18.4 17.0	—	38.0	19.0	9.4
9[c]	1.8	10.9	14.6 17.3	15.3 17.0	—	26.9	9.2	51.5

[a]Natural subgrade.
[b]Clayey soil compacted to 1.8 gm/cc of dry density.
[c]Sandy soil compacted to 1.8 gm/cc of dry density.

TABLE 3

COMPARISON OF CBR VALUES OBTAINED FROM IN SITU TEST AND UNDISTURBED SAMPLES OF CORE CUTTER (AFTER SOAKING)

Test Pit	Dry Density (gm/cc)	In Situ Soaking			Undisturbed Samples in Lab			Undisturbed Samples Without Surcharge Weights		
		CBR	Moisture (%)		CBR	Moisture (%)		CBR	Moisture (%)	
			3 In.	6 In.		Top	Bottom		Top	Bottom
1[a]	1.6	1.4	20.5	22.0	2.3	22.1	23.0	1.4	23.4	24.5
2	1.6	2.9	20.7	20.8	3.4	21.0	22.0	1.98	22.5	24.0
3	1.55	2.0	24.2	21.7	2.3	22.0	22.0	2.0	22.6	23.4
4	1.55	1.6	24.2	24.8	1.8	24.1	24.5	1.7	22.0	22.6
5[b]	1.8	1.6	21.4	22.5	3.4	20.5	19.9	1.2	21.9	23.3
6	1.8	3.4	21.4	22.5						
7[c]	1.8	4.7	13.1	12.7	5.4	13.9	15.2	2.4	14.2	14.8
8	1.8	3.9	13.1	12.7						

[a]Natural subgrade.
[b]Clayey soil compacted to 1.8 gm/cc of dry density.
[c]Sandy soil compacted to 1.8 gm/cc of dry density.

TABLE 4

COMPARISON OF CBR VALUES TESTED IN SITU AND ON UNDISTURBED SAMPLES FROM THE STABILIZED SOIL BASE AFTER SOAKING IN SITU AND IN THE LABORATORY

Test Pit	Dry Density (gm/cc)	Soaked CBR			Soaked Moisture (%)				Soil Characteristics		
		In Situ Soaking		Lab Soaking	In Situ Soaking		Lab Soaking		LL	PI	SC
		In Situ Test	Undisturbed Sample	Undisturbed Sample	3 In.	6 In.	Top	Bottom			
1[a]	1.8	21.9	21.1	20.9	19.3	18.5	18.8	20.8	40.7	12.7	12.8
2	1.8	21.9	21.8	21.5	19.3	18.5	17.8	17.3	40.7	12.7	12.8
3	1.8	27.4	24.1	21.5							
4	1.8	19.5	22.6		19.3	18.5			40.7	12.7	12.8
5[b]	1.8	19.5	23.0	18.9	18.9	18.9	17.6	19.2	42.2	14.5	8.0
6	1.8	23.5	24.3	23.2	18.9	18.9			42.2	14.5	8.0
7	1.8	14.1	12.2								
8	1.8	26.1	23.8	24.9	18.9	18.9	16.6	19.8	42.2	14.5	8.0

[a]Stabilized with 2 percent lime and 7 days curing before soaking. Compacted at 1.8 gm/cc of dry density.
[b]Stabilized with 2 percent cement and 7 days curing before soaking. Compacted at 1.8 gm/cc of dry density.

of obtaining undisturbed samples for determining the load carrying capacity of natural subgrade and suitable pavement thicknesses is necessary.

To achieve this objective, thin-walled steel core cutters having a 6-in. internal diameter were used for obtaining the undisturbed samples. Results have been very satisfactory. A comparative study of CBR tests in situ and undisturbed samples obtained by the core cutter method was made to ascertain that the core cutter method and in situ CBR tests gave identical results. The actual results are given in Tables 1 to 4.

STEEL CORE CUTTER SPECIFICATIONS

The core cutter sampling arrangement consists of two parts: (a) a thin-walled open-ended steel cylinder with a 6-in. internal and 6.25-in. external diameter and a 5-in. length, with one end sharpened to serve as a cutting edge; and (b) a steel cap with an inside collar of the same dimensions as the core cutter so that when the cap is placed over the core cutter, the collar sits exactly on the rim. These parts along with other accessories are shown in Figure 3. The height of the cap is 1.5 in. and that of the internal collar 0.75 in., so that the soil specimen projects out this far from the core cutter to allow the finishing of the top. The percentage area ratio of the cylinder comes to only 8.5. Because it is less than 10, the distortion or disturbance of the sample obtained by such core cutters is almost negligible.

Procedure of Obtaining Undisturbed Samples

As in the case of obtaining undisturbed samples with the CBR mold, the ground surface is leveled and the core cutter with the steel cap is pressed vertically with the cutting edge downward (Fig. 4a). It is then carefully hammered down by an 18-lb rammer (Fig. 4b). A hard wooden block is placed over the cap to avoid damaging the steel cap. The hammering is continued until the edge of the cap just touches the ground; then some soil is excavated along the rim of the cap to a depth of about 2 in. and hammering is resumed to fill the core cutter (Fig. 4c). Care is taken that the soil coming into the cutter does not get pressed by the cap. This can be watched through a $\frac{1}{2}$-in. diameter hole in the top of the cap. The condition of the top of the soil specimen can be seen by removing the cap. If some disturbance of the soil has taken place, the upper layers,

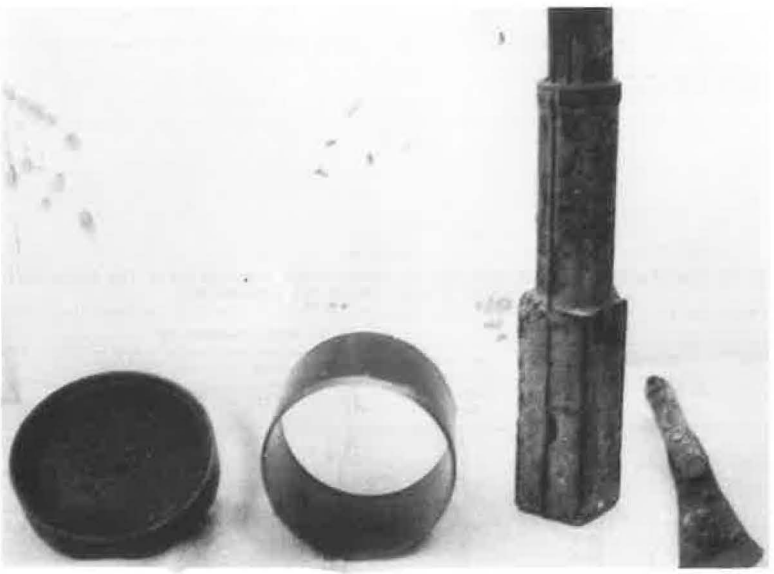

Figure 3.

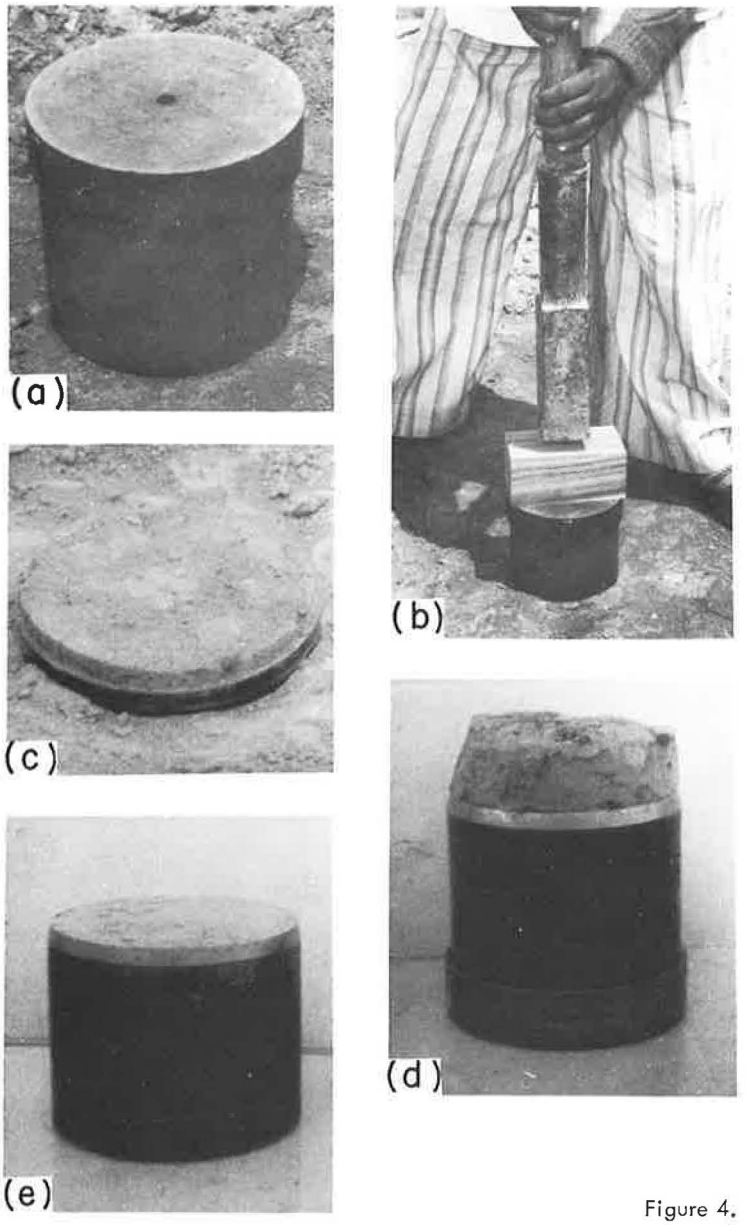

Figure 4.

which are projecting out of the core cutter due to the use of collared cap, are trimmed to the level of the cutter rim. If necessary, the cap can be replaced and the core cutter lowered further into the ground by resuming hammering until a clean and firm undisturbed specimen is obtained. The cutter is then removed from the ground by digging the soil from the sides and cutting the sample at the bottom in the same manner as mentioned in the CBR method. Figure 4d shows the result. The sample is trimmed to the rim on both sides (Fig. 4e). For determining CBR, undisturbed samples may be transferred to the CBR standard mold by means of a jack arrangement

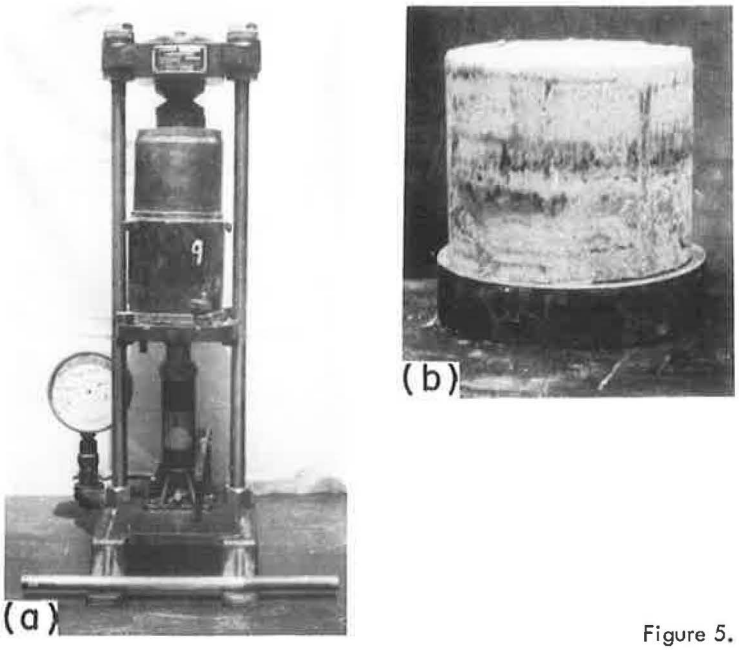

Figure 5.

(Fig. 5a). A CBR test can also be conducted on the specimen in the core cutter itself. Figure 5b shows the undisturbed soil specimen taken out of the cutter by the jack assembly.

DISCUSSION OF RESULTS

Table 1 compares the density of the natural ground with that of undisturbed specimens obtained from near the same place, in order to make sure that the use of the core cutter does not interfere with this property. Notice that there was no significant variation in the density of the ground and that of the undisturbed samples collected by core cutters. Similarly, the inside and outside depth as measured from the rim of the core cutter remained unchanged during the lowering of the cutter into the ground. These results confirm that the samples obtained by the core cutter method are not disturbed during the extraction process.

Table 2 compares the CBR values obtained in situ with undisturbed samples collected by core cutters after natural moisture content has been drawn. Eleven points having a CBR range varying from 3 to 25 were tested and results obtained by the two methods were in very close agreement.

Table 3 compares the soaked CBR value obtained in situ with undisturbed samples soaked in the laboratory. The undisturbed samples were soaked with and without using surcharge weights. Moisture content of the soil at a 3 and 6-in. depth (in situ test) and at the top and bottom of the soaked undisturbed samples (core cut) is also given in Table 3. The results of the 8 points tested were almost identical for the two test methods. The CBR test results of the undisturbed samples soaked without surcharge were closer to the in situ test.

In Table 4 soaked CBR test results of the soil bases stabilized with lime and cement, as obtained by the in situ and core cutter methods, are given. Table 4 also shows a comparison of CBR results of undisturbed specimens obtained after in situ soaking and laboratory soaking. In all cases, the results showed reasonable agreement with each other.

REFERENCES

1. Soil Mechanics for Road Engineers. DSIR, Road Research Laboratory, Harmondsworth, 1961, 541 pp.
2. Peck, R. B., Hanson, W. E., and Thornburn, T. H. Foundation Engineering. John Wiley and Sons, N.Y., 1953, 410 pp.
3. Bertram, George E., and Labaugh, W. C., Jr. Soil Tests. ARBA Tech. Bull. 107, 1964.
4. Soils Manual for Design of Asphalt Pavement Structures. Asphalt Institute, Manual Series 10, June 1961.